

Universität Stuttgart

Supersolid phases in cold atomic gases

Supersolide Phasen in kalten atomaren
Gasen

Diplomarbeit von

Adam Bühler

Hauptberichter: Prof. Dr. H. P. Büchler

Mitberichter: Prof. Dr. G. Wunner

Institut für Theoretische Physik III
Universität Stuttgart

January 15, 2011

Contents

1	Introduction	7
2	Basic concepts	9
2.1	Optical lattice	9
2.2	Bose-Hubbard Model	10
2.2.1	Extended Bose-Hubbard Hamiltonian	12
2.3	Quantum Phase Transition	12
2.3.1	Mott Insulator - Superfluid Transition	13
2.3.2	Supersolid Phase	16
2.4	Rotor Model	17
2.5	^{52}Cr Experiments	18
3	Bogoliubov theory	21
3.1	Fourier transformation of the Bose-Hubbard Hamiltonian	21
3.1.1	Fourier transformation of the first part of the Hamiltonian	22
3.1.2	Fourier transformation of the second part	23
3.1.3	Fourier transformation of the third part	24
3.1.4	Fourier transformed Hamiltonian	25
3.2	Analysis of the Bogoliubov Hamiltonian	25
3.2.1	Calculation of the Instability	29
4	Mean-field Calculations for Rotor Model	31
4.1	Deriving the Rotor-Model	31
4.1.1	Calculation of the kinetic part	32
4.1.2	Calculation of the on-site interaction part	33
4.1.3	Calculation of the nearest-neighbor interaction part	34
4.1.4	The Rotor-Hamiltonian	34
4.2	Fourier Transformation of the Rotor-Hamiltonian	34
4.2.1	Fourier Transformation of the kinetic part	35
4.2.2	Fourier Transformation of the interaction parts	37
4.2.3	The Fourier transformed Rotor-Hamiltonian	38
4.3	Diagonalization of the Rotor-Hamiltonian	38
4.4	Calculation of the Instability	41
4.5	Calculating the number of particles	44
4.5.1	Calculation of the mean-field number fluctuations	46
4.6	Calculating the energy of the new groundstate	47

4.6.1	Calculation of \bar{c} and \bar{d}	49
4.7	Calculation of the phase transition	51
4.8	Supersolid Phase	54
4.9	Validity for the mean-field theory	56
5	Stability of the supersolid phase	59
5.1	Rotor-Hamiltonian in real space	59
5.1.1	Analysis of the linear order in Δn_i	63
5.1.2	Comparing the Hamiltonians	65
5.1.3	Calculating the mean-field part	68
5.1.4	The final Rotor-Hamiltonian in real space	69
5.2	Fourier Transformation of the Rotor-Hamiltonian	70
5.2.1	Fourier Transformation Part1	70
5.2.2	Fourier Transformation Part2	72
5.2.3	Fourier Transformation Part3	74
6	Experimental Realization	81
6.1	Energy of the BEC in a trap	81
6.2	Calculation of U, V, t	83
6.2.1	Calculation of the on-site interaction U	83
6.2.2	Calculation of the nearest-neighbor interaction V	85
6.2.3	Expressing the Instability	88
6.2.4	The hopping term t	90
6.3	Experimental Proposal	90
7	Summary & Outlook	93
A	Sortation of Rotor-Hamiltonian	95
B	Calculations of Chapter 5	97
B.1	Computing $2n$	97
B.2	Calculation of U_0	98
B.3	Calculation of U_1	99
	Bibliography	101
	Acknowledgements	105

List of Figures

2.1	Different optical lattices	9
2.2	Description of an optical lattice	10
2.3	Mott Insulator and Superfluid in an optical lattice	13
2.4	Dependence of hopping t and on-site interaction U on depth of optical lattice V_0	14
2.5	Phasediagram of the Bose-Hubbard Model	15
2.6	Possible cloud shapes of dipolar BEC	18
2.7	Number of particles in condensate depending on scattering length and trap shape	20
2.8	Stability diagram for a dipolar BEC	20
4.1	Dispersion relations in mean-field theory	43
4.2	Energy density e_g at phase transition	53
4.3	Supersolid phase on an optical lattice	55
4.4	Comparison of the scaling behaviors	57
5.1	Dispersion relation of the supersolid phase in 1D	79
6.1	BEC confined in cylindrical shaped trap	83
6.2	Two BECs confined in two traps	85

Chapter 1

Introduction

A solid is characterized by a periodic structure, i.e. a long-range ordering of atoms. This ordering forms a lattice, where each lattice site is occupied by one or more atoms. Depending on the solid, one or more lattice sites form the basis of it. The solid is then simply formed by adding a number of basis together, see [28].

On the other hand, superfluidity is characterized by a frictionless flow of particles. This means, that the flow of particles does not suffer an energy loss due to friction, see [2]. The arising question now is, are the properties of a solid and the superfluid flow compatible? Theoretical thoughts, on behalf to this question, were made by Leggett [33], Chester [13] and Guyer [21]. They proposed, that these two possible properties of a system can only be compatible, if the system has diagonal and off-diagonal elements in its reduced density matrix. Diagonal elements in the reduced density matrix refers to a crystalline, solid structure, i.e. diagonal long-range order, where off-diagonal elements are a sign of superfluidity. The concept of diagonal and off-diagonal long-range order were introduced by Penrose and Onsager [39], and Yang [57].

The following question then is: Does a solid with superfluid properties exist in nature? A natural candidate for such properties would be solid ^4He . Despite this proposal for a candidate, the question of the existence of a superfluid solid was answered for a long time with no. For many years the answer stayed negative, until Kim and Chan [25] did their experiment with solid ^4He . They showed an indication of non-classical rotational inertia. Leggett proposed in 1970 [33] that non-classical rotational inertia is the first signature of the compatibility of a solid structure and superfluidity. The experiment and discovery of Kim and Chan are still highly debated by the community. This means, that a rigorous proof of the existence of a superfluid solid in nature is still due.

Possible candidates for such experiments are cold atomic gases, since they offer a wide range of applications, especially when loaded into an optical lattice. Gases are referred to be cold, if they are in a temperature regime of micro (10^{-6}) to nano (10^{-9}) Kelvin or lower. Often alkali atoms like lithium Li, rubidium Rb and cesium Cs are cooled to such temperatures. Other common atoms used for cooling are chromium Cr and helium He. In principle, all atoms or even some molecules like LiCs, CaO and SrF, can be cooled to the desired temperature regime. Possible applications for cold gases are e.g. high precession measurements, investigation of new quantum phases and many more. The most prominent example of the application of cold gases is the experimental realization of the Mott Insulator to superfluid transition done in 2002 by Greiner *et.al.* [19].

Further introductions into the field of BECs and possible phases in optical lattices can be found in [15], [36], [17], [16], [54], [7], [23], [30]. For more insight into supersolids, confront [10], [56], [40], [49], [5], [46], [41], [47], [4], [37], [6]. For the subject of cold gases, [9] can also be taken into account.

The motivation for the presented work is the following: Until now, the superfluid and Mott Insulator quantum phase have been achieved in experiments. Still due is to proof the existence of the supersolid within an experiment. So far, calculations for the supersolid phase have been done with low filling factors n at each lattice site of an optical lattice. In this work, we consider a regime, where we assume to have a high filling factor $n \gg 1$ at each lattice site. This is a totally different approach and therefore we want to investigate, if the supersolid phase even occurs in that regime.

The work is structured as follows: In chapter 2 we give the tools to understand the discussions in the following chapters and give some insight into the field of cold gases. Then, in chapter 3 we begin our calculations for a system of a dilute Bose gas and investigate the superfluid phase there. Within chapter 4 we investigate rigorously various considerations relevant to mean-field calculations. Then chapter 5 concludes the preceded chapters by the stability determination of the proposed new phase. In the last chapter 6 of this work, we consider an experimental setup to achieve the argued situations within an experiment.

Chapter 2

Basic concepts

In recent years, the technique of loading Bose-Einstein condensates (BEC) into optical lattices has opened up new and interesting physics. The following sections will give an introduction to the required tools.

2.1 Optical lattice

An optical lattice is a periodic potential, which is generated by overlapping two counterpropagating laser beams. The periodic structure is due to the interference between these two laser beams, resulting in an optical standing wave with a periodicity of $\lambda/2$. Atoms can now be confined in the standing wave. Depending on how many laser beams are used, different lattice structures can be realized. Using two laser beams reveals a 1D optical lattice, which looks like stacked pancakes, see figure 2.1. Using four superimposed orthogonal laser beams gives a 2D lattice, containing of 1D potential tubes and six laser beams gives a 3D simple cubic lattice, where each lattice site confines atoms in a harmonic oscillator potential.

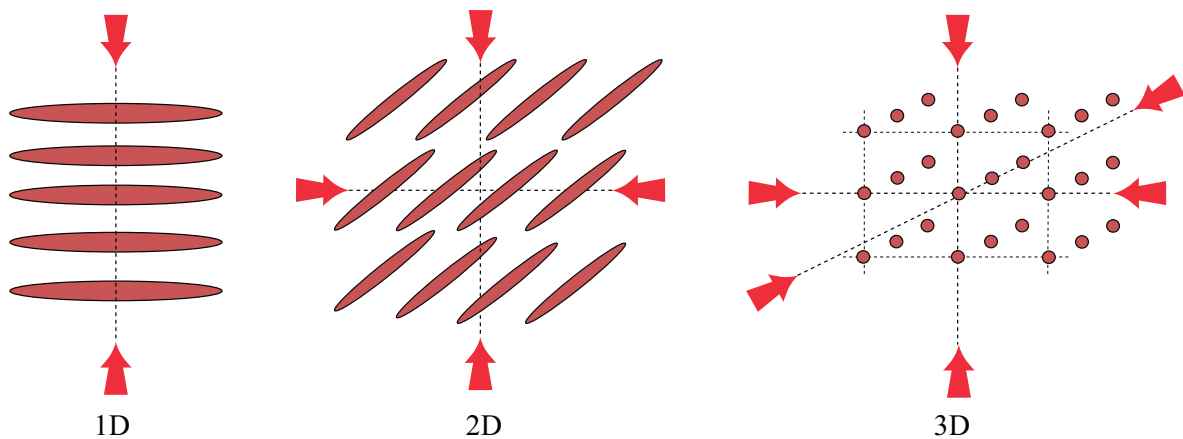


Figure 2.1: Depending on how many counterpropagating laser beams are used, one, two or three dimensional optical lattices can be created.

The optical lattice, i.e. the standing wave, can be described approximately as the sum of a homogeneous periodic lattice potential

$$V_{lat}(x, y, z) = V_0 (\sin^2(kx) + \sin^2(ky) + \sin^2(kz)) = V_{lat}(\mathbf{r}), \quad (2.1)$$

with V_0 being the depth of the potential and $k = 2\pi/\lambda$ is the wave vector of the laser beam. In addition, the harmonic potential at each lattice site can be described as

$$V_{site}(x, y, z) = \frac{m}{2} (\omega_x^2 x^2 + \omega_y^2 y^2 + \omega_z^2 z^2) = V_{site}(\mathbf{r}), \quad (2.2)$$

where m is the mass of the confined atoms and $\omega_{x,y,z}$ are the trapping frequencies in the corresponding direction. See also figure 2.2.

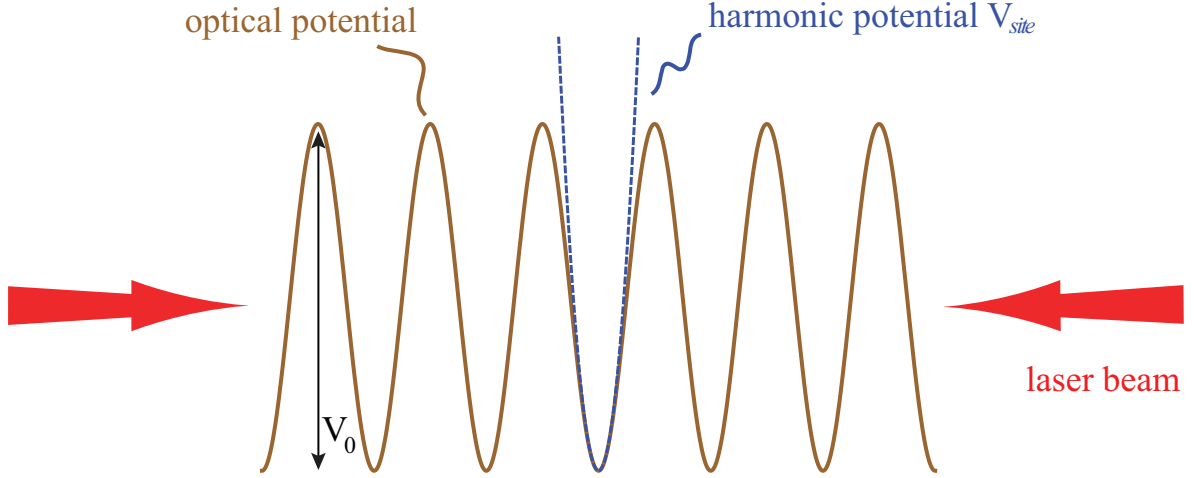


Figure 2.2: An optical lattice is created by counterpropagating laser beams. It is described as a standing wave, where each valley can be approximated with a harmonic potential. V_0 tunes the depth of the optical lattice.

This gives an approximation for the confining potential of the atoms in the BEC

$$V(x, y, z) = V_0 (\sin^2(kx) + \sin^2(ky) + \sin^2(kz)) + \frac{m}{2} (\omega_x^2 x^2 + \omega_y^2 y^2 + \omega_z^2 z^2) = V(\mathbf{r}). \quad (2.3)$$

2.2 Bose-Hubbard Model

As a next step a model is required, which can describe a BEC in an optical lattice. Jaksch *et.al.* [22] proposed, that the known Bose-Hubbard model can be applied to describe this situation.

The starting point is a Hamiltonian for interacting bosonic particles in a trapping potential $V(\mathbf{r})$ as described above

$$\mathbf{H} = \int d\mathbf{r} \psi^\dagger(\mathbf{r}) \left(-\frac{\hbar^2}{2m} \nabla^2 + V(\mathbf{r}) \right) \psi(\mathbf{r}) + \frac{1}{2} \frac{4\pi a_s \hbar^2}{m} \int d\mathbf{r} \psi^\dagger(\mathbf{r}) \psi^\dagger(\mathbf{r}) \psi(\mathbf{r}) \psi(\mathbf{r}), \quad (2.4)$$

where $\psi(\mathbf{r})$ are bosonic field operators, a_s the s-wave scattering length, m is the mass of the atoms and $V_T(\mathbf{r})$ is an additional potential.

Assuming that energies in the system are much smaller than the first excited state, i.e. excitations to higher bands can be neglected, only the lowest Bloch band is considered. In the following an ansatz for the field operators with Wannier functions $w(\mathbf{r} - \mathbf{r}_i)$ is introduced, since they are well localized at each lattice site i ,

$$\psi(\mathbf{r}) = \sum_i b_i w(\mathbf{r} - \mathbf{r}_i) , \quad (2.5)$$

and

$$\psi^\dagger(\mathbf{r}) = \sum_i b_i^\dagger w^*(\mathbf{r} - \mathbf{r}_i) . \quad (2.6)$$

The Wannier functions $w(\mathbf{r} - \mathbf{r}_i)$ are defined by the Fourier transformation of Bloch wave functions $\phi_{n,\mathbf{q}}(\mathbf{r})$

$$w_n(\mathbf{r} - \mathbf{r}_i) = \frac{1}{\sqrt{\mathcal{N}}} \sum_{\mathbf{q}} e^{-i\mathbf{q}\cdot\mathbf{r}_i} \phi_{n,\mathbf{q}}(\mathbf{r}) , \quad (2.7)$$

where n denotes the Bloch band, q the momentum and \mathcal{N} the normalization constant. The Bloch wave functions can be written as a product of a plane wave and a function $u_{n,\mathbf{q}}(\mathbf{r})$, which has the same periodicity as the periodic potential

$$u_{n,\mathbf{q}}(\mathbf{r} + \mathbf{R}) = u_{n,\mathbf{q}}(\mathbf{r}) , \quad (2.8)$$

with \mathbf{R} being a lattice vector, this gives

$$\phi_{n,\mathbf{q}}(\mathbf{r}) = u_{n,\mathbf{q}}(\mathbf{r}) e^{i\mathbf{q}\cdot\mathbf{r}} . \quad (2.9)$$

Now the ansatz eq. (2.5) and eq. (2.6) can be inserted into the Hamiltonian eq. (2.4), which then becomes

$$H = -t \sum_{\langle i,j \rangle} (b_j^\dagger b_i + b_i^\dagger b_j) + \sum_i \epsilon_i b_i^\dagger b_i + \frac{U}{2} \sum_i b_i^\dagger b_i^\dagger b_i b_i \quad (2.10)$$

where the hopping coefficient t between nearest neighboring sites, the energy offset ϵ_i and the on-site interaction U of each lattice site are calculated as

$$t = \int d\mathbf{r} w^*(\mathbf{r} - \mathbf{r}_i) \left[-\frac{\hbar^2}{2m} \nabla^2 + V_{lat}(\mathbf{r}) \right] w(\mathbf{r} - \mathbf{r}_j) , \quad (2.11)$$

$$\epsilon_i = \int d\mathbf{r} V_{site}(\mathbf{r}) |w(\mathbf{r} - \mathbf{r}_i)|^2 , \quad (2.12)$$

$$U = \frac{4\pi a_s \hbar^2}{m} \int d\mathbf{r} |w(\mathbf{r})|^4 , \quad (2.13)$$

with $V_{lat}(\mathbf{r})$ as in eq. (2.1) and $V_{site}(\mathbf{r})$ as in eq. (2.2).

The creation b_i^\dagger and annihilation b_i operators obey the commutation relation

$$[b_i, b_j^\dagger] = \delta_{ij}. \quad (2.14)$$

Introducing the number operator

$$\hat{n}_i = b_i^\dagger b_i, \quad (2.15)$$

the Hamiltonian of eq. (2.10) finally becomes the well-known Bose-Hubbard Hamiltonian

$$H = -t \sum_{\langle i, j \rangle} (b_j^\dagger b_i + b_i^\dagger b_j) + \sum_i \epsilon_i \hat{n}_i + \frac{U}{2} \sum_i \hat{n}_i (\hat{n}_i - 1). \quad (2.16)$$

The first term of the Bose-Hubbard Hamiltonian describes the hopping of bosons between neighboring sites, i.e. the tunneling of bosons. The hopping term t determines the strength of the hopping between the sites. The second term, the energy offset ϵ_i is zero for a homogeneous system. The third term describes the interaction of n bosons with $n - 1$ other bosons at the same lattice site. In this case, U determines the repulsion strength between atoms.

2.2.1 Extended Bose-Hubbard Hamiltonian

The Hamiltonian eq. (2.16) can be extended for the case of arbitrary interactions and for a grand canonical ensemble. It then reads

$$H = -t \sum_{\langle i, j \rangle} (b_j^\dagger b_i + b_i^\dagger b_j) + \sum_i \epsilon_i \hat{n}_i + \frac{U}{2} \sum_i \hat{n}_i (\hat{n}_i - 1) + \frac{1}{2} \sum_{i \neq j} V_{ij} \hat{n}_i \hat{n}_j - \mu \sum_i \hat{n}_i, \quad (2.17)$$

the fourth term accounts the nearest-neighbor interactions, where V_{ij} goes over to V when only nearest-neighbor interactions are considered. The fifth term consists the chemical potential μ , which fixes the mean number of particles in the case of a grand canonical ensemble.

When only nearest-neighbor interactions and a homogeneous system is considered, the extended Bose-Hubbard Hamiltonian reads

$$H = -t \sum_{\langle i, j \rangle} (b_j^\dagger b_i + b_i^\dagger b_j) + \frac{U}{2} \sum_i \hat{n}_i (\hat{n}_i - 1) + \frac{V}{2} \sum_{\langle i, j \rangle} \hat{n}_i \hat{n}_j - \mu \sum_i \hat{n}_i. \quad (2.18)$$

2.3 Quantum Phase Transition

A phase transition is characterized by a change of phases when some physical quantities are tuned, e.g. water can change its phase from solid (ice), to liquid or vapor, depending on temperature and applied pressure. This means classical phase transitions are driven by thermal fluctuations. In recent years a new field of research opened up, when temperatures near $T = 0$ were reached and new physics observed. In a classical sense, all thermal fluctuations are frozen out, when $T = 0$ is reached, i.e. no classical phase transition appears at $T = 0$. If temperatures reach $T = 0$, the system becomes quantum mechanical and such effects as the Heisenberg uncertainty principle come into play. The Heisenberg uncertainty principle is responsible for the appearance of quantum fluctuations, which can drive the system even at

$T = 0$ into different phases. This means quantum phase transitions at $T = 0$ are solely driven by quantum fluctuations. For a further introduction into this field see [43].

A well-known quantum phase transition is the transition of a system from the Mott Insulator to the superfluid ground state.

2.3.1 Mott Insulator - Superfluid Transition

The Bose-Hubbard Hamiltonian eq. (2.16) describes a quantum system, which contains an optical lattice that can confine atoms, which are in a BEC. The two main quantities are the hopping t eq. (2.11) and the on-site interaction U eq. (2.13). The hopping term in eq. (2.16) tends to delocalize the bosons over the lattice, where the on-site interaction term tends to localize the bosons to a lattice site. The two quantities t and U are in competition with each other. In the superfluid ground state the hopping t is much larger than the on-site interaction U , meaning that a hopping of bosons through the lattice sites, i.e. delocalization, is favorable. In the Mott Insulator ground state, the hopping t is suppressed by a larger on-site interaction U , where a integer filling of lattice sites is preferred and no hopping. See also figure 2.3.

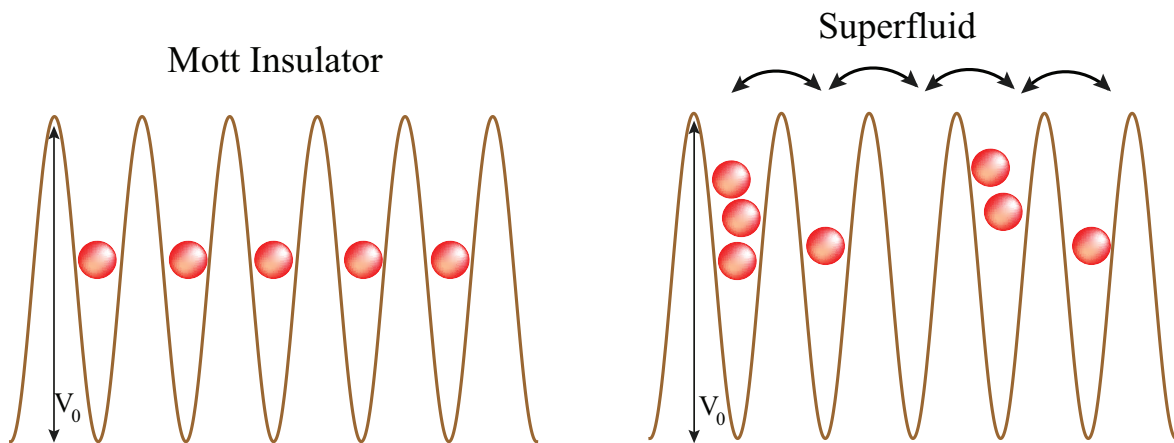


Figure 2.3: **Left figure:** Mott Insulator, each boson is confined to a lattice site. The hopping between different lattice sites is suppressed by the depth of the optical potential. **Right figure:** Superfluid, the boson can hop freely between lattice sites, without being constraint to a certain lattice site. In this case a delocalization of the boson over the lattice is favored.

The tunable quantity in this system is the depth of the optical potential V_0 as introduced in eq. (2.1). With a low V_0 the bosons can easily overcome the potential barrier V_0 and hop through the lattice, i.e. tunnel between lattice sites. It is not energetically favorable to localize the bosons to specific lattice sites, since the cost of kinetic energy is low compared to the on-site interaction U . As the depth of the potential V_0 is raised, the cost of hopping nearly free through the lattice increases. At a critical value $(U/t)_c = z \cdot 5.8$ the transition between the superfluid ground state to the Mott Insulator ground state occurs, where z is the number of nearest neighbors. The cost in energy for hopping is now much higher than the localization of each boson to a lattice site. In this regime, the on-site interaction term in eq. (2.16) becomes dominant and pins each lattice site with an integer filling of bosons, also see figure 2.4.

For larger fillings $n \gg 1$, the critical value is $(U/t)_c = z \cdot 4n$, where n is the mean number of atoms, see also figure 2.5.

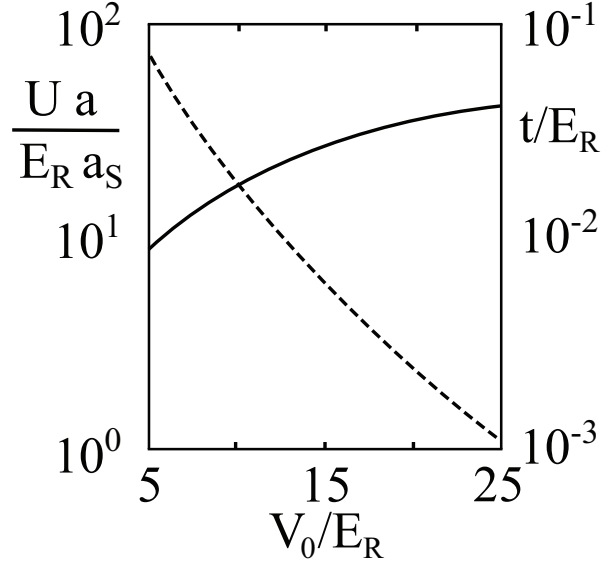


Figure 2.4: Dependence of the hopping term t and the on-site interaction U on the depth of the optical lattice V_0 . At low values for V_0 the hopping in the system is dominant. The bosons are delocalized over the lattice, the system is in the superfluid phase. As the depth is raised, hopping becomes suppressed and the bosons become localized to a certain lattice site. In this case, it becomes much harder to overcome the barrier created by V_0 . The system then is transferred into the Mott Insulator phase, with an integer filling of each lattice site. Diagram is qualitatively taken from [22].

The Bose-Hubbard phase diagram for the superfluid to Mott Insulator transition is given in figure 2.5. The lobes at integer filling n are characteristic for the Mott Insulator. In the regions outside of the Mott lobes, the system is superfluid. The critical value $(t/U)_c$ corresponds to the tip of each Mott lobe. For higher fillings n , the critical value $(t/U)_c$ for the transition scales as $\sim 1/n$.

With the system being in the Mott Insulator ground state, there are two possible ways to drive it into the superfluid regime. Either the hopping t is increased, beyond the critical value $(t/U)_c$ until the bosons confined to single lattice sites can easily overcome the potential barrier. Or some bosons are added to the system, which leads to non-integer filling of lattice sites and a raise in chemical potential μ . The system is then in the superfluid regime until there are more bosons added. The Mott Insulator is again achieved, if the filling results in an integer value per lattice site and the hopping t is lowered.

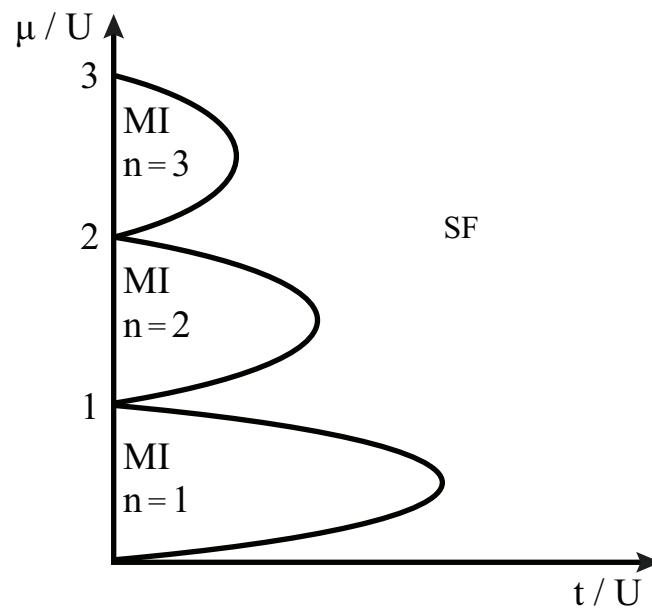


Figure 2.5: Phasediagram of the Mott Insulator to Superfluid transition in the Bose-Hubbard Model. μ is the chemical potential given in units of the on-site interaction energy U and t the hopping term in units of U . The characteristic Mott lobes for different filling factors n per lattice site i is given. See also [7].

2.3.2 Supersolid Phase

Another interesting quantum phase is the supersolid. This kind of phase is characterized by a solid-like crystalline long-range ordering and the existence of superfluidity. The notation "supersolid" refers to the two properties of the phase. The existence was proposed by Leggett [33] and Chester [13], that a solid can also exhibit superfluidity and has been discussed controversial.

To describe a solid structure, the number density $\rho(\mathbf{r})$ has to be considered. Here \mathbf{r} denotes the position vector in the solid structure. The solid is described by a peak structure in the number density, since particles can only be found on certain sites within the structure. This can be expressed as

$$\rho(\mathbf{r}) = \sum_{\mathbf{1}} \delta(\mathbf{r} - \mathbf{R}_{\mathbf{1}}) , \quad (2.19)$$

where $\mathbf{R}_{\mathbf{1}}$ considers all possible lattice sites.

A fluid or superfluid can be described by the one particle density matrix

$$\rho_1(\mathbf{r}, \mathbf{r}') = N \int dr_2 dr_3 \dots dr_N \rho^*(r, r_2 \dots r_N) \rho(r', r_2 \dots r_N) , \quad (2.20)$$

where N is a normalization constant. It gives the density of two different coordinates \mathbf{r} and \mathbf{r}' . A superfluid is translational invariant, therefore the density matrix $\rho(\mathbf{r}, \mathbf{r}')$ can be written as $\rho(\mathbf{r} - \mathbf{r}')$. Now, the nature of two far apart positions within the superfluid system is investigated

$$\rho(\mathbf{r} - \mathbf{r}') \xrightarrow{\mathbf{r} - \mathbf{r}' \rightarrow \infty} const. . \quad (2.21)$$

This means, that at every position between \mathbf{r} and \mathbf{r}' the system has a constant value in its density. Thus, no peak structure can be found within a superfluid system, the density is constant.

To give a short summary, a solid is described by a peak structured number density $\rho(\mathbf{r})$, whereas a superfluid has a constant value in its density, if two far apart positions \mathbf{r} and \mathbf{r}' are analyzed. For a more rigorous introduction into this subject, see [12]. In the following, a more detailed description is given.

A crystalline solid is characterized by a diagonal long-range order (DLRO) in its density matrix. A solid is a many-particle system which is defined by a many-particle wave function $\Psi_k(\mathbf{r}_1, \mathbf{r}_2, \dots, \mathbf{r}_N)$, where k denotes the state and $\mathbf{r}_1 \dots \mathbf{r}_N$ the position. For the further considerations, it is assumed, that the system is in its ground state, thus the many-particle wave function becomes $\Psi_0(\mathbf{r}_1, \mathbf{r}_2, \dots, \mathbf{r}_N)$. The diagonal many-particle density matrix is defined as the square of the wave function and gives the probability density for finding a particle at position \mathbf{r}_j

$$\rho_N(\mathbf{r}_1, \mathbf{r}_2, \dots, \mathbf{r}_N) = |\Psi_0(\mathbf{r}_1, \mathbf{r}_2, \dots, \mathbf{r}_N)|^2 , \quad (2.22)$$

the diagonal density matrix ρ_N is normalized, thus a integral over all positions gives unity

$$1 = \int d^3r_1 \dots d^3r_N \rho_N(\mathbf{r}_1, \mathbf{r}_2, \dots, \mathbf{r}_N) . \quad (2.23)$$

Now the concept of superfluidity and off-diagonal long-range order (ODLRO) is given. A general density matrix is defined as the product of two wave functions with different coordinates

$$\tilde{\rho}_N(\mathbf{r}_1, \mathbf{r}_2, \dots, \mathbf{r}_N; \mathbf{r}'_1, \mathbf{r}'_2, \dots, \mathbf{r}'_N) = \Psi_0^*(\mathbf{r}_1, \mathbf{r}_2, \dots, \mathbf{r}_N) \Psi_0(\mathbf{r}'_1, \mathbf{r}'_2, \dots, \mathbf{r}'_N), \quad (2.24)$$

where again the system is assumed to be in its ground state with $\mathbf{k} = 0$. If the two sets of coordinates are identical, the general density matrix $\tilde{\rho}_N$ becomes the diagonal density matrix ρ_N of eq. (2.22).

The one-particle density matrix $\tilde{\rho}_1(\mathbf{r}_1, \mathbf{r}'_1)$ is obtained, when all but one set of coordinates in $\tilde{\rho}_N$ eq. (2.24) are set equal and integrated over

$$\tilde{\rho}_1(\mathbf{r}_1, \mathbf{r}'_1) = \int d^3r_2 d^3r_3 \dots d^3r_N \tilde{\rho}_N(\mathbf{r}_1, \mathbf{r}_2, \dots, \mathbf{r}_N; \mathbf{r}'_1, \mathbf{r}_2, \dots, \mathbf{r}_N). \quad (2.25)$$

A system is superfluid, i.e. Bose condensed, if the density matrix $\tilde{\rho}_1$ eq. (2.25) has an eigenvalue which is proportional to the number of atoms in the system.

The condensate fraction in the ground state $n_{\mathbf{k}=0}$, i.e. the number of particles, is calculated as

$$n_0 = \frac{1}{\nu} \int d^3r_1 d^3r'_1 \tilde{\rho}_N(\mathbf{r}_1, \mathbf{r}'_1), \quad (2.26)$$

with ν being the system volume.

A system is called to have an ODLRO, if the condensate fraction n_0 has a value greater than zero. This implies that a system which has ODLRO in its ground state is superfluid. Thus, Bose-Einstein condensation is the simplest form of an ODLRO in the density matrix $\tilde{\rho}_N$ eq. (2.24), see also [34] for an introduction into ODLRO.

Hence the supersolid phase has to have a diagonal and off-diagonal long-range order in its density matrix to exhibit superfluidity and the properties of a solid.

For further insight into ODLRO see [39], [57], [52], [14], [45], [55], [58].

2.4 Rotor Model

The Bose-Hubbard Hamiltonian eq. (2.18) is only valid for small filling factors $n \geq 1$. If filling factors much larger than one are considered, i.e. $n \gg 1$, the Bose-Hubbard Hamiltonian becomes inaccurate. For this case a new Hamiltonian has to be found, which then can describe the system.

If each lattice site contains many bosons, it can be considered, that each lattice holds a Bose-Einstein condensate of its own. This means that the bosons within each lattice site can now be described by a macroscopic wave function, with a defined phase φ and a particle density n . Under these assumptions the following ansatz for the creation and annihilation operators for the bosons can be made

$$\begin{aligned} b_i &= \sqrt{n_i} e^{i\varphi_i}, \\ b_i^\dagger &= \sqrt{n_i} e^{-i\varphi_i}. \end{aligned} \quad (2.27)$$

This means that each lattice site contains a quasi-condensate with a particle density n_i and a defined phase φ_i .

Inserting the ansatz eq. (2.27) into the Bose-Hubbard Hamiltonian eq. (2.18) and applying once more the commutation relation for bosonic operators eq. (2.14), at the on-site interaction term, reveals the Hamiltonian in the Rotor-Model

$$H_{Rotor} = -2t \sum_{\langle i,j \rangle} \sqrt{n_i n_j} \cos(\varphi_i - \varphi_j) + \frac{U}{2} \sum_i n_i^2 + \frac{V}{2} \sum_{\langle i,j \rangle} n_i n_j - \mu \sum_i n_i. \quad (2.28)$$

See chapter 4 for a rigorous derivation of the Rotor-Hamiltonian.

The presented Hamiltonian eq. (2.28) in the Rotor-Model is valid for higher filling factors n , where $n \gg 1$. For a filling factor $n \approx 1$ it becomes invalid, because each lattice site is no longer populated by many particles. A description of each lattice site, containing a quasi-condensate, expressed by a macroscopic wave function, becomes invalid. Hence, it depends on the filling factor n , if the Rotor-Hamiltonian H_{Rotor} eq. (2.28) or the Bose-Hubbard Hamiltonian H eq. (2.18) can be applied.

The Rotor-Hamiltonian is related to the topic of Josephson Junction arrays, see [24], [8], [42],[11], [48], for an introduction into this field. The concept of quasi-condensates is introduced in [35], [50].

2.5 ^{52}Cr Experiments

The properties of chromium (^{52}Cr) atoms and possible applications are under high investigations by the group of Tilman Pfau at the University of Stuttgart.

In 2005 they first reported of the experimental realization of a BEC of chromium [20]. Before that, only BECs of alkali atoms have been achieved, where the atoms mainly interact via an effective contact interaction. The interesting feature of chromium is its very high magnetic moment of $6 \mu_B$ (μ_B is the Bohr magneton) and therefore its significant long-range and anisotropic dipole-dipole interaction. In their experiment, a pure dipolar BEC with up to 10^5 atoms was achieved, where the magnetic dipole-dipole interactions play a dominant role.

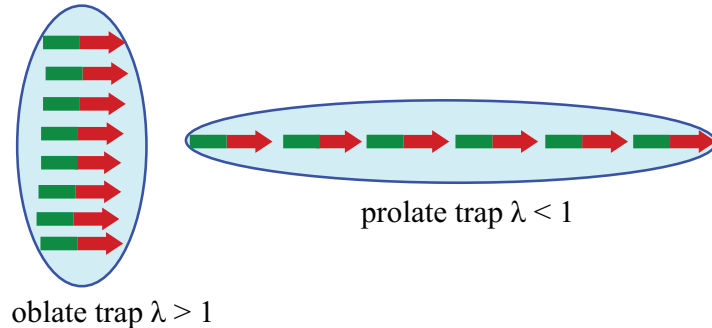


Figure 2.6: Possible cloud shapes for a dipolar BEC. The left figure shows a oblate, pancake shaped trap. The right a prolate, cigar shaped trap.

As a next step, they investigated the influence of the dipole-dipole interaction on the behavior of the dynamics of the chromium BEC [51], [31]. They applied a homogeneous magnetic field to the BEC and found that the atoms align along the magnetization direction, which leads to a squeezed orthogonal direction. This alignment could even be seen, when the BEC was released from the trap and measured in a time of flight experiment. Further, they studied the characteristics of the BEC with strong dipolar interactions by tuning the contact interactions, via a Feshbach resonance, to be small. In the same work they used different trap sizes, by applying different magnetic fields.

Then they examined the stability of a dipolar BEC depending on the scattering length a and the trap size [27]. One conclusion was, that the stability strongly depends on the trap size. A dipolar BEC is stable, if its loaded into a pancake-shaped trap (aspect ratio $\lambda = \omega_z/\omega_r > 1$, with $\omega_{r,z}$ being the trap frequencies in r - or z -direction), because the dipoles predominantly repel each other. It becomes unstable, if the trap is cigar-shaped ($\lambda < 1$), which leads to attractive forces and thus to a collapse. Another conclusion was, that the scattering length a also plays an important role in the stability. The scattering length a is responsible for tuning the contact interaction. A scattering length $a = 0$ means, that now the pure dipolar regime is reached. The higher the value of a , the more the effect of the contact interaction is important. If the dipolar BEC is within an isotropic trap ($\lambda = 1$), it can only handle positive scattering lengths a . On the other hand, if the BEC is loaded into a pancake-shaped trap ($\lambda = 10$), it can even handle slightly negative scattering lengths a , before collapsing, see figure 2.7.

They could also give a stability diagram of a dipolar BEC, which depends on the critical scattering length a_{crit} and the trap aspect ratio λ . The critical scattering length a_{crit} determines, if the dipolar BEC is stable at a given set of trap aspect ratio and scattering length a . At aspect ratios of $\lambda \gg 1$ the scattering length can be tuned to $a = 0$, which leads to the pure dipolar regime, without the BEC collapsing, see figure 2.8.

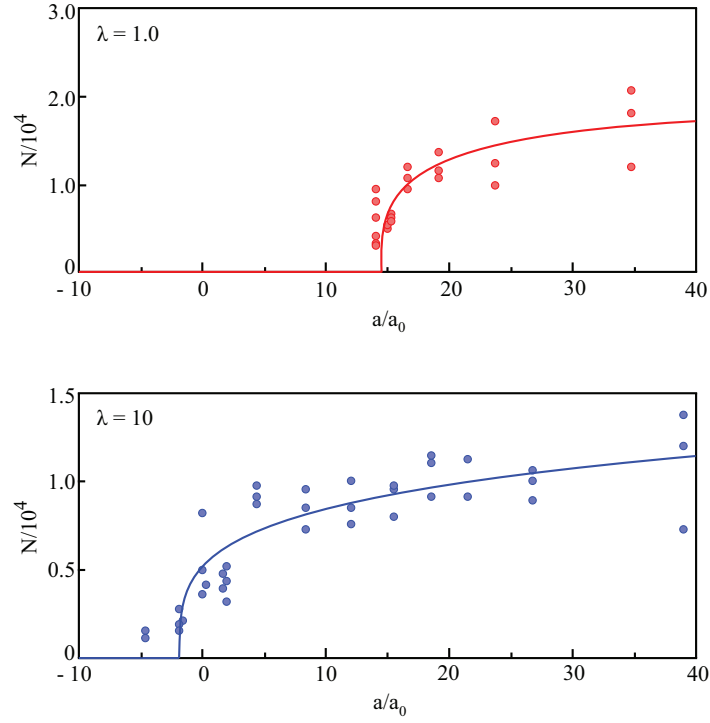


Figure 2.7: Number of particles in a dipolar condensate at given trap ratios λ and tuning the scattering length a . In the above figure, the trap is prolate. The dipolar BEC collapses at a positive scattering length a . The bottom figure shows that the collapse of a BEC, within an oblate trap, occurs at slightly negative scattering lengths. The figure is qualitatively taken from [27].

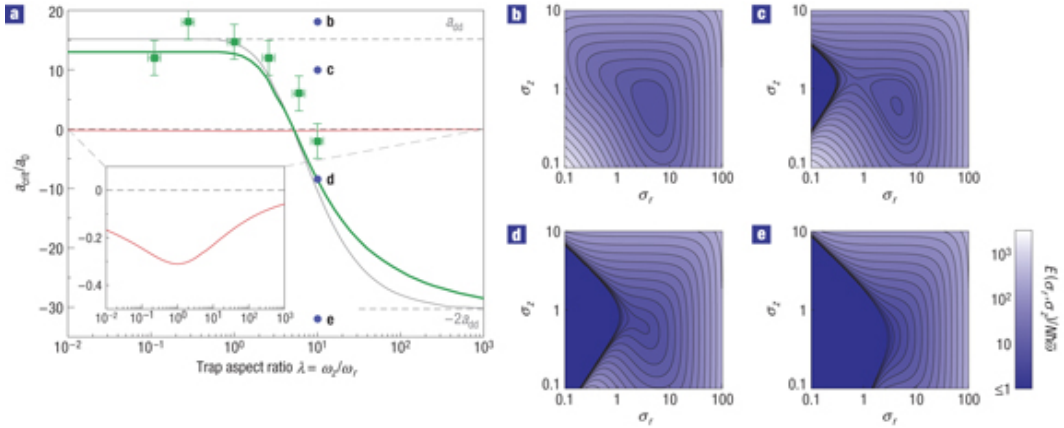


Figure 2.8: Stability diagram of a dipolar BEC. The stability at different scattering lengths a depends strongly on the trap aspect ratio λ . At a cigar shaped trap, $\lambda < 1$, the BEC can only handle positive scattering lengths before collapsing. Within a pancake shaped trap, $\lambda \gg 1$, the BEC can even handle negative scattering lengths before collapsing. In the region above the green curve, the dipolar BEC is stable, beneath it, it becomes unstable and collapses. On the right side of the figure, there are the energy planes, for different scattering lengths. The figure is taken from [27].

Chapter 3

Bogoliubov theory

In the theory of a dilute Bose gas, the interactions between particles are relatively small. Only s-wave scattering processes between particles are considered. Further, the scattering can be regarded as isotropic and triple collisions are neglected. The interaction between particles is assumed to be repulsive, i.e. the scattering amplitude a_S is positive.

Bogoliubov was the first, who found the energy spectrum for such a system at $T = 0$. For sake of simplicity, he assumed that the particles in the Bose gas have spin zero. In [1] a detailed introduction to the theory of a dilute Bose gas can be found.

The following calculation is carried out similarly as in [1], whereas here, nearest-neighbor interactions V are accounted.

3.1 Fourier transformation of the Bose-Hubbard Hamiltonian

For calculating the energy spectrum $\varepsilon(k)$ as in [1] of a dilute Bose gas, the first step is to Fourier transform the following Hamiltonian

$$H = -t \sum_{\langle i, j \rangle} (b_j^\dagger b_i + b_i^\dagger b_j) + \frac{U}{2} \sum_i \hat{n}_i \hat{n}_i + \frac{V}{2} \sum_{\langle i, j \rangle} \hat{n}_i \hat{n}_j. \quad (3.1)$$

It is the extended Bose-Hubbard Hamiltonian, as introduced in sec.2.2.1, for a canonical ensemble, i.e. $\mu = 0$. The on-site interaction U is as in eq. (2.13), V only considers nearest-neighbor interactions.

The Fourier transformations for the creation b_i^\dagger , annihilation b_i and number operator \hat{n}_i are

$$b_i^\dagger = \frac{1}{\sqrt{N}} \sum_{k'} e^{-ik'x_i} b_{k'}^\dagger, \quad (3.2)$$

$$b_i = \frac{1}{\sqrt{N}} \sum_k e^{ikx_i} b_k, \quad (3.3)$$

$$\hat{n}_i = \frac{1}{N} \sum_k e^{ikx_i} \hat{n}_k. \quad (3.4)$$

To obtain the energy spectrum from eq. (3.1), by diagonalizing it, the following simplification has to be made: In an ideal Bose gas the particles are not interacting with each other. In

a dilute Bose gas, the ground state slightly differs from that of an ideal gas, because of the weakly interactions. Although, the occupation of the ground state in a dilute gas exceeds the occupations of excited levels. In this case, only interactions of particles in the ground state of the dilute gas and particles in the weakly excited states with particles in the ground state have to be considered. Interactions of excited particles with each other are neglected.

The following sections compute the Fourier transformation of eq. (3.1).

3.1.1 Fourier transformation of the first part of the Hamiltonian

Now the first part of the Hamiltonian eq. (3.1) can be transformed, it reads

$$H_1 = -t \sum_{\langle i, j \rangle} \left(b_j^\dagger b_i + b_i^\dagger b_j \right). \quad (3.5)$$

Inserting the Fourier transformations eq. (3.2, 3.3) gives

$$\begin{aligned} H_1 &= -t \sum_{\langle i, j \rangle} \frac{1}{N} \left(\sum_{q'} e^{-iq'x_j} b_{q'}^\dagger \sum_k e^{ikx_i} b_k + \sum_{k'} e^{-ik'x_j} b_{k'}^\dagger \sum_q e^{iqx_i} b_q \right) \\ &= -\frac{t}{N} \sum_{\langle i, j \rangle} \left(\sum_{q', k} e^{-i(q'x_j - kx_i)} b_{q'}^\dagger b_k + \sum_{k', q} e^{i(qx_j - k'x_i)} b_{k'}^\dagger b_q \right). \end{aligned} \quad (3.6)$$

Since the Bose-Hubbard Hamiltonian describes the physics on an optical lattice, each lattice site x_j is accompanied by nearest-neighboring sites of x_i afar by a unity vector e_j . Using this fact gives

$$\begin{aligned} &= -\frac{t}{N} \sum_{\langle i, j \rangle} \left(\sum_{q', k} e^{-i((q'-k)x_i + q'e_j)} b_{q'}^\dagger b_k + \sum_{k', q} e^{i((q-k')x_i + q'e_j)} b_{k'}^\dagger b_q \right) \\ &= -\frac{t}{N} \sum_j \left(\sum_{q'} N e^{-iq'e_j} b_{q'}^\dagger b_{q'} + \sum_q N e^{iqe_j} b_q^\dagger b_q \right) \\ &= -t \sum_j \left(\sum_{q'} e^{-iq'e_j} b_{q'}^\dagger b_{q'} + \sum_q e^{iqe_j} b_q^\dagger b_q \right). \end{aligned} \quad (3.7)$$

The summations $\sum_{q'}$ and \sum_q run over all possible q - and q' -values, hence the summation index q' can be rewritten as q

$$\begin{aligned} &= -t \sum_{j, q} b_q^\dagger b_q (e^{-iqe_j} + e^{iqe_j}) \\ &= -2t \sum_{j, q} b_q^\dagger b_q \cos(qe_j) \\ \Rightarrow H_1 &= -4t \sum_{q, \alpha} b_q^\dagger b_q \cos(q_\alpha a). \end{aligned} \quad (3.8)$$

Depending on the dimension of the lattice, the summation index α is one for a 1D lattice, two for 2 D and three for a three dimensional lattice. For the case, where each lattice site is equidistant apart, the summation \sum_j over all possible unity vectors e_j each time gives a , a lattice constant.

3.1.2 Fourier transformation of the second part

The second part of the Hamiltonian eq. (3.1) reads

$$H_2 = \frac{U}{2} \sum_i \hat{n}_i \hat{n}_i. \quad (3.9)$$

Here, the number operators have to be Fourier transformed with eq. (3.4). In the following the symbols for the operator $\hat{}$ are omitted, since the nature of n_i is clear. The Fourier transformation of the first number operator thus is

$$\begin{aligned} n_{k_1}^{(1)} &= \sum_i e^{-ik_1 x_i} n_i \\ &= \sum_i e^{-ik_1 x_i} b_i^\dagger b_i \\ &= \sum_i e^{-ik_1 x_i} \frac{1}{\sqrt{N}} \sum_{q'} e^{-iq' x_i} b_{q'}^\dagger \frac{1}{\sqrt{N}} \sum_q e^{iq x_i} b_q \\ &= \frac{1}{N} \sum_{i, q', q} e^{-i(k_1 + q' - q)x_i} b_{q'}^\dagger b_q \\ &= \frac{1}{N} \sum_{q', q} N \delta_{(k_1 + q')_q} b_{q'}^\dagger b_q \\ \Rightarrow n_{k_1}^{(1)} &= \sum_{q'} b_{q'}^\dagger b_{q' + k_1}. \end{aligned} \quad (3.10)$$

Hence, the first number operator reads

$$n_i^{(1)} = \frac{1}{N} \sum_{k_1} e^{ik_1 x_i} n_{k_1}^{(1)} = \frac{1}{N} \sum_{k_1, q'} e^{ik_1 x_i} b_{q'}^\dagger b_{q' + k_1}. \quad (3.11)$$

The Fourier transformation of the second number operator is done identically and gives

$$n_i^{(2)} = \frac{1}{N} \sum_{k_2, q'_2} e^{ik_2 x_i} b_{q'_2}^\dagger b_{q'_2 + k_2} \quad (3.12)$$

Inserting both Fourier transformed number operators into the second part of the Hamiltonian eq. (3.9)

$$\begin{aligned} H_2 &= \frac{U}{2} \sum_i n_i^{(1)} n_i^{(2)} \\ &= \frac{U}{2N^2} \sum_{i, k_1, k_2} \sum_{q'_1, q'_2} e^{i(k_1 + k_2)x_i} b_{q'_1}^\dagger b_{q'_1 + k_1} b_{q'_2}^\dagger b_{q'_2 + k_2}, \end{aligned} \quad (3.13)$$

to sum over all lattice sites i , k_2 must be $-k_1$

$$H_2 = \frac{U}{2N^2} \sum_{k_1, k_2} \sum_{q'_1, q'_2} \delta_{-k_1 k_2} N b_{q'_1}^\dagger b_{q'_1+k_1} b_{q'_2}^\dagger b_{q'_2+k_2}. \quad (3.14)$$

The summation over all possible k_2 and renaming the variable k_1 as k gives a more compact form for the Fourier transformed second part of the Hamiltonian eq. (3.9)

$$H_2 = \frac{U}{2N} \sum_k \sum_{q'_1, q'_2} b_{q'_1}^\dagger b_{q'_1+k} b_{q'_2}^\dagger b_{q'_2-k}. \quad (3.15)$$

3.1.3 Fourier transformation of the third part

The third part of the Hamiltonian eq. (3.1) is

$$H_3 = \frac{V}{2} \sum_{\langle i, j \rangle} \hat{n}_i \hat{n}_j. \quad (3.16)$$

The Fourier transformations for both number operators are done identically as in eq. (3.10 + 3.11), the symbols for the operators are again omitted and the results are

$$n_i = \frac{1}{N} \sum_{k, k_1} e^{ikx_i} b_{k_1}^\dagger b_{k_1+k} \quad (3.17)$$

$$n_j = \frac{1}{N} \sum_{q, q_1} e^{iqx_j} b_{q_1}^\dagger b_{q_1+q}. \quad (3.18)$$

These Fourier transformed number operators can be inserted into eq. (3.16). The relation between nearest-neighboring sites, introduced in section 3.1.1 $x_j = x_i + e_j$, is also used

$$\begin{aligned} H_3 &= \frac{V}{2} \sum_{\langle i, j \rangle} \left(\frac{1}{N} \sum_{k, k_1} e^{ikx_i} b_{k_1}^\dagger b_{k_1+k} \right) \left(\frac{1}{N} \sum_{q, q_1} e^{iqx_j} b_{q_1}^\dagger b_{q_1+q} \right) \\ &= \frac{V}{2N^2} \sum_{\langle i, j \rangle} \sum_{k, k_1, q, q_1} e^{i(k+q)x_i} e^{iqe_j} b_{k_1}^\dagger b_{k_1+k} b_{q_1}^\dagger b_{q_1+q} \\ &= \frac{V}{2N^2} \sum_j \sum_{k, k_1, q, q_1} N \delta_{q-k} e^{iqe_j} b_{k_1}^\dagger b_{k_1+k} b_{q_1}^\dagger b_{q_1+q} \\ \Rightarrow H_3 &= \frac{V}{N} \sum_{k, k_1, q_1, \alpha} b_{k_1}^\dagger b_{k_1+k} b_{q_1}^\dagger b_{q_1-k} \cos(k_\alpha a) \end{aligned} \quad (3.19)$$

The summation index α again accounts for the dimensionality of the considered lattice, as introduced in section 3.1.1.

3.1.4 Fourier transformed Hamiltonian

Since now, all three parts of the Hamiltonian eq. (3.1) have been Fourier transformed. To get the whole Fourier transformation eq. (3.8, 3.12, 3.19) have to be summed. All the different summation indices can be renamed as: $q'_1 \rightarrow q$, $q'_2 \rightarrow q'$, $k_1 \rightarrow q$, $q_1 \rightarrow q'$, $q \rightarrow k$. This is for sake of simplicity and to achieve a more compact form for the following Bogoliubov Hamiltonian

$$H = -4t \sum_{k,\alpha} b_k^\dagger b_k \cos(k_\alpha a) + \frac{U}{2N} \sum_{k,q,q'} b_q^\dagger b_{q+k} b_{q'}^\dagger b_{q'-k} \underbrace{\left[1 + 2\gamma \sum_{\alpha} \cos(k_\alpha a) \right]}_{=V(k)}. \quad (3.20)$$

At renaming all the different summation indices, one has to be caution not to miss the different natures of the summations. False renaming could lead to a false behavior of the system.

3.2 Analysis of the Bogoliubov Hamiltonian

With the Hamiltonian eq. (3.1) completely Fourier transformed, the analysis of the Bogoliubov Hamiltonian eq. (3.20) can be done. For this reason different values for the indices k , q , q' are inserted. The analysis begins with the kinetic part of eq. (3.20)

$$H_{\text{kin}} = -2t \sum_{k,\alpha} \left(b_k^\dagger b_k + b_{-k}^\dagger b_{-k} \right) \cos(k_\alpha a) \quad (3.21)$$

$$k = 0 : \quad H_{\text{kin},0} = -2t \left(b_0^\dagger b_0 + b_0^\dagger b_0 \right) = -4t N_0. \quad (3.22)$$

If all the summation indices k , q , q' are set equally to zero, nearly all particles are in the ground state. This means, that the creation b_0^\dagger and annihilation operator b_0 of the ground state with $k = q = q' = 0$ can be treated as c-numbers and can be replaced by $\sqrt{N_0}$, i.e. $b_0^\dagger = b_0 = \sqrt{N_0}$. The number of particles in the ground state $\sqrt{N_0}$ is such a large number, that b_0^\dagger nearly behaves like b_0 . This justifies the replacement of b_0^\dagger and b_0 by $\sqrt{N_0}$. Further we introduce a quantity, which lets us write later equations more compact: $n_0 = N_0/N$. This quantity, n_0 , is the density of particles in the ground state, where N are the number of lattice sites.

As a next step, the interaction part of the Bogoliubov Hamiltonian eq. (3.20)

$$H_{\text{int}} = \frac{U}{2N} \sum_{k,q,q'} b_q^\dagger b_{q+k} b_{q'}^\dagger b_{q'-k} V(k), \quad (3.23)$$

is analyzed, by starting with the ground state. Here all the summation indices k , q , q' are set equally to zero. This gives the contribution of the interactions to the ground state energy, since in this case only particles in the ground state interacting with each other are considered

$$H_{\text{int},0} = \frac{U}{2N} b_0^\dagger b_0 b_0^\dagger b_0 V(0) = \frac{U}{2} N_0 n_0 V(0). \quad (3.24)$$

Hence, the energy of the ground state can be calculated by summing eq. (3.22) and eq. (3.24)

$$E_0 = -4tN_0 + \frac{U}{2} N_0 n_0 V(0) = N_0 \left(\frac{U}{2} n_0 V(0) - 4t \right). \quad (3.25)$$

Now the interaction part of the Bogoliubov Hamiltonian eq. (3.23) is further analyzed for the case of interactions between particles in an excited state and in the ground state, as reasoned in section 3.1. For this reason the values k, q, q' are chosen in such a way, that only one set of particles is in the excited state and the other set remains in the ground state

$$k = q = 0 : \quad H_{\text{int},1} = \frac{U}{2N} \sum_{q'} b_0^\dagger b_0 b_{q'}^\dagger b_{q'} V(0) = \frac{U}{2} n_0 \sum_{q'} b_{q'}^\dagger b_{q'} V(0), \quad (3.26)$$

$$q' = q = 0 : \quad H_{\text{int},2} = \frac{U}{2N} \sum_k b_0^\dagger b_k b_0^\dagger b_{-k} V(k) = \frac{U}{2} n_0 \sum_k b_k b_{-k} V(k). \quad (3.27)$$

In the next step, the annihilation operator b_{q+k} is permuted with the creation operator $b_{q'}^\dagger$. This is possible, since they act on different k values

$$[b_{q+k}, b_{q'}^\dagger] = 0. \quad (3.28)$$

With the two operators permuted, the case with $q = 0$ and $q' = k$ can be considered

$$q = 0, q' = k : \quad H_{\text{int},3} = \frac{U}{2N} \sum_k b_0^\dagger b_k^\dagger b_k b_0 V(k) = \frac{U}{2} n_0 \sum_k b_k^\dagger b_k V(k). \quad (3.29)$$

The two operators b_{q+k} and $b_{q'}^\dagger$ can now be permuted back and hence the other possible values for k, q, q' are analyzed

$$q = -k, q' = 0 : \quad H_{\text{int},4} = \frac{U}{2N} \sum_k b_{-k}^\dagger b_0 b_0^\dagger b_{-k} V(k) = \frac{U}{2} n_0 \sum_k b_{-k}^\dagger b_{-k} V(k), \quad (3.30)$$

$$q = -k, q' = k : \quad H_{\text{int},5} = \frac{U}{2N} \sum_k b_{-k}^\dagger b_0 b_k^\dagger b_0 V(k) = \frac{U}{2} n_0 \sum_k b_{-k}^\dagger b_k^\dagger V(k), \quad (3.31)$$

$$q' = k = 0 : \quad H_{\text{int},6} = \frac{U}{2N} \sum_q b_q^\dagger b_q b_0^\dagger b_0 V(0) = \frac{U}{2} n_0 \sum_q b_q^\dagger b_q V(0). \quad (3.32)$$

The terms, where the summations are carried out for the values q and q' can be renamed as summations carried out for all possible k -values. This can be done, since all possible values for q and q' are considered with a summation over k . The equations (3.26) and (3.32) then can be written as

$$H_{\text{int},1} = \frac{U}{4} n_0 V(0) \sum_k \left(b_k^\dagger b_k + b_{-k}^\dagger b_{-k} \right), \quad (3.33)$$

$$H_{\text{int},6} = \frac{U}{4} n_0 V(0) \sum_k \left(b_k^\dagger b_k + b_{-k}^\dagger b_{-k} \right). \quad (3.34)$$

It has to be kept in mind, that the number of particles in the system \bar{N} is fixed. Thus the number of particles in the ground state N_0 can be written as

$$N_0 = \bar{N} - \frac{1}{2} \sum_{k \neq 0} \left(b_k^\dagger b_k + b_{-k}^\dagger b_{-k} \right). \quad (3.35)$$

The number of particles in the ground state can now be expressed by eq. (3.35). Terms which appear linearly in N_0 can directly be expressed as \bar{N} the number of particles in the system, because N_0 is such a larger number that it is in the order of \bar{N} . Only terms which appear in quadratic order in N_0 have to be replaced by eq. (3.35). Inserting this into the ground state energy of a dilute Bose gas eq. (3.25) and keeping only linear terms in the creation and annihilation operators, thus gives

$$E_0 = \frac{U}{2N} \bar{N}^2 V(0) - \frac{U}{2N} \bar{N} \sum_{k \neq 0} \left(b_k^\dagger b_k + b_{-k}^\dagger b_{-k} \right) V(0) - 4t\bar{N} + \mathcal{O} \left(b_k^{\dagger 2}, b_k^2 \right). \quad (3.36)$$

Higher orders of creation and annihilation operators are neglected, since only weakly excited states are considered.

To finally achieve the Bogoliubov Hamiltonian for a dilute Bose gas, equations (3.21, 3.27, 3.29 - 3.31, 3.33 - 3.34) have to be summed

$$H = E' + \frac{1}{2} \sum_k \left\{ E'_k \left(b_k^\dagger b_k + b_{-k}^\dagger b_{-k} \right) + V'_k \left(b_k^\dagger b_{-k}^\dagger + b_{-k} b_k \right) \right\}, \quad (3.37)$$

where

$$E' = \bar{N} \left(\frac{U}{2} n V(0) - 4t \right) \quad (3.38)$$

$$E'_k = 2\epsilon_k + U n V(k) = -4t \sum_\alpha \cos(k_\alpha a) + U n \left(1 + 2\gamma \sum_\alpha \cos(k_\alpha a) \right) \quad (3.39)$$

$$V'_k = U n V(k) = U n \left(1 + 2\gamma \sum_\alpha \cos(k_\alpha a) \right), \quad (3.40)$$

and $n = \bar{N}/N$ being the particle density.

The presented Bogoliubov Hamiltonian eq. (3.37) is obviously not diagonal. To diagonalize it, a set of new operators are introduced, similarly done in [1],

$$b_k = \frac{1}{\sqrt{1 - A_k^2}} \left(\alpha_k + A_k \alpha_{-k}^\dagger \right), \quad b_k^\dagger = \frac{1}{\sqrt{1 - A_k^2}} \left(\alpha_k^\dagger + A_k \alpha_{-k} \right) \quad (3.41)$$

$$b_{-k} = \frac{1}{\sqrt{1 - A_k^2}} \left(\alpha_{-k} + A_k \alpha_k^\dagger \right), \quad b_{-k}^\dagger = \frac{1}{\sqrt{1 - A_k^2}} \left(\alpha_{-k}^\dagger + A_k \alpha_k \right) \quad (3.42)$$

where the introduced operators $\alpha_{\pm k}^\dagger$, $\alpha_{\pm k}$ are again creation and annihilation operators. The coefficient A_k has to be calculated in such a way, that the Hamiltonian eq. (3.37) becomes diagonal.

Now the introduced relations between the old operators $b_{\pm k}$, $b_{\pm k}^\dagger$ and the new operators $\alpha_{\pm k}$, $\alpha_{\pm k}^\dagger$ eq. (3.41 + 3.42) can be inserted into eq. (3.37)

$$\begin{aligned} H_\alpha = E' + \frac{1}{2} \sum_k \frac{1}{1 - A_k^2} & \left\{ (E'_k (1 + A_k^2) + 2 A_k V'_k) (\alpha_{-k}^\dagger \alpha_{-k} + \alpha_k^\dagger \alpha_k) \right. \\ & + (2 E'_k A_k + V'_k (1 + A_k^2)) (\alpha_k^\dagger \alpha_{-k}^\dagger + \alpha_k \alpha_{-k}) \\ & \left. + 2 A_k (E'_k A_k + V'_k) \right\}. \end{aligned} \quad (3.43)$$

In the next step, the coefficient A_k is determined in such a way, that the off-diagonal term $(\alpha_k^\dagger \alpha_{-k}^\dagger + \alpha_k \alpha_{-k})$ vanishes

$$\underbrace{(2 E'_k A_k + V'_k (1 + A_k^2))}_{=0} \underbrace{(\alpha_k^\dagger \alpha_{-k}^\dagger + \alpha_k \alpha_{-k})}_{\neq 0} \stackrel{!}{=} 0, \quad (3.44)$$

the operators $\alpha_{\pm k}^\dagger$, $\alpha_{\pm k}$ can not become zero, hence

$$\begin{aligned} 2 E'_k A_k + V'_k (1 + A_k^2) &= 0 \\ \Rightarrow A_k &= -\frac{E'_k}{V'_k} \pm \sqrt{\frac{E_k'^2}{V_k'^2} - 1}, \end{aligned} \quad (3.45)$$

where only one solution for A_k is kept for the further calculation

$$A_k = -\frac{E'_k}{V'_k} + \sqrt{\frac{E_k'^2}{V_k'^2} - 1}, \quad (3.46)$$

since the other solution for A_k is physically irrelevant.

With the calculated value for A_k eq. (3.46) being inserted into the not-diagonal Hamiltonian H_α eq. (3.43), the diagonal Bogoliubov Hamiltonian is obtained

$$H_\alpha = E' + \frac{1}{2} \sum_k \varepsilon(k) (\alpha_{-k}^\dagger \alpha_{-k} + \alpha_k^\dagger \alpha_k) - \frac{1}{2} \sum_k \left(E'_k - \sqrt{E_k'^2 - V_k'^2} \right). \quad (3.47)$$

The dispersion relation $\varepsilon(k)$ is hereby

$$\varepsilon(k) = \sqrt{E_k'^2 - V_k'^2}. \quad (3.48)$$

The coefficient E' is as defined in eq. (3.38), E'_k as in eq. (3.39) and V'_k as in eq. (3.40).

3.2.1 Calculation of the Instability

To calculate the instability, it is necessary, that the dispersion relation $\varepsilon(k)$ in eq. (3.47) has to vanish. A disappearing dispersion relation at a certain value of γ , the ratio between nearest-neighbor and on-site interaction, means, that the system becomes unstable at this ratio. The instability is the first sign of a phase transition to some kind of ordering of the boson. This also means, that a symmetry-breaking occurs, because there is no diagonal long-range order in the superfluid phase. At the onset of the instability, some kind of structure sets in. What we suppose this structure is, will be argued later. For the instability to happen, there has to be

$$\varepsilon(k) = \sqrt{E_k'^2 - V_k'^2} \stackrel{!}{=} 0. \quad (3.49)$$

Next, the equations (3.39) and (3.40) are inserted into eq. (3.49) and further simplified

$$\begin{aligned} 0 &= \left[\left(-4t \sum_{\alpha} \cos(k_{\alpha}a) + U n \left(1 + 2\gamma \sum_{\alpha} \cos(k_{\alpha}a) \right) \right)^2 \right. \\ &\quad \left. - \left(U n \left(1 + 2\gamma \sum_{\alpha} \cos(k_{\alpha}a) \right) \right)^2 \right]^{1/2} \\ &\quad - 2t \left(\frac{z}{2} - \sum_{\alpha} \cos(k_{\alpha}a) \right) = U n \left(1 + 2\gamma \sum_{\alpha} \cos(k_{\alpha}a) \right). \end{aligned} \quad (3.50)$$

With the simplified eq. (3.50), it can be solved for the desired ratio γ

$$\begin{aligned} -\frac{2t}{Un} \left(\frac{z}{2} - \sum_{\alpha} \cos(k_{\alpha}a) \right) &= 1 + 2\gamma \sum_{\alpha} \cos(k_{\alpha}a) \\ \gamma &= -\frac{t}{Un \sum_{\alpha} \cos(k_{\alpha}a)} \left(\frac{z}{2} - \sum_{\alpha} \cos(k_{\alpha}a) \right) - \frac{1}{2 \sum_{\alpha} \cos(k_{\alpha}a)}. \end{aligned} \quad (3.51)$$

For a further simplification, it has to be mentioned, that the number of nearest neighbors z can be expressed as

$$z = -2 \sum_{\alpha} \cos(k_{\alpha}a). \quad (3.52)$$

This is possible, because the function $-2 \sum_{\alpha} \cos(k_{\alpha}a)$ has its maximum value at the boundary of the first Brillouin zone $k = \pi/a$. Depending on the dimensionality of the lattice, \sum_{α} accounts for that, the possible values for the function $-2 \sum_{\alpha} \cos(k_{\alpha}a)$ are 2 in 1D, 4 in 2D and 6 in 3D, which is exactly the number of nearest neighboring sites in the given dimension. Inserting the relation eq. (3.52) into eq. (3.51) reveals

$$\gamma = \frac{2t}{Un} + \frac{1}{z}. \quad (3.53)$$

Hence, the system of a dilute Bose gas becomes unstable, if the ratio γ of nearest-neighbor and on-site interaction is tuned to eq. (3.53). This is the first sign of an appearance of a new possible phase in the system.

Chapter 4

Mean-field Calculations for Rotor Model

In chapter 3 the instability of the dispersion relation was calculated in a dilute Bose gas. In this regime, small filling factors $n \geq 1$ were considered. We are now interested in a regime with high filling factors, i.e. $n \gg 1$. This means, the presented Bose-Hubbard Hamiltonian eq. (2.18) becomes invalid and we have to use the Rotor-Hamiltonian H_{Rotor} eq. (2.28), as introduced in section 2.4.

4.1 Deriving the Rotor-Model

We consider a regime with high filling factors $n \gg 1$. We are interested on how the system behaves, when each lattice site i contains a particle density n_i , which is much larger than one. The particle density n_i consists out of a mean number of particles n , which is fixed, and mean-field fluctuations δn_i . The mean-field fluctuations δn_i are small compared to the mean number of particles n . The total number of particles in the system is fixed, thus the calculation is carried out in the canonical ensemble, i.e. the chemical potential $\mu = 0$.

As mentioned in section 2.4, we now carry out the derivation of the Rotor-Hamiltonian. Therefore, we start with the extended Bose-Hubbard Hamiltonian eq. (2.18) in a homogeneous system with $\mu = 0$ and transform it into a Rotor-Hamiltonian. The extended Bose-Hubbard-Hamiltonian, for our considerations, reads

$$H = -t \sum_{\langle i, j \rangle} (b_i^\dagger b_j + b_j^\dagger b_i) + \frac{U}{2} \sum_i \hat{n}_i (\hat{n}_i - 1) + \frac{1}{2} \sum_{i \neq j} V_{ij} \hat{n}_i \hat{n}_j \quad (4.1)$$

where t is the hopping parameter, b_i^\dagger the annihilation, b_i^\dagger the creation operator for particles on lattice site i or j , U the on-site interaction, \hat{n}_i the number operator for lattice site i or j and V_{ij} is the neighbor interaction. For the following calculations we only assume nearest-neighbor interactions, thus $V_{ij} \rightarrow V$.

For the further derivation, we replace each creation and annihilation operator by the following ansatz, as argued in section 2.4

$$b_i = \sqrt{n + \delta n_i} e^{i\varphi_i} \quad b_i^\dagger = \sqrt{n + \delta n_i} e^{-i\varphi_i} \quad (4.2)$$

where n is the mean number of particles per lattice site and δn_i is the mean-field fluctuation of particles at lattice site i or j . The ansatz is justified, because we consider a regime with high filling factors, thus each lattice contains a quasi-condensate, which can be described by a macroscopic wave function.

4.1.1 Calculation of the kinetic part

Now the different parts of the Bose-Hubbard Hamiltonian eq. (4.1) are transformed, by inserting the ansatz eq. (4.2). Starting with the kinetic part

$$\begin{aligned} H_1 &= -t \sum_{\langle i, j \rangle} (b_i^\dagger b_j + b_j^\dagger b_i) \\ &= -t \sum_{\langle i, j \rangle} \left[\sqrt{n + \delta n_i} e^{-i\varphi_i} \sqrt{n + \delta n_j} e^{i\varphi_j} + \sqrt{n + \delta n_j} e^{-i\varphi_j} \sqrt{n + \delta n_i} e^{i\varphi_i} \right] \\ &= -tn \sum_{\langle i, j \rangle} \sqrt{\left(1 + \frac{\delta n_i}{n}\right) \left(1 + \frac{\delta n_j}{n}\right)} \left[e^{-i(\varphi_i - \varphi_j)} + e^{i(\varphi_i - \varphi_j)} \right] \\ &= -tn \sum_{\langle i, j \rangle} \sqrt{\left(1 + \frac{\delta n_i}{n}\right) \left(1 + \frac{\delta n_j}{n}\right)} 2 \cos(\varphi_i - \varphi_j). \end{aligned} \quad (4.3)$$

Since we only consider small deviations of the neighboring phases φ_i and φ_j , the difference $\varphi_i - \varphi_j$ is small. Hence, the cosine $\cos(\varphi_i - \varphi_j)$ in eq. (4.3) can be expanded to second order

$$\cos x \approx 1 - \frac{x^2}{2}. \quad (4.4)$$

The expansion is only carried out to second order, because higher orders are irrelevant for the further calculation.

As mentioned before, the mean-field fluctuations δn_i are small compared to the mean number of particles in a lattice site n , thus, the root can be expanded to second order too

$$\sqrt{1+x} \approx 1 + \frac{x}{2} - \frac{x^2}{8}. \quad (4.5)$$

Again, the expansion is only carried out to second order, because the contributions of higher orders can be neglected.

After inserting the expansions eq. (4.4 + 4.5) into the Hamiltonian eq. (4.3), it reads

$$\begin{aligned} H_1 &= -2tn \sum_{\langle i, j \rangle} \left(1 + \frac{1}{2} \frac{\delta n_i}{n} - \frac{1}{8} \left(\frac{\delta n_i}{n} \right)^2 \right) \left(1 + \frac{1}{2} \frac{\delta n_j}{n} - \frac{1}{8} \left(\frac{\delta n_j}{n} \right)^2 \right) \\ &\quad \times \left(1 - \frac{(\varphi_i - \varphi_j)^2}{2} \right). \end{aligned} \quad (4.6)$$

For the further calculation, all terms containing δn_i in a linear order and higher order than $\mathcal{O}\{\delta n_i^2\}$ are neglected, since they only mean a chemical shift. This means, only quadratic orders in δn_i are kept. Now the above Hamiltonian eq. (4.6) becomes

$$\begin{aligned} H_1 = & -2tn \sum_{\langle i,j \rangle} \left[1 - \frac{1}{8} \left(\frac{\delta n_j}{n} \right)^2 + \frac{1}{4n^2} \delta n_i \delta n_j - \frac{1}{8} \left(\frac{\delta n_i}{n} \right)^2 \right] \\ & + tn \sum_{\langle i,j \rangle} \left[1 - \frac{1}{8} \left(\frac{\delta n_j}{n} \right)^2 + \frac{1}{4n^2} - \frac{1}{8} \left(\frac{\delta n_i}{n} \right)^2 \right] (\varphi_i - \varphi_j)^2 \end{aligned} \quad (4.7)$$

Next, all terms of the form $\delta n_i^2 (\varphi_i - \varphi_j)^2$ are neglected, because their contribution is of higher order, than we are interested in

$$\begin{aligned} H_1 = & -2tn \sum_{\langle i,j \rangle} \left[-\frac{1}{8} \left(\left(\frac{\delta n_i}{n} \right)^2 + \left(\frac{\delta n_j}{n} \right)^2 \right) \right. \\ & \left. + \frac{1}{4n^2} \delta n_i \delta n_j - \frac{1}{2} (\varphi_i - \varphi_j)^2 \right] - 2tznN. \end{aligned} \quad (4.8)$$

The summation of $\sum_{\langle i,j \rangle} 1$ was done and contributes the last term in eq. (4.8). The quantity z is the number of nearest neighbors to a certain lattice site and N is the number of lattice sites in the system.

4.1.2 Calculation of the on-site interaction part

Now the second part of the Hamiltonian eq. (4.1) is calculated, which is the on-site interaction part. Again the ansatz eq. (4.2) is inserted. The commutation relation for bosonic operators has to be applied at first, before inserting the ansatz

$$H_2 = \frac{U}{2} \sum_i \hat{n}_i (\hat{n}_i - 1) \rightarrow \frac{U}{2} \sum_i b_i^\dagger b_i^\dagger b_i b_i. \quad (4.9)$$

Then, the ansatz eq. (4.2) can be inserted

$$\begin{aligned} H_2 &= \frac{U}{2} \sum_i b_i^\dagger b_i^\dagger b_i b_i \\ &= \frac{U}{2} \sum_i (n + \delta n_i) (n + \delta n_i) \\ &= \frac{U}{2} N n^2 + \frac{U}{2} \sum_i (2n \delta n_i) + \frac{U}{2} \sum_i \delta n_i \delta n_i, \end{aligned} \quad (4.10)$$

where N is the number of lattice sites in the system. Here, once more, the part with the linear order in δn_i can be neglected, because it again means a chemical shift. With this, the second part eq. (4.10) becomes

$$H_2 = \frac{U}{2} N n^2 + \frac{U}{2} \sum_i \delta n_i \delta n_i. \quad (4.11)$$

4.1.3 Calculation of the nearest-neighbor interaction part

The third part of the Bose-Hubbard Hamiltonian eq. (4.1) is now being calculated. Again, the ansatz eq. (4.2) is inserted

$$\begin{aligned}
H_3 &= \frac{V}{2} \sum_{\langle i, j \rangle} \hat{n}_i \hat{n}_j \\
&= \frac{V}{2} \sum_{\langle i, j \rangle} (n + \delta n_i) (n + \delta n_j) \\
&= \frac{V}{2} z N n^2 + \frac{V}{2} \sum_{\langle i, j \rangle} (n (\delta n_i + \delta n_j) + \delta n_i \delta n_j), \tag{4.12}
\end{aligned}$$

where z is the number of nearest neighbors.

With the same reasoning as in sec. 4.1.2, the part with linear order in δn_i is neglected. The third part then reads

$$H_3 = \frac{V}{2} z N n^2 + \frac{V}{2} \sum_{\langle i, j \rangle} \delta n_i \delta n_j. \tag{4.13}$$

4.1.4 The Rotor-Hamiltonian

As the calculated parts of the Hamiltonians eq. (4.8, 4.11, 4.13) being summed, we get the Rotor-Hamiltonian for a system with high filling factors n

$$\begin{aligned}
H &= E_0 - 2tn \sum_{\langle i, j \rangle} \left[\frac{1}{4n^2} \delta n_i \delta n_j - \frac{1}{8} \left(\left(\frac{\delta n_i}{n} \right)^2 + \left(\frac{\delta n_j}{n} \right)^2 \right) - \frac{1}{2} (\varphi_i - \varphi_j)^2 \right] \\
&\quad + \frac{U}{2} \sum_i \delta n_i \delta n_i + \frac{V}{2} \sum_{\langle i, j \rangle} \delta n_i \delta n_j, \tag{4.14}
\end{aligned}$$

where

$$E_0 = 2tnzN \left[\frac{n}{4tz} (U + zV) - 1 \right], \tag{4.15}$$

is the energy of the ground state in this system.

At this point, it should be reminded, that we derived the Rotor-Hamiltonian eq. (4.14) out of the extended Bose-Hubbard Hamiltonian eq. (4.1) by expanding the root $\sqrt{n + \delta n_i}$ and the cosine $\cos(\varphi_i - \varphi_j)$ to second order and neglecting terms of linear order in δn_i , terms containing a mixture of $\varphi_i \cdot \delta n_i$ and terms of higher order than quadratic.

4.2 Fourier Transformation of the Rotor-Hamiltonian

With the Rotor-Hamiltonian calculated, a Fourier transformation has to be performed to reach the desired dispersion relation. Following Fourier transformations are valid for the phase φ_i and the mean-field fluctuation δn_i

$$\varphi_i = \frac{1}{\sqrt{N}} \sum_k e^{ikx_i} \varphi_k \quad , \quad \delta n_i = \frac{1}{\sqrt{N}} \sum_k e^{ikx_i} \delta n_k, \quad (4.16)$$

where the factor $1/\sqrt{N}$ is the normalization constant and N is the number of lattice sites.

With these definitions eq. (4.16), the relevant parts of the Rotor-Hamiltonian eq. (4.14) are transformed

$$(\varphi_i - \varphi_j)^2 = \frac{1}{N} \left[2 \sum_k \varphi_k \varphi_{-k} - \sum_{k,q} e^{i(kx_i - qx_j)} \varphi_k \varphi_{-q} - \sum_{k,q} e^{i(qx_j - kx_i)} \varphi_q \varphi_{-k} \right]. \quad (4.17)$$

The nearest neighboring sites x_j can be expressed as $x_j = x_i + e_j$, where e_j is an unity vector. This was introduced in section 3.1.1. Inserting this into eq. (4.17) gives

$$= \frac{1}{N} \left[2 \sum_k \varphi_k \varphi_{-k} - \sum_{k,q} \left(e^{i(k-q)x_i} \varphi_k \varphi_{-q} e^{-iqe_j} + e^{-i(k-q)x_i} \varphi_q \varphi_{-k} e^{iqe_j} \right) \right]. \quad (4.18)$$

The next relevant parts of the Rotor-Hamiltonian eq. (4.14) are

$$\delta n_i \delta n_j = \frac{1}{N} \sum_{k',q'} e^{i(k'x_i + q'x_j)} \delta n_{k'} \delta n_{q'} \quad (4.19)$$

$$= \frac{1}{N} \sum_{k',q'} e^{i(k'+q')x_i} e^{iq'e_j} \delta n_{k'} \delta n_{q'}, \quad (4.20)$$

and

$$\begin{aligned} \delta n_i \delta n_i &= \frac{1}{N} \sum_k e^{ikx_i} \delta n_k \sum_q e^{iqx_i} \delta n_q \\ &= \frac{1}{N} \sum_{k,q} e^{i(k+q)x_i} \delta n_k \delta n_q. \end{aligned} \quad (4.21)$$

4.2.1 Fourier Transformation of the kinetic part

Now these Fourier transformations can be inserted into the Rotor-Hamiltonian parts eq. (4.8, 4.11, 4.13) to compute the corresponding parts in k -space.

We begin with the kinetic part eq. (4.8)

$$\begin{aligned}
H_1 &= -2tn \sum_{\langle i, j \rangle} \left[\frac{1}{4n^2} \left(\frac{1}{N} \sum_{k', q'} e^{i(k'+q')x_i} e^{iq'e_j} \delta n_{k'} \delta n_{q'} \right) \right. \\
&\quad - \frac{1}{8n^2} \left(\frac{1}{N} \sum_{k, q} e^{i(k+q)x_i} \delta n_k \delta n_q \right) - \frac{1}{8n^2} \left(\frac{1}{N} \sum_{k', q'} e^{i(k'+q')x_j} \delta n_{k'} \delta n_{q'} \right) \\
&\quad \left. - \frac{1}{2N} \left(2 \sum_k \varphi_k \varphi_{-k} - \sum_{k, q} \left(e^{i(k-q)x_i} \varphi_k \varphi_{-q} e^{-iqe_j} + e^{-i(k-q)x_i} \varphi_q \varphi_{-k} e^{iqe_j} \right) \right) \right] \\
&\quad - 2tnzN \\
&= -2tn \sum_j \left[\frac{1}{4n^2 N} \sum_{k', q'} N \delta_{-k' q'} e^{iq'e_j} \delta n_{k'} \delta n_{q'} \right. \\
&\quad - \frac{1}{8n^2 n} \sum_{k, q} N \delta_{-k q} \delta n_k \delta n_q - \frac{1}{8n^2 N} \sum_{k', q'} z e^{i(k'+q')x_j} \delta n_{k'} \delta n_{q'} \\
&\quad \left. - \frac{1}{2N} \left(2 \sum_k N \varphi_k \varphi_{-k} - \sum_{k, q} N \delta_{k q} e^{-iqe_j} \varphi_k \varphi_{-q} - \sum_{k, q} N \delta_{k q} e^{iqe_j} \varphi_q \varphi_{-k} \right) \right] - 2tnzN \\
&= -2tn \left[\frac{1}{4n^2} \sum_{k', \alpha} 2 \cos(k'_\alpha a) \delta n_{k'} \delta n_{-k'} \right. \\
&\quad - \frac{z}{8n^2} \sum_k \delta n_k \delta n_{-k} - \frac{z}{8n^2 N} \sum_{k', q'} N \delta_{-k' q'} \delta n_{k'} \delta n_{q'} \\
&\quad \left. - \frac{1}{2} \left(2z \sum_k \varphi_k \varphi_{-k} - \sum_{k, \alpha} 4 \cos(k_\alpha a) \varphi_k \varphi_{-k} \right) \right] - 2tnzN, \tag{4.22}
\end{aligned}$$

where a is the lattice constant, as introduced in section 3.1.1.

All summation indices k' can be renamed as k , since the summations have to be carried out over all possible k -values. This gives, after further simplification

$$\begin{aligned}
H_1 &= -2tn \left[\frac{1}{2n^2} \sum_{k, \alpha} \delta n_k \delta n_{-k} \cos(k_\alpha a) - \frac{z}{4n^2} \sum_k \delta n_k \delta n_{-k} \right. \\
&\quad \left. - \left(z \sum_k \varphi_k \varphi_{-k} - 2 \sum_{k, \alpha} \varphi_k \varphi_{-k} \cos(k_\alpha a) \right) \right] - 2tnzN \\
&= -\frac{t}{n} \sum_{k, \alpha} \delta n_k \delta n_{-k} \cos(k_\alpha a) + \frac{tz}{2n} \sum_k \delta n_k \delta n_{-k} \\
&\quad + 2tn \sum_k \varphi_k \varphi_{-k} \left[z - 2 \sum_\alpha \cos(k_\alpha a) \right] - 2tnzN. \tag{4.23}
\end{aligned}$$

Finally we get the Fourier transformed kinetic part of the Rotor-Hamiltonian

$$\begin{aligned}
H_1 &= -2tnzN + 2tn \sum_k \varphi_k \varphi_{-k} \left[z - 2 \sum_\alpha \cos(k_\alpha a) \right] \\
&\quad + \frac{t}{n} \sum_k \delta n_k \delta n_{-k} \left[\frac{z}{2} - \sum_\alpha \cos(k_\alpha a) \right].
\end{aligned} \tag{4.24}$$

4.2.2 Fourier Transformation of the interaction parts

Now that the kinetic part of the Rotor-Hamiltonian H_1 has been Fourier transformed, the next step is to transform the on-site interaction part H_2 eq. (4.11) by using the Fourier transformation eq. (4.21)

$$\begin{aligned}
H_2 &= \frac{U}{2} N n^2 + \frac{U}{2} \sum_i \delta n_i \delta n_i \\
&= \frac{U}{2} N n^2 + \frac{U}{2} \sum_i \frac{1}{\sqrt{N}} \sum_k e^{ikx_i} \delta n_k \frac{1}{\sqrt{N}} \sum_q e^{iqx_i} \delta n_q \\
&= \frac{U}{2} N n^2 + \frac{U}{2N} \sum_{i,k,q} e^{i(k+q)x_i} \delta n_k \delta n_q \\
&= \frac{U}{2} N n^2 + \frac{U}{2N} \sum_{k,q} N \delta_{-kq} \delta n_k \delta n_q.
\end{aligned} \tag{4.25}$$

Hence, the Fourier transformed on-site interaction part is obtained

$$H_2 = \frac{U}{2} N n^2 + \frac{U}{2} \sum_k \delta n_k \delta n_{-k}. \tag{4.26}$$

In the following, the third part of the Rotor-Hamiltonian eq. (4.14), for the nearest-neighbor interaction, is due. For this case the Fourier transformation eq. (4.20) is needed

$$\begin{aligned}
H_3 &= \frac{V}{2} zN n^2 + \frac{V}{2} \sum_{\langle i,j \rangle} \delta n_i \delta n_j \\
&= \frac{V}{2} zN n^2 + \frac{V}{2} \sum_{\langle i,j \rangle} \frac{1}{\sqrt{N}} \sum_k e^{ikx_i} \delta n_k \frac{1}{\sqrt{N}} \sum_q e^{iqx_j} \delta n_q \\
&= \frac{V}{2} zN n^2 + \frac{V}{2N} \sum_{\langle i,j \rangle} \sum_{k,q} e^{i(kx_i+qx_j)} \delta n_k \delta n_q \\
&= \frac{V}{2} zN n^2 + \frac{V}{2N} \sum_{\langle i,j \rangle} \sum_{k,q} e^{i(k+q)x_i} e^{iqe_j} \delta n_k \delta n_q \\
&= \frac{V}{2} zN n^2 + \frac{V}{2N} \sum_{j,k,q} N \delta_{-kq} e^{iqe_j} \delta n_k \delta n_q \\
&= \frac{V}{2} zN n^2 + \frac{V}{2} \sum_{j,k} e^{-ike_j} \delta n_k \delta n_{-k}.
\end{aligned} \tag{4.27}$$

It follows the last part for the Rotor-Hamiltonian, the Fourier transformed nearest-neighbor interaction part

$$H_3 = \frac{V}{2} z N n^2 + V \sum_{k, \alpha} \delta n_k \delta n_{-k} \cos(k_\alpha a). \quad (4.28)$$

4.2.3 The Fourier transformed Rotor-Hamiltonian

The whole Fourier transformed Rotor-Hamiltonian is obtained by summing all three Fourier transformed parts eq. (4.24, 4.26, 4.28)

$$\begin{aligned} H = E_0 &+ 2tn \sum_k \varphi_k \varphi_{-k} \left[z - 2 \sum_\alpha \cos(k_\alpha a) \right] \\ &+ \frac{t}{n} \sum_k \delta n_k \delta n_{-k} \left[\frac{z}{2} - \sum_\alpha \cos(k_\alpha a) \right] \\ &+ \frac{U}{2} \sum_k \delta n_k \delta n_{-k} + V \sum_{k, \alpha} \delta n_k \delta n_{-k} \cos(k_\alpha a), \end{aligned} \quad (4.29)$$

where E_0 is as in eq. (4.15) defined.

Thus, the Rotor-Hamiltonian in k -space is

$$\begin{aligned} H = E_0 &+ 2tn \sum_k \varphi_k \varphi_{-k} \left[z - 2 \sum_\alpha \cos(k_\alpha a) \right] \\ &+ \sum_k \delta n_k \delta n_{-k} \left[\frac{t}{n} \left(\frac{z}{2} - \sum_\alpha \cos(k_\alpha a) \right) + \frac{U}{2} \left(1 + 2\gamma \sum_\alpha \cos(k_\alpha a) \right) \right] \end{aligned}$$

and γ is the ratio of the nearest-neighbor and on-site interaction V/U .

4.3 Diagonalization of the Rotor-Hamiltonian

Still due is the calculation of the dispersion relation for a system with high filling factors n . A step in this direction was the realization of a Rotor-Hamiltonian in real space eq. (4.14) for a system, where each lattice site contains a quasi-condensate, which is described by a macroscopic wave function. The next step was the Fourier transformation of this Rotor-Hamiltonian eq. (4.30). The final step, which is up next, is to diagonalize the Fourier transformed Rotor-Hamiltonian eq. (4.30), to finally achieve the desired dispersion relation.

Since the Rotor-Hamiltonian eq. (4.30) is of quadratic order, it can be solved by diagonalizing, similar to the harmonic oscillator. For a further introduction in the solving mechanism of the harmonic oscillator by diagonalization, see [44]. To do this, creation and annihilation operators are introduced for the phase $\varphi_{k, -k}$ and mean-field fluctuation $\delta n_{k, -k}$, similarly as in [44]. The phase $\varphi_{k, -k}$ of the quasi-condensate can be interpreted as the momentum p and the mean-field

fluctuation $\delta n_{k,-k}$ as the position x of the particles in the harmonic oscillator system. Thus, following relations between the old values $\varphi_{k,-k}$, $\delta n_{k,-k}$ and the new operators are made

$$\varphi_k = i\beta_k (a_k^\dagger - a_{-k}), \quad (4.30)$$

$$\varphi_{-k} = i\beta_{-k} (a_{-k}^\dagger - a_k), \quad (4.31)$$

$$\delta n_k = \gamma_k (a_k + a_{-k}^\dagger), \quad (4.32)$$

$$\delta n_{-k} = \gamma_{-k} (a_{-k} + a_k^\dagger), \quad (4.33)$$

where β_k and γ_k are coefficients, which still need to be calculated. The operator a_k^\dagger creates a particle with momentum k and the operator a_k annihilates a particle with momentum k . To determine the coefficients β_k and γ_k , it is necessary to know, that the phase φ_k and the mean-field fluctuation δn_k are connected via following commutator relation

$$[\varphi_k, \delta n_k] = i. \quad (4.34)$$

It has to be kept in mind, that $\gamma \neq \gamma_k$. The coefficient γ_k is for diagonalization purposes and γ is the ratio of the nearest-neighbor to on-site interaction. With the commutator relation eq. (4.34) above, we achieve a relation between β_k and γ_k

$$\beta_k = -\frac{1}{2\gamma_k}. \quad (4.35)$$

This relation between β_k and γ_k is inserted into eq. (4.30 + 4.31)

$$\varphi_k = -\frac{i}{2\gamma_k} (a_k^\dagger - a_{-k}), \quad (4.36)$$

$$\varphi_{-k} = -\frac{i}{2\gamma_{-k}} (a_{-k}^\dagger - a_k). \quad (4.37)$$

By using the commutator relation eq. (4.34) and inserting it into eq. (4.30 + 4.31), we obtained that the equations for the phase $\varphi_{k,-k}$ eq. (4.36, 4.37) and mean-field fluctuation $\delta n_{k,-k}$ eq. (4.32, 4.33) only depend of the coefficient γ_k . The coefficient γ_k is determined in a later step.

Finally the equations (4.32, 4.33, 4.36, 4.37) are inserted into the Rotor-Hamiltonian eq. (4.30)

$$\begin{aligned}
\text{H} &= E_0 - 2tn \sum_k \frac{1}{4|\gamma_k|^2} \left(a_k^\dagger a_{-k}^\dagger - a_k^\dagger a_k - a_{-k} a_{-k}^\dagger + a_{-k} a_k \right) \underbrace{\left[z - 2 \sum_\alpha \cos(k_\alpha a) \right]}_{=:\epsilon_k} \\
&+ \sum_k |\gamma_k|^2 \left(a_k a_{-k} + a_k a_k^\dagger + a_{-k}^\dagger a_{-k} + a_{-k}^\dagger a_k^\dagger \right) \\
&\times \underbrace{\left[\frac{t}{n} \left(\frac{z}{2} - \sum_\alpha \cos(k_\alpha a) \right) + \frac{U}{2} \left(1 + 2\gamma \sum_\alpha \cos(k_\alpha a) \right) \right]}_{=:V_k} \\
&= E_0 - \frac{tn}{2} \sum_k \frac{1}{|\gamma_k|^2} \left(-a_k^\dagger a_k - a_{-k} a_{-k}^\dagger \right) \epsilon_k + \sum_k |\gamma_k|^2 \left(a_k a_k^\dagger + a_{-k}^\dagger a_{-k} \right) V_k \\
&- \frac{tn}{2} \sum_k \frac{1}{|\gamma_k|^2} \left(a_k^\dagger a_{-k}^\dagger + a_{-k} a_k \right) \epsilon_k + \sum_k |\gamma_k|^2 \left(a_k a_{-k} + a_{-k}^\dagger a_k^\dagger \right) V_k. \quad (4.38)
\end{aligned}$$

To further diagonalize the Rotor-Hamiltonian eq. (4.38), the off-diagonal elements have to vanish. This is accomplished by calculating the coefficient γ_k

$$\begin{aligned}
\Rightarrow 0 &= -\frac{tn}{2} \sum_k \frac{1}{|\gamma_k|^2} \left(a_k^\dagger a_{-k}^\dagger + a_{-k} a_k \right) + \sum_k |\gamma_k|^2 \left(a_k a_{-k} + a_{-k}^\dagger a_k^\dagger \right) V_k \\
0 &= \sum_k \underbrace{\left(-\frac{tn}{2} \frac{1}{|\gamma_k|^2} + |\gamma_k|^2 V_k \right)}_{=0} \left(a_k^\dagger a_{-k}^\dagger + a_{-k} a_k \right). \quad (4.39)
\end{aligned}$$

Since the operators $a_{\pm k}^\dagger$, $a_{\pm k}$ can not become zero, the bracket has to be always zero. This leads to

$$\begin{aligned}
\frac{tn}{2} \frac{\epsilon_k}{|\gamma_k|^2} &= |\gamma_k|^2 V_k \\
\Rightarrow |\gamma_k| &= \pm \left(\frac{tn}{2} \frac{\epsilon_k}{V_k} \right)^{1/4}. \quad (4.40)
\end{aligned}$$

The calculated coefficient γ_k of eq. (4.40) has to be inserted into the Rotor-Hamiltonian eq. (4.38) to further reduce it

$$\begin{aligned}
\text{H} &= E_0 + \frac{tn}{2} \sum_k \left(\frac{tn}{2} \frac{\epsilon_k}{V_k} \right)^{-1/2} \left(a_k^\dagger a_k + a_{-k} a_{-k}^\dagger \right) \epsilon_k \\
&+ \sum_k \sqrt{\frac{tn}{2} \frac{\epsilon_k}{V_k}} \left(a_k a_k^\dagger + a_{-k}^\dagger a_{-k} \right) V_k. \quad (4.41)
\end{aligned}$$

The presented Rotor-Hamiltonian eq. (4.41) can be diagonalized further by applying the commutator relation for the creation $a_{\pm k}^\dagger$ and annihilation operator $a_{\pm k}$

$$\left[a_k^\dagger, a_k \right] = -1. \quad (4.42)$$

With this, the Rotor-Hamiltonian eq. (4.41) is finally diagonalized and we achieve the energy spectrum for this system

$$H = E_0 + \sum_k E_k \left(a_k^\dagger a_k + \frac{1}{2} \right). \quad (4.43)$$

Since the summation \sum_k runs over all possible k -values, operators a_{-k} can be renamed as a_k . By this renaming, no values for k are missed or lost. The Rotor-Hamiltonian eq. (4.43) now is of the same form as the harmonic oscillator Hamiltonian, see [44]. The ground state energy E_0 is as defined in eq. (4.15). The dispersion relation E_k for a system with high filling factors $n \gg 1$ reads

$$E_k = \sqrt{8tnV_k\epsilon_k}, \quad (4.44)$$

where the coefficients V_k and ϵ_k are

$$V_k = \frac{t}{n} \left(\frac{z}{2} - \sum_\alpha \cos(k_\alpha a) \right) + \frac{U}{2} \left(1 + 2\gamma \sum_\alpha \cos(k_\alpha a) \right) \quad (4.45)$$

$$\epsilon_k = \left[z - 2 \sum_\alpha \cos(k_\alpha a) \right]. \quad (4.46)$$

4.4 Calculation of the Instability

Until now, we have calculated the energy spectrum eq. (4.43) of a system with high filling factors $n \gg 1$, where each lattice site contains a quasi-condensate. The question, which now arises is: Is the system stable in the presence of the mean-field fluctuations $\delta n_{\pm k}$ and the appearance of nearest-neighbor interaction V or does an instability in its dispersion relation eq. (4.44) occur? An instability in the dispersion relation means, that at some certain ratio γ it becomes zero. This indicates a quantum phase transition.

We are now interested in the calculation of the instability. For this, we have to determine the ratio of $\gamma = V/U$ where the dispersion relation E_k of eq. (4.44) becomes zero, again. The dispersion relation E_k eq. (4.44) can be brought into following form

$$E'_k = \left\{ \underbrace{\left[4t^2 \left(z - 2 \sum_\alpha \cos(k_\alpha a) \right) + 4tnU \left(1 + 2\gamma \sum_\alpha \cos(k_\alpha a) \right) \right]}_{E'_1} \times \underbrace{\left[z - 2 \sum_\alpha \cos(k_\alpha a) \right]}_{E'_2} \right\}. \quad (4.47)$$

Since the quantity E'_2 is not always zero, only at certain values for k , the quantity E'_1 has to be

$$\begin{aligned}
E'_1 &= \sqrt{4t^2 \left[z - 2 \sum_{\alpha} \cos(k_{\alpha}a) \right] + 4tnU \left[1 + 2\gamma \sum_{\alpha} \cos(k_{\alpha}a) \right]} \stackrel{!}{=} 0 \\
&\quad -t \left[z - 2 \sum_{\alpha} \cos(k_{\alpha}a) \right] = Un \left(1 + 2\gamma \sum_{\alpha} \cos(k_{\alpha}a) \right) \\
\Rightarrow \quad \gamma &= -\frac{t}{Un \sum_{\alpha} \cos(k_{\alpha}a)} \left(\frac{z}{2} - \sum_{\alpha} \cos(k_{\alpha}a) \right) - \frac{1}{2 \sum_{\alpha} \cos(k_{\alpha}a)}. \quad (4.48)
\end{aligned}$$

As introduced in section 3.2.1, the following relation for the number of nearest neighbors z is valid

$$z = -2 \sum_{\alpha} \cos(k_{\alpha}a). \quad (4.49)$$

This relation eq. (4.49) is inserted into eq. (4.48) and reveals the ratio γ for which the instability in the dispersion relation E_k eq. (4.44) occurs

$$\gamma = \frac{2t}{Un} + \frac{1}{z}. \quad (4.50)$$

This has the following consequence for the system: At low ratios $\gamma \approx 1$, the nearest-neighbor interaction is of the order of the on-site interaction. The bosons are in the superfluid phase, thus they can freely hop between lattice site, i.e. delocalize over the lattice. Despite the hopping, there is always a large number of particles in each lattice site. As the ratio γ is being raised, the influence of the nearest-neighbor interaction becomes stronger. The bosons are still free to hop between lattice site, but are aware of this influence. As the nearest-neighbor interaction is getting stronger, more and more bosons become confined to a certain lattice site. Many are still free to hop, in spite of the strong nearest-neighbor interaction. When the critical ratio γ eq. (4.50) is reached the superfluid phase becomes unstable and leads to a phase transition.

In figure 4.1 the dispersion relation is plotted for two different kind of ratios γ . The top figure shows the dispersion relation for $\gamma = 1$. For that case, the system is in the superfluid phase. The bottom figure shows the dispersion relation for the critical γ -ratio eq. (4.50). Here, the system undergoes an instability, which is a sign for a phase transition.

At this point, the calculated value for the critical ratio γ eq. (4.50) within the Rotor-Model should be compared to the value of the Bogoliubov theory eq. (3.53). In the Bogoliubov description only a low filling factor $n \propto 1$ is considered, where as in the Rotor-Model, the filling factor is much larger than one $n \gg 1$. The arising question now is, how does this discrepancy affect the critical ratio of nearest-neighbor to on-site interaction and therefore the occurrence of the instability of the superfluid phase? We find, that the two ratios are identical, despite the two different descriptions. Never the less, we have to keep the properties of the two different models in mind, when considering one of them.

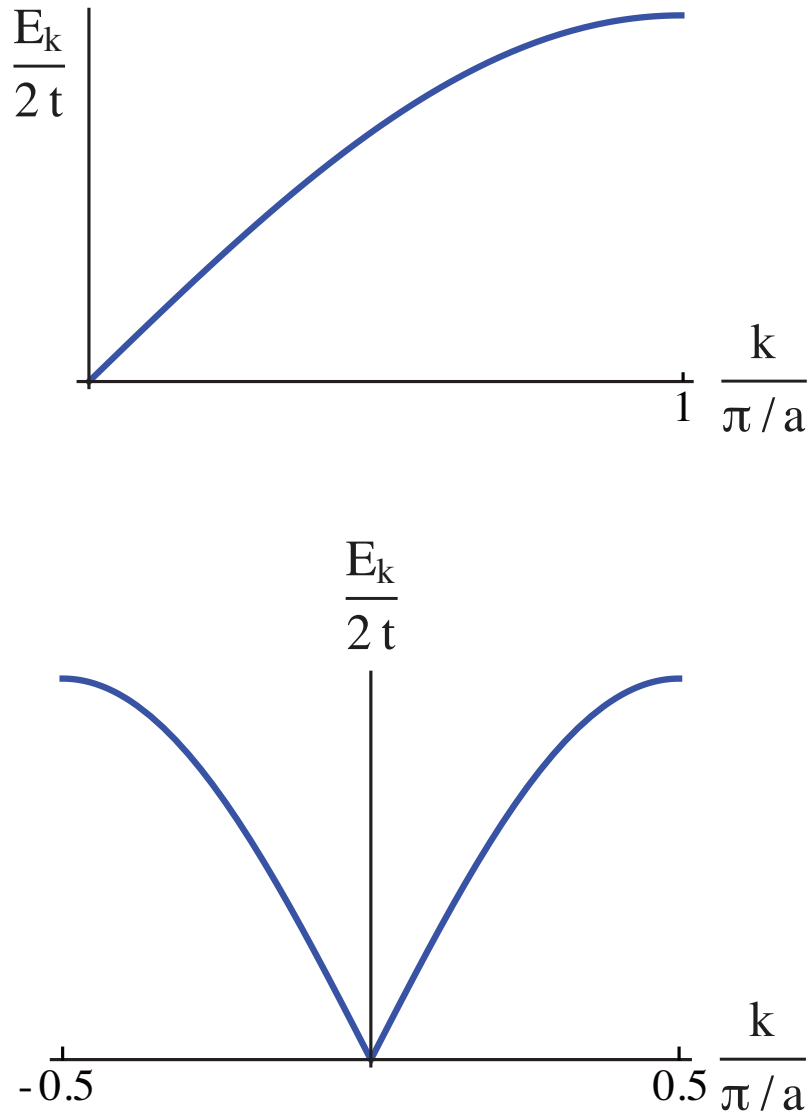


Figure 4.1: **Top:** Dispersion relation in units of $k = \pi/a$, where a is the lattice constant. The ratio $\gamma = 1$, thus the system is in the superfluid phase. **Bottom:** Dispersion relation in units of $k = \pi/a$. In this case, the system is tuned to the critical ratio γ of eq. (4.50). Here the superfluid phase becomes unstable and a phase transition occurs.

4.5 Calculating the number of particles

So far we have assumed our optical lattice is constructed of an one atomic basis. Therefore we did not make any comments about the possible structures on the optical lattice. With this assumption we saw, that the superfluid phase suffers an instability. In the next step, we propose a possible structure on the lattice. Since the one atomic basis is unstable at a critical ratio γ_c , we suggest a two atomic basis. This proposal has to be investigated, if it is viable on an optical lattice. In the following calculations and considerations this is due.

In section 4.3 we have calculated the energy spectrum for a system with high filling factors n . The previous section 4.4 investigated the stability for that system and revealed, that it becomes unstable at a critical ratio γ eq. (4.50). In the calculations above, we have used the quantity n_i , the particle density at a certain lattice site, without even knowing the nature of this quantity. As the next step we are going to determine n_i and if a realization of a two atomic basis is doable. The mean number of particles per lattice site is calculated by

$$n_i = \langle b_i^\dagger b_i \rangle, \quad (4.51)$$

where b_i^\dagger is the creation operator and b_i the annihilation operator for a particle in lattice site i . The brackets $\langle \rangle$ indicate, that the mean value is carried out.

The mean-field operators $\langle b_k \rangle$ are known for two k -values, $k_0 = 0$ and $k_1 = \pi/a$, i.e. at the center of the first Brillouin zone $k_0 = 0$ and at the boundary of the first zone $k_1 = \pi/a$, a is the lattice constant. The values for these operators are

$$\langle b_{k_0} \rangle = c e^{i\varphi_0} \quad , \quad \langle b_{k_0}^\dagger \rangle = c^* e^{-i\varphi_0} \quad (4.52)$$

$$\langle b_{k_1} \rangle = d e^{i\varphi_1} \quad , \quad \langle b_{k_1}^\dagger \rangle = d^* e^{-i\varphi_1} \quad (4.53)$$

where c, d are constants, which have to be calculated, see section 4.6.1. The quantities φ_0, φ_1 are the phases at $k_0 = 0$ and $k_1 = \pi/a$. The symbol $*$ indicates, that the complex conjugate of the according quantity has to be taken.

Since we are not aware of the values for the creation $\langle b_i^\dagger \rangle$ and annihilation operator $\langle b_i \rangle$ in real space, we have to Fourier transform the number of particles n_i at first

$$n_q = \sum_i e^{-iqx_i} n_i \quad (4.54)$$

$$= \sum_i e^{-iqx_i} \langle b_i^\dagger b_i \rangle, \quad (4.55)$$

where the Fourier transformations for the creation and annihilation operators read

$$\langle b_i \rangle = l \sum_i e^{ik'x_i} \langle b_{k'} \rangle, \quad \langle b_i^\dagger \rangle = l^* \sum_i e^{-ikx_i} \langle b_k^\dagger \rangle, \quad (4.56)$$

where l, l^* are normalization constants. These constants are determined by the fact, that the two operators b_i^\dagger, b_i obey the commutator relation

$$\left[b_i^\dagger, b_i \right] = -1. \quad (4.57)$$

This gives the following result for the normalization constants

$$l = l^* = \frac{1}{\sqrt{N}}, \quad (4.58)$$

thus, the constants in eq. (4.56) can be replaced by their calculated values eq. (4.58).

At the next step, the Fourier transformations for the creation and annihilation operators eq. (4.56) are inserted into the Fourier transformation for the number operator eq. (4.55)

$$\begin{aligned} n_q &= \sum_i e^{-iqx_i} \left(\frac{1}{\sqrt{N}} \sum_k e^{-ikx_i} \langle b_k^\dagger \rangle \right) \left(\frac{1}{\sqrt{N}} \sum_{k'} e^{ik'x_i} \langle b_{k'} \rangle \right) \\ &= \frac{1}{N} \sum_{i, k, k'} e^{-ix_i(q+k-k')} \langle b_k^\dagger b_{k'} \rangle \\ &= \frac{1}{N} \sum_{k, k'} N \delta_{(q+k)k'} \langle b_k^\dagger b_{k'} \rangle \\ &= \sum_k \langle b_k^\dagger b_{q+k} \rangle, \end{aligned} \quad (4.59)$$

hence, we achieved the Fourier transformation for the number of particles n_q .

To finally get the number of particles per lattice site i , the Fourier transformation has to be carried out backwards

$$\begin{aligned} n_i &= \frac{1}{N} \sum_q e^{iqx_i} n_q \\ &= \frac{1}{N} \sum_q e^{iqx_i} \sum_k \langle b_k^\dagger b_{q+k} \rangle \\ &= \frac{1}{N} \sum_{q, k} e^{iqx_i} \langle b_k^\dagger b_{q+k} \rangle, \end{aligned} \quad (4.60)$$

at this point, we accomplished to evaluate the number of particles at lattice site i , expressed by the mean-field operators $\langle b_k^\dagger b_{q+k} \rangle$. Thus we are able to determine n_i , because we know the values of the mean-field operators at certain points in k -space.

With the number of particles per lattice site i eq. (4.60) calculated, an analysis of the possible k, q -values has to be done

$$q = 0 : \quad \frac{1}{N} \left(\langle b_{k_0}^\dagger b_{k_0} \rangle + \langle b_{k_1}^\dagger b_{k_1} \rangle \right) = \frac{1}{N} \left(|c|^2 + |d|^2 \right) \quad (4.61)$$

$$\begin{aligned} q = \frac{\pi}{a} : & \quad \frac{1}{N} e^{i\frac{\pi}{a}x_i} \left(\langle b_{k_0}^\dagger b_{k_1} \rangle + \langle b_{k_1}^\dagger b_{k_0} \rangle \right) \\ &= \frac{1}{N} e^{i\frac{\pi}{a}x_i} \left(c^* d e^{-i\varphi_0} e^{i\varphi_1} + d^* c e^{-i\varphi_1} e^{i\varphi_0} \right), \end{aligned} \quad (4.62)$$

if the assumption is made, that c, d are all real quantities, i.e. $c^* = c$ and $d^* = d$, then eq. (4.62) becomes

$$\begin{aligned} &= \frac{cd}{N} e^{i\frac{\pi}{a}x_i} \left(e^{-i(\varphi_0 - \varphi_1)} + e^{i(\varphi_0 - \varphi_1)} \right) \\ &= \frac{cd}{N} \left(e^{-i(\varphi' - \frac{\pi}{a}x_i)} + e^{i(\varphi' + \frac{\pi}{a}x_i)} \right). \end{aligned} \quad (4.63)$$

Here we used the expression $\varphi' = \varphi_0 - \varphi_1$ and took advantage of the periodicity of the lattice considered. This allows us to put $-\frac{\pi}{a}x_i = +\frac{\pi}{a}x_i$. With this, eq. (4.63) then becomes

$$\frac{1}{N} e^{i\frac{\pi}{a}x_i} \left(\langle b_{k_0}^\dagger b_{k_1} \rangle + \langle b_{k_1}^\dagger b_{k_0} \rangle \right) = 2 \frac{cd}{N} \cos \left(\varphi' + \frac{\pi}{a}x_i \right). \quad (4.64)$$

If eq. (4.61 + 4.64) are summed, they reveal the number of particles at lattice site i

$$n_i = \frac{1}{N} \left[|c|^2 + |d|^2 + 2cd \cos \left(\varphi' + \frac{\pi}{a}x_i \right) \right], \quad (4.65)$$

where $\varphi' = \varphi_0 - \varphi_1$ is the difference between the two phases at $k_0 = 0$ and $k_1 = \pi/a$.

4.5.1 Calculation of the mean-field number fluctuations

We still are not aware of the value for the mean-field fluctuations δn_i . One step closer was the calculation of the number of particles at lattice site i eq. (4.65), because n_i consists of the mean number of particles n and δn_i . Thus, the mean-field fluctuations can be expressed as

$$\delta n_i = n_i - \langle n \rangle. \quad (4.66)$$

where n_i is the number of particles per lattice site i , as in eq. (4.65), and $\langle n \rangle$ is the mean number of particle per lattice site.

There are two possible ways to determine the mean-field fluctuations δn_i , either by direct calculation or by evaluating the mean number of particles per lattice site $\langle n \rangle$. For the following consideration, we have chosen the latter possibility. Use of the Fourier transformations for the mean-field operators eq. (4.56) is advantageous.

$$\begin{aligned} \langle n \rangle &= \frac{1}{N} \sum_i \langle b_i^\dagger b_i \rangle \\ &= \frac{1}{N} \sum_i \left(\frac{1}{\sqrt{N}} \sum_{k'} e^{-ik'x_i} \langle b_{k'}^\dagger \rangle \right) \left(\frac{1}{\sqrt{N}} \sum_k e^{-ikx_i} \langle b_k^\dagger \rangle \right) \\ &= \frac{1}{N^2} \sum_k N \delta_{kk'} \langle b_{k'}^\dagger b_k \rangle \\ &= \frac{1}{N} \sum_k \langle b_k^\dagger b_k \rangle. \end{aligned} \quad (4.67)$$

Now, the possible k -values for the equation above eq. (4.67) are analyzed and inserted are the possible mean fields of eq. (4.52, 4.53). We then obtain the mean number of particles $\langle n \rangle$

$$\langle n \rangle = \frac{1}{N} \left(|c|^2 + |d|^2 \right). \quad (4.68)$$

The next step is to insert the calculated mean number of particles eq. (4.68) into the proposed relation between the mean-field fluctuations δn_i and the number of particles at lattice site i eq. (4.66), to achieve

$$\delta n_i = \frac{2cd}{N} \cos \left(\varphi' + \frac{\pi}{a} x_i \right). \quad (4.69)$$

For further calculations, normalized quantities c , d are introduced

$$\bar{c} = \frac{c}{\sqrt{N}}, \quad \bar{d} = \frac{d}{\sqrt{N}}, \quad (4.70)$$

they are normalized to the number of lattice sites N in the considered system.

As the normalized quantities \bar{c} , \bar{d} are inserted into the number of particles at lattice site i eq. (4.65), we get

$$n_i = \langle n \rangle + \delta n_i \quad (4.71)$$

$$= \left(\bar{c}^2 + \bar{d}^2 \right) + \left(2\bar{c}\bar{d} \cos \left(\varphi' + \frac{\pi}{a} x_i \right) \right). \quad (4.72)$$

This has the following consequence for the system: Each lattice site is occupied by a mean number of particles $\langle n \rangle$ as assumed in sec. 4.1, accompanied by a mean-field fluctuation δn_i . The fluctuation δn_i depends on the lattice i and is driven by the phase difference φ' . The phase difference has to be adjusted in such a way, that the fluctuations can be seen, i.e. they have to be at the different lattice sites i . If φ' is detuned, the fluctuations appear in between the different lattice sites and have no effect on the mean number of particles $\langle n \rangle$. Hence, the phase difference φ' has to be chosen carefully. This counter checks our proposal of a two atomic basis viability, since it can be realized by tuning the phase difference φ' correctly.

4.6 Calculating the energy of the new groundstate

Until now, we have found, that a system with high filling factors $n \gg 1$ on an optical lattice exhibits an instability in its dispersion relation and that number of particles per lattice site fluctuates around its mean value $\langle n \rangle$. Next, we want to calculate the energy of the new ground state of the system, after the instability in the dispersion relation happened. The instability is the sign of a phase transition, see section 4.7 for further analysis of the nature of the phase transition.

To determine the new ground state energy, we take the Rotor-Hamiltonian eq. (2.28) in a homogeneous and canonical ensemble. Into this Hamiltonian

$$H_{Rotor} = -2t \sum_{\langle i,j \rangle} \sqrt{n_i n_j} \cos(\varphi_i - \varphi_j) + \frac{U}{2} \sum_i n_i^2 + \frac{V}{2} \sum_{\langle i,j \rangle} n_i n_j, \quad (4.73)$$

we plug in the ansatz for a two atomic basis, as mentioned in the previous section

$$n_i = (\bar{c} + \bar{d})^2, \quad (4.74)$$

$$n_j = (\bar{c} - \bar{d})^2. \quad (4.75)$$

As can be seen in the above equations, the fluctuations of particle numbers at the different lattice sites are considered in the factors $(\bar{c} + \bar{d})$ and $(\bar{c} - \bar{d})$. The coefficients \bar{c} , \bar{d} are as introduced in section 4.5.1 and still need to be computed.

Analyzing the first part

The first part of the Hamiltonian eq. (4.73) is the kinetic part. The ansatz eq. (4.74 + 4.75) are inserted

$$\begin{aligned} H_1 &= -2t \sum_{\langle i, j \rangle} \sqrt{(\bar{c} + \bar{d})^2 (\bar{c} - \bar{d})^2} \cos(\varphi_i - \varphi_j) \\ &= -2t (\bar{c}^2 - \bar{d}^2) \sum_{\langle i, j \rangle} \cos(\varphi_i - \varphi_j). \end{aligned} \quad (4.76)$$

We carry out the evaluation, while being within a quasi-condensate at a lattice site i . Hence, the phase difference $\varphi_i - \varphi_j$ becomes zero. The first part then reads

$$H_1 = -2ztN (\bar{c}^2 - \bar{d}^2), \quad (4.77)$$

where z is the number of nearest neighbors and N the number of lattice sites in the system.

Analyzing the second part

The second part considers the on-site interaction between particles at the same site i

$$H_2 = \frac{U}{2} \sum_i n_i^2. \quad (4.78)$$

The Hamiltonian above has to be split into two parts, because there are two different possible lattice sites available, one with a large number of particle n_i and one with few n_j . The summation over all lattice sites i then also has to be split into two parts, one summing all i - $N/2$ and one all j - $N/2$ sites. The Hamiltonian eq. (4.78) becomes, with inserting the ansatz of equations (4.74 + 4.75)

$$\begin{aligned} H_2 &= \frac{U}{2} \left[\sum_i^{N/2} n_i n_i + \sum_j^{N/2} n_j n_j \right] \\ &= \frac{U}{2} \left[\sum_i^{N/2} (\bar{c} + \bar{d})^2 (\bar{c} + \bar{d})^2 + \sum_j^{N/2} (\bar{c} - \bar{d})^2 (\bar{c} - \bar{d})^2 \right] \\ &= \frac{UN}{4} \left[(\bar{c}^2 + \bar{d}^2 + 2\bar{c}\bar{d}) (\bar{c}^2 + \bar{d}^2 + 2\bar{c}\bar{d}) \right. \\ &\quad \left. + (\bar{c}^2 + \bar{d}^2 - 2\bar{c}\bar{d}) (\bar{c}^2 + \bar{d}^2 - 2\bar{c}\bar{d}) \right]. \end{aligned} \quad (4.80)$$

For further simplification, $\bar{c}^2 + \bar{d}^2 = n$ can be used, as in eq. (4.68) calculated. The on-site interaction part thus becomes

$$H_2 = \frac{1}{2}UNn^2 + 2UN\bar{c}^2\bar{d}^2. \quad (4.81)$$

Analyzing the third part

The third part of the Hamiltonian accounts for the nearest-neighbor interactions. With the ansatz eq. (4.74 + 4.75) put in, it gets

$$\begin{aligned} H_3 &= \frac{V}{2} \sum_{\langle i,j \rangle} n_i n_j \\ &= \frac{V}{2} \sum_{\langle i,j \rangle} (\bar{c} + \bar{d})^2 (\bar{c} - \bar{d})^2 \\ &= \frac{V}{2} zN (\bar{c}^2 + \bar{d}^2 + 2\bar{c}\bar{d}) (\bar{c}^2 + \bar{d}^2 - 2\bar{c}\bar{d}) \\ &= \frac{V}{2} zN (n + 2\bar{c}\bar{d}) (n - 2\bar{c}\bar{d}). \end{aligned} \quad (4.82)$$

Thus, the third part of the Hamiltonian then becomes

$$H_3 = \frac{1}{2}zVNn^2 - 2zVN\bar{c}^2\bar{d}^2. \quad (4.83)$$

Now all three parts of the Hamiltonian can be written together, equations (4.77, 4.81, 4.83). We achieve a Hamiltonian, which only depends of the normalized coefficients \bar{c} and \bar{d}

$$H(\bar{c}, \bar{d}) = \frac{n^2 N}{2} (U + zV) - 2tzN (\bar{c}^2 - \bar{d}^2) + 2N\bar{c}^2\bar{d}^2 (U - zV). \quad (4.84)$$

For further calculations, the energy density of the ground state is introduced as

$$e_g = \frac{H}{N} = \frac{n^2}{2} (U + zV) - 2zt (\bar{c}^2 - \bar{d}^2) + 2\bar{c}^2\bar{d}^2 (U - zV). \quad (4.85)$$

4.6.1 Calculation of \bar{c} and \bar{d}

The energy density of the ground state eq. (4.85) is expressed in the normalized coefficients \bar{c} and \bar{d} . We still do not know their value. The computation of these coefficients is due in this section.

The coefficients \bar{c} and \bar{d} are linked via the constraint $\bar{c}^2 + \bar{d}^2 = n$, as introduced in section 4.5.1. By inserting this constraint into energy density eq. (4.85), we obtain the energy density solely depending on \bar{c} or \bar{d}

$$e_g(\bar{d}) = \frac{n^2}{2} (U + zV) - 2ztn + 4zt\bar{d}^2 + 2(U - zV) (n\bar{d}^2 - \bar{d}^4). \quad (4.86)$$

The energy density is now expressed in orders of \bar{d} . This means, that here the energy density e_g has to be an extremal value. Hence, the coefficient \bar{d} has to be extremal. Therefore the first derivative with respect to \bar{d} has to be taken

$$\begin{aligned}\frac{\partial e_g}{\partial \bar{d}} &= 8zt\bar{d} + 2(U - zV) \left(2n\bar{d} - 4\bar{d}^3 \right) \\ &= \bar{d} \left(8zt + 2(U - zV) \left(2n - 4\bar{d}^2 \right) \right) \stackrel{!}{=} 0.\end{aligned}\quad (4.87)$$

The coefficient \bar{d} can not be zero, thus the bracket has to be. Hence, we obtain the value for \bar{d} by solving eq. (4.87)

$$\bar{d} = \pm \sqrt{\frac{n}{2} + \frac{zt}{(U - zV)}}. \quad (4.88)$$

The value for the coefficient \bar{c} can be calculated via the before introduced constraint $\bar{c}^2 = n - \bar{d}^2$. This gives

$$\bar{c} = \pm \sqrt{\frac{n}{2} - \frac{zt}{(U - zV)}}. \quad (4.89)$$

New ground state energy

The values for the coefficient \bar{c} eq. (4.89) and \bar{d} eq. (4.88) have now been computed. Therefore the value for the energy density of the new ground state can be determined, by inserting the values for \bar{c} and \bar{d} into eq. (4.85)

$$e_g = \frac{2z^2t^2}{(U - zV)} + Un^2. \quad (4.90)$$

Energy difference between the two phases

The energy density of the new ground state is

$$e_g = \frac{2z^2t^2}{U - zV} + Un^2, \quad (4.91)$$

where the energy density of the old, superfluid phase is

$$e_0 = -2ztn. \quad (4.92)$$

The difference between these two energy densities becomes

$$\Delta E = e_g - e_0 = 2ztn \left(\frac{zt}{Un(1 - z\gamma)} + \frac{nU}{2zt} + 1 \right). \quad (4.93)$$

4.7 Calculation of the phase transition

Still due are the considerations about the order of the phase transition, which occurs at the critical value γ eq. (4.50). To get more insight into the behavior of the phase transition, the energy density eq. (4.86) can be rewritten in a different form

$$e_g(\bar{d}) = 2zt \left[-n + \frac{Un^2}{4t} \left(\frac{1}{z} + \gamma \right) + 2\bar{d}^2 + \frac{U}{t} \left(\frac{1}{z} - \gamma \right) (n\bar{d}^2 - \bar{d}^4) \right]. \quad (4.94)$$

At this point, we introduce a new normalization for the coefficient \bar{d}

$$\tilde{d} = \frac{\bar{d}}{\sqrt{n}}. \quad (4.95)$$

This normalizes the coefficient \bar{d} to the mean number of particles in a lattice site n . Thus we can write the energy density eq. (4.94) as

$$e_g(\tilde{d}) = 2ztn \left[-1 + \frac{Un}{4t} \left(\frac{1}{z} + \gamma \right) + 2\tilde{d}^2 + \frac{Un}{t} \left(\frac{1}{z} - \gamma \right) (\tilde{d}^2 - \tilde{d}^4) \right], \quad (4.96)$$

but we have to be aware, that the normalized coefficient \tilde{d} is only valid for values $-1 < \tilde{d} < +1$.

To make clear, on how the energy density eq. (4.96) e_g depends on the order of \tilde{d} , it can be expressed as

$$e_g(\tilde{d}) = 2znt \left[-1 + \frac{Un}{4t} \left(\frac{1}{z} + \gamma \right) + \left(2 + \frac{Un}{t} \left(\frac{1}{z} - \gamma \right) \right) \tilde{d}^2 - \frac{Un}{t} \left(\frac{1}{z} - \gamma \right) \tilde{d}^4 \right]. \quad (4.97)$$

This form clearly shows, that the two parts, \tilde{d}^2 and \tilde{d}^4 , are in competition with each other. We are now interested at which point the \tilde{d}^4 -part becomes dominant. The transition from the \tilde{d}^2 - to \tilde{d}^4 -dominance is the transition between different phases. Hence, we search for the critical ratio γ_c , which leads to this transition

$$e_g(\tilde{d}) = 2ztn \left[-1 + \underbrace{\left(2 + \frac{Un}{t} \left(\frac{1}{z} - \gamma \right) \right)}_{\stackrel{!}{=} 0} \tilde{d}^2 - \frac{Un}{t} \left(\frac{1}{z} - \gamma \right) \tilde{d}^4 \right] \quad (4.98)$$

$$0 \stackrel{!}{=} 2 + \frac{Un}{t} \left(\frac{1}{z} - \gamma \right) \quad (4.99)$$

$$\Rightarrow \gamma_c = \frac{2t}{Un} + \frac{1}{z}.$$

This means, that at the critical value γ_c eq. (4.99) the \tilde{d}^2 -part vanishes and the \tilde{d}^4 -part becomes dominant. Thus, for small γ -values, i.e. for a small ratio V/U , the \tilde{d}^2 -part is dominant and the system is superfluid. For large γ -values, the system transforms into a new phase, with a dominant \tilde{d}^4 -part. It is a smooth transition at the critical ratio γ_c , i.e. the system undergoes a second order phase transition, from a superfluid to a new phase. In figure 4.2 there are three

plots for different values of the ratio γ . The top figure shows the behavior of the system with \tilde{d}^2 -dominance, at $\gamma \approx 1$. In this case, the nearest-neighbor interaction V is of the order of the on-site interaction U . The middle figure shows the system at the transition point with $\gamma = \gamma_c$. There is no gap in the energy density, which is a clear indication of a second order phase transition. The bottom figure shows the energy density at $\gamma > \gamma_c$. In this region the \tilde{d}^4 -part of eq. (4.97) prevails. This kind of form of the energy density is called a "mexican hat", which again is a property of an underlying second order phase transition.

The determined critical ratio γ_c eq. (4.99) is compared to the computed ratios within the Bogoliubov theory eq. (3.53) and the Rotor-Model eq. (4.50). All three critical ratios are identical, which means, that our calculations so far are consistent. The phase transition occurs at the point, where the superfluid phase becomes unstable.

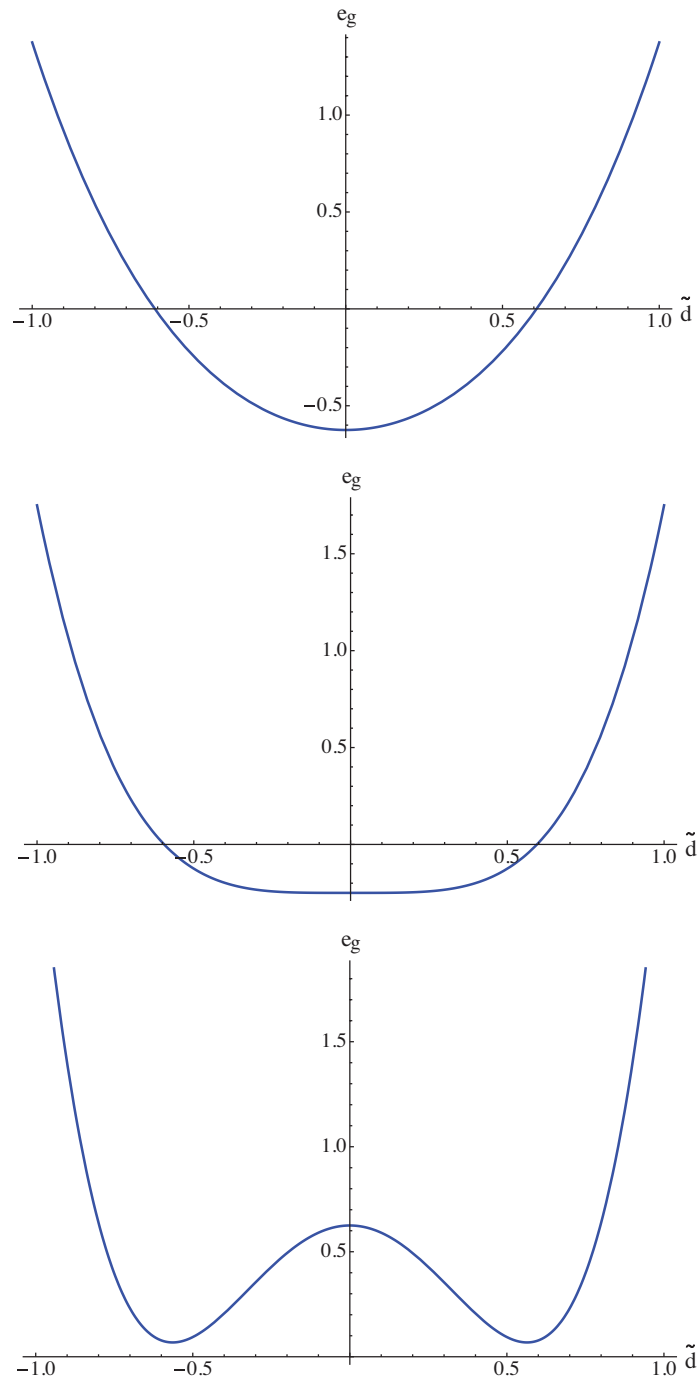


Figure 4.2: **Top:** Superfluid region, the energy density e_g is dominated by \tilde{d}^2 . The ratio between nearest neighbor and on-site interaction is of the order of one, $\gamma \approx 1$. **Middle:** The system is tuned to the critical ratio $\gamma = \gamma_c$ and undergoes a second order phase transition. **Bottom:** The ratio γ is tuned to reach the \tilde{d}^4 -dominant part, with $\gamma > \gamma_c \gg 1$. The new phase prevails.

4.8 Supersolid Phase

The big question now is: What kind of new phase occurs beyond γ_c ?

So far, we deeply investigated the phase transition. We started within a superfluid regime, where the bosons were free to hop between lattice sites. Then we found, that by raising the ratio between nearest-neighbor and on-site interaction γ , the system suffers an instability in its dispersion relation eq. (4.44). That was the first sign of the occurrence of a phase transition. Next, we looked at the number of particles at the lattice site i and obtained, that it fluctuates depending on the phase difference φ' eq. (4.72). Then we proposed an ansatz for the creation and annihilation operator eq. (4.74 + 4.75), which considers the fluctuations of particle numbers at lattice sites i . In this calculation we achieved an expression for the energy density of the new ground state. Finally we investigated the phase transition of the superfluid regime to the new phase. All these conclusions tell us the following: In the superfluid phase, all bosons are delocalized over the optical lattice. As the ratio γ is being raised, more and more bosons become confined to a certain lattice site i . Still, some bosons can overcome the barrier, which arises from the nearest-neighbor interaction, and hop through the lattice sites. At the critical ratio γ_c , most of the bosons are localized at the lattice sites i creating a structure on the optical lattice. In this regime, there are still bosons, which can hop through the different lattice sites i . Thus, the new phase has the property of a superfluid, i.e. bosons are delocalized, and of a crystalline solid, because of the structure on the optical lattice. Hence, the new phase is a supersolid, as introduced in section 2.3.2.

In figure 4.3 a supersolid is plotted. The crystalline structure is arranged as follows: One lattice site contains many bosons, the neighboring site is only occupied by few particles. The number of particles n_i eq. (4.72) indicates the occupation of each site i . The presented structure can be referred to as a checkerboard, where a white area can be imagined as a lattice site occupied by many bosons and a black area, a site containing few particles. Although, the system is not static, the bosons are still able to hop between lattice, but the checkerboard pattern prevails.

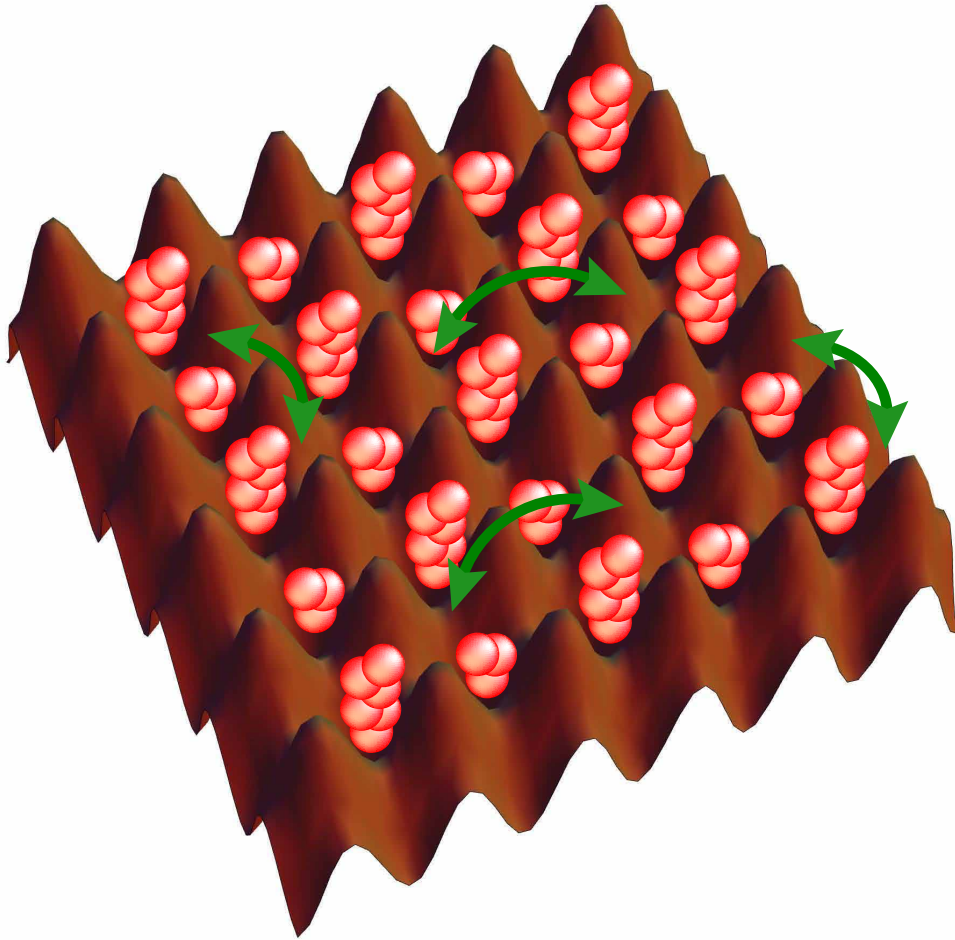


Figure 4.3: Supersolid phase on an optical lattice. The structure can be referred to as a checkerboard, because one lattice site contains many bosons, the neighboring site is occupied by few and vice versa. The bosons are still free to hop between sites, indicated by the green arrows.

4.9 Validity for the mean-field theory

Another question which arises is: Why is a mean-field calculation used to determine such a delicate phase as the supersolid?

In chapter 3 we calculated the instability within the Bogoliubov theory. In this regime, a dilute Bose gas was considered, where only few bosons occupy each optical lattice site. Another phase transition, where few particles in an optical lattice is considered, is the well-known Mott Insulator to Superfluid transition, see section 2.3.1. For such a system, the instability $(t/U)_c$ scales as $\sim 1/n$. Since we were interested in a system with a high filling factor $n \gg 1$, this lead us to the application of the Rotor-Hamiltonian eq. (2.28). The Rotor-Hamiltonian considers a system where each lattice site is occupied by a quasi-condensate, similar to an array of Josephson Junctions, [11]. The usage of the Rotor-Hamiltonian gave us the instability for such a system

$$\gamma_c = \frac{2t}{Un} + \frac{1}{z}. \quad (4.100)$$

To find out the scaling properties of the critical ratio $\gamma_c = V/U$, it can be rewritten into

$$\left(\frac{t}{U}\right)_c = \frac{1}{2} \left(\frac{V}{U} - \frac{1}{z}\right) n, \quad (4.101)$$

where t is the hopping term, U the on-site, V the nearest-neighbor interaction, z the number of nearest neighbors and n is the filling factor.

Equation (4.101) tells us, that the instability in the Rotor-Model regime scales with $\sim n$. This means, the higher we choose the filling factor n , the more accurate the used mean-field calculation becomes. Although, if small filling factors n are considered the assumptions in the Rotor-Model become inaccurate and the instability invalid. Figure 4.4 the two different scaling behaviors within the Bose-Hubbard- and Rotor-Model are compared.

In this work we only consider high filling factors n , thus do not make any estimates, what happens at small filling factors $n \leq 1$. This is the reason for the dashed area in figure 4.4. Until now, the behavior of a system with small filling factors $n \leq 1$ on an optical lattice is not fully understood and under high investigation. Our discussions exclude the regime with $n \leq 1$.

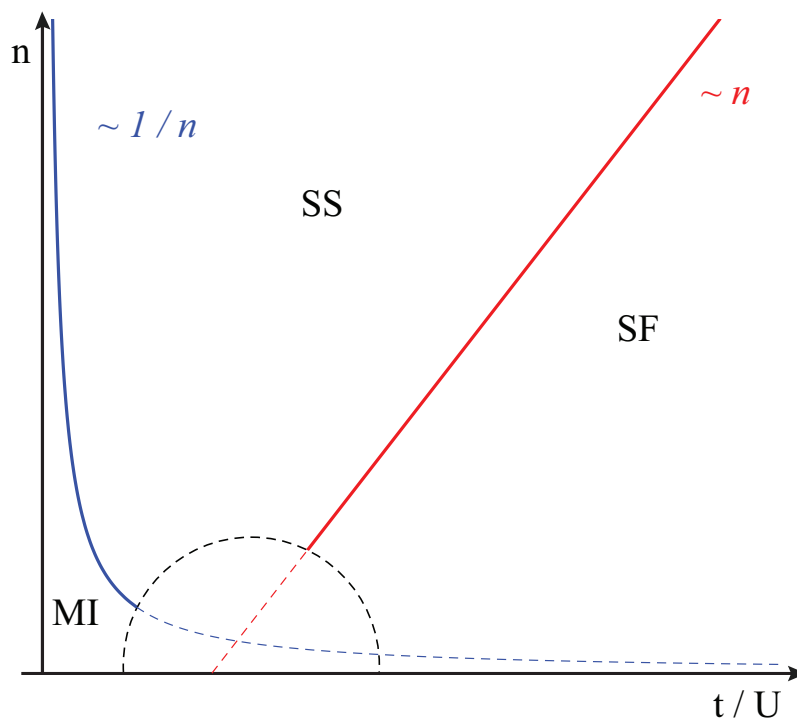


Figure 4.4: Comparison of the scaling behaviors in the Bose-Hubbard- and Rotor-Model. The instability within the Bose-Hubbard Model, indicated in blue, scale with n like $\sim 1/n$. In the Rotor-Model, marked as red, the instability scales as $\sim n$. In the dashed area small filling factors $n \leq 1$ are considered, what happens there is not fully understood and therefore excluded from the discussion.

Chapter 5

Stability of the supersolid phase

In the previous chapter, we claimed that the new phase, which occurs after the system is tuned across the critical value γ_c eq. (4.50), is a supersolid. Then we proposed an ansatz for the creation and annihilation operator eq. (4.74 + 4.75), where the number fluctuations at each lattice site were considered. This supersolid phase has the properties of a crystalline solid, the long-range ordering and of a superfluid, the delocalization of the bosons over the lattice site.

The question now is: Is the supersolid phase stable against quantum fluctuations?

To answer this question, we consider the system in the grand canonical ensemble, where quantum fluctuations are allowed. To control the number of particles in the system, we therefore introduce the chemical potential μ . In the following we use the Rotor-Hamiltonian, as given in eq. (2.28) of section 2.4 and derived in section 4.1.

The desired goal of the calculation is again the dispersion relation for a system with high filling factors $n \gg 1$, mean-field and quantum fluctuations.

5.1 Rotor-Hamiltonian in real space

As argued above, we start our investigation with the Rotor-Hamiltonian eq. (2.28) for a homogeneous system

$$H_{Rotor} = -2t \sum_{\langle i,j \rangle} \sqrt{n_i n_j} \cos(\varphi_i - \varphi_j) + \frac{U}{2} \sum_i n_i^2 + \frac{V}{2} \sum_{\langle i,j \rangle} n_i n_j - \mu \sum_i n_i. \quad (5.1)$$

Mentioned above, we now allow quantum fluctuations in our system. Thus the number of particles at lattice sites i consist of the mean-field number of particles \bar{n}_i and quantum fluctuations Δn_i

$$n_i = \underbrace{(\bar{c} + \bar{d})^2}_{=\bar{n}_i} + \Delta n_i \quad n_j = \underbrace{(\bar{c} - \bar{d})^2}_{=\bar{n}_j} + \Delta n_j. \quad (5.2)$$

The mean-field coefficients \bar{c} and \bar{d} are as in eq. (4.89) and eq. (4.88) calculated. For a further introduction into the Rotor-Model, see section 2.4 and section 2.4.

In the following, the given values for the number of particles eq. (5.2) are inserted into the Rotor-Hamiltonian eq. (5.1).

Kinetic part

As the first step, we insert the ansatz eq. (5.2) into the kinetic part of the Rotor-Hamiltonian eq. (5.1) and transform it into a more convenient form.

Hence, the kinetic part reads

$$H_1 = -2t \sum_{\langle i,j \rangle} \sqrt{\bar{n}_j \bar{n}_i} \sqrt{1 + \frac{\Delta n_j}{\bar{n}_j}} \sqrt{1 + \frac{\Delta n_i}{\bar{n}_i}} \cos(\varphi_i - \varphi_j). \quad (5.3)$$

We assume that the mean-field number of particles \bar{n}_i are much larger than the quantum fluctuations Δn_i , therefore we are allowed to expand the terms containing roots to quadratic order

$$\sqrt{1+x} \approx 1 + \frac{1}{2}x - \frac{1}{8}x^2. \quad (5.4)$$

This is being inserted into eq. (5.3) to further reduce the kinetic part of the Rotor-Hamiltonian

$$\begin{aligned} H_1 &= -2t \sum_{\langle i,j \rangle} \sqrt{\bar{n}_j \bar{n}_i} \left(1 + \frac{1}{2} \frac{\Delta n_j}{\bar{n}_j} - \frac{1}{8} \left(\frac{\Delta n_j}{\bar{n}_j} \right)^2 \right) \\ &\quad \left(1 + \frac{1}{2} \frac{\Delta n_i}{\bar{n}_i} - \frac{1}{8} \left(\frac{\Delta n_i}{\bar{n}_i} \right)^2 \right) \cos(\varphi_i - \varphi_j) \\ &= -2t \sum_{\langle i,j \rangle} \sqrt{\bar{n}_j \bar{n}_i} \left(1 + \frac{1}{2} \left(\frac{\Delta n_j}{\bar{n}_j} + \frac{\Delta n_i}{\bar{n}_i} \right) + \frac{1}{4} \frac{\Delta n_j \Delta n_i}{\bar{n}_j \bar{n}_i} \right. \\ &\quad \left. - \frac{1}{8} \left(\left(\frac{\Delta n_j}{\bar{n}_j} \right)^2 + \left(\frac{\Delta n_i}{\bar{n}_i} \right)^2 \right) \right) \cos(\varphi_i - \varphi_j). \end{aligned} \quad (5.5)$$

Next, all terms of higher order than quadratic in the quantum fluctuations Δn_i are neglected, because the contributions of higher orders are irrelevant for the stability consideration. The cosine term in eq. (5.5) can also be expanded to second order, with the same argumentation as in section 4.1.1

$$\cos x \approx 1 - \frac{1}{2}x^2. \quad (5.6)$$

With the expansion of the cosine term put into eq. (5.5) and taking only terms purely in Δn_i and φ_i into account, we arrive at

$$\begin{aligned} H_1 &= -2t \sum_{\langle i,j \rangle} \sqrt{\bar{n}_i \bar{n}_j} \left[1 + \frac{1}{2} \left(\frac{\Delta n_j}{\bar{n}_j} + \frac{\Delta n_i}{\bar{n}_i} \right) + \frac{1}{4} \frac{\Delta n_j \Delta n_i}{\bar{n}_j \bar{n}_i} \right. \\ &\quad \left. - \frac{1}{8} \left(\left(\frac{\Delta n_j}{\bar{n}_j} \right)^2 + \left(\frac{\Delta n_i}{\bar{n}_i} \right)^2 \right) - \frac{1}{2} (\varphi_i - \varphi_j)^2 \right], \end{aligned} \quad (5.7)$$

the kinetic part of the Rotor-Hamiltonian adjusted for our system. The selection of only pure terms Δn_i and φ_i was also done in section 4.1.1.

On-site interaction part

Our next item to do, is to compute the on-site interaction term of the Rotor-Hamiltonian for the considered system. As argued in section 4.6, there are two possible lattice sites available in the system, one with particle numbers n_i and the other with n_j . This has to be kept in mind at the further consideration

$$\begin{aligned}
H_2 &= \frac{U}{2} \sum_i n_i^2 \\
&= \frac{U}{2} \left[\sum_i n_i^2 + \sum_j n_j^2 \right] \\
&= \frac{U}{2} \left[\sum_i (\bar{n}_i + \Delta n_i)^2 + \sum_j (\bar{n}_j + \Delta n_j)^2 \right] \\
&= \frac{U}{2} \left[\sum_i (\bar{n}_i^2 + \Delta n_i^2 + 2\bar{n}_i \Delta n_i) + \sum_j (\bar{n}_j^2 + \Delta n_j^2 + 2\bar{n}_j \Delta n_j) \right]. \quad (5.8)
\end{aligned}$$

The two parts in the on-site interaction term can be combined, because they are of the same structure. Conclusively the summation index j can be renamed as i without missing a lattice site. This gives a more compact form for the on-site interaction part of the Rotor-Hamiltonian

$$H_2 = \frac{U}{2} \sum_i (\bar{n}_i^2 + \Delta n_i^2 + 2\bar{n}_i \Delta n_i). \quad (5.9)$$

When the summation of the on-site interaction part eq. (5.9) is carried out, we have to be careful, at which site i we are looking at. There are two possibilities, either a site with a large particle number n_i are one with few n_j . This has to be kept in mind for further calculations.

Nearest-neighbor interaction part

Now we look at the nearest-neighbor interaction term of the Rotor-Hamiltonian. Inserting the number of particles eq. (5.2) gives

$$\begin{aligned}
H_3 &= \frac{V}{2} \sum_{\langle i, j \rangle} n_i n_j \\
&= \frac{V}{2} \sum_{\langle i, j \rangle} (\bar{n}_i + \Delta n_i) (\bar{n}_j + \Delta n_j).
\end{aligned}$$

Hence, the nearest-neighbor interaction part for the Rotor-Hamiltonian becomes

$$H_3 = \frac{V}{2} \sum_{\langle i, j \rangle} (\bar{n}_i \bar{n}_j + \bar{n}_i \Delta n_j + \bar{n}_j \Delta n_i + \Delta n_i \Delta n_j). \quad (5.10)$$

Chemical potential part

Finally we analyze the term containing the chemical potential in the Rotor-Hamiltonian eq. (5.1). The chemical potential μ takes care of the total number of particles in the system. Again, we have to be careful at the summation over all possible lattice sites i , since there are two possibilities

$$\begin{aligned} H_4 &= -\mu \sum_i n_i \\ &= -\mu \left[\sum_i (\bar{n}_i + \Delta n_i) + \sum_j (\bar{n}_j + \Delta n_j) \right]. \end{aligned}$$

The summation index j in the equation above, can again be renamed as i . If the summation over all lattice sites i is carried out, the nature of the lattice sites has to be reminded. The chemical potential part for the Rotor-Hamiltonian reduces to

$$H_4 = -\mu \sum_i (\bar{n}_i + \Delta n_i). \quad (5.11)$$

The unsorted Rotor-Hamiltonian

With all parts of the Rotor-Hamiltonian computed for our considered system, we have to sum all four parts to obtain it

$$\begin{aligned} H &= -2t \sum_{\langle i,j \rangle} \sqrt{\bar{n}_i \bar{n}_j} \left[1 + \frac{1}{2} \left(\frac{\Delta n_j}{\bar{n}_j} + \frac{\Delta n_i}{\bar{n}_i} \right) + \frac{1}{4} \frac{\Delta n_j \Delta n_i}{\bar{n}_j \bar{n}_i} \right. \\ &\quad \left. - \frac{1}{8} \left(\left(\frac{\Delta n_j}{\bar{n}_j} \right)^2 + \left(\frac{\Delta n_i}{\bar{n}_i} \right)^2 \right) - \frac{1}{2} (\varphi_i - \varphi_j)^2 \right] \\ &\quad + \frac{U}{2} \sum_i (\bar{n}_i^2 + \Delta n_i^2 + 2\bar{n}_i \Delta n_i) \\ &\quad + \frac{V}{2} \sum_{\langle i,j \rangle} (\bar{n}_i \bar{n}_j + \bar{n}_i \Delta n_j + \bar{n}_j \Delta n_i + \Delta n_i \Delta n_j) \\ &\quad - \mu \sum_i (\bar{n}_i + \Delta n_i). \end{aligned} \quad (5.12)$$

The sorted Rotor-Hamiltonian

The next step is to sort the Rotor-Hamiltonian eq. (5.12) in orders of $\mathcal{O}(\Delta n_i)$. The linear parts of the quantum fluctuations Δn_i have to vanish and for this reason the sortation is carried out. Appendix A contains the procedure, only the result is given

$$\begin{aligned}
H = & -2t \sum_{\langle i,j \rangle} \sqrt{\bar{n}_i \bar{n}_j} \left(1 - \frac{1}{2} (\varphi_i - \varphi_j)^2 \right) + \frac{U}{2} \sum_i \bar{n}_i^2 + \frac{V}{2} \sum_{\langle i,j \rangle} \bar{n}_i \bar{n}_j - \mu \sum_i \bar{n}_i \\
& - 2t \sum_{\langle i,j \rangle} \sqrt{\frac{\bar{n}_j}{\bar{n}_i}} \Delta n_i + U \sum_i \bar{n}_i \Delta n_i + V \sum_{\langle i,j \rangle} \bar{n}_j \Delta n_i - \mu \sum_i \Delta n_i \\
& + \frac{1}{2} \sum_{\langle i,j \rangle} \Delta n_i \Delta n_j \left[V - \frac{t}{\sqrt{\bar{n}_i \bar{n}_j}} \right] + \frac{t}{2} \sum_{\langle i,j \rangle} \frac{\sqrt{\bar{n}_i \bar{n}_j}}{\bar{n}_i^2} \Delta n_i^2 + \frac{U}{2} \sum_i \Delta n_i^2.
\end{aligned} \tag{5.13}$$

5.1.1 Analysis of the linear order in Δn_i

The part of the Rotor-Hamiltonian eq. (5.13), which is of linear order in Δn_i has to vanish. The linear part reads

$$H_{\text{linear}} = -2t \sum_{\langle i,j \rangle} \sqrt{\frac{\bar{n}_j}{\bar{n}_i}} \Delta n_i + U \sum_i \bar{n}_i \Delta n_i + V \sum_{\langle i,j \rangle} \bar{n}_j \Delta n_i - \mu \sum_i \Delta n_i. \tag{5.14}$$

There are two possible cases of lattice site occupation, when the summation over all possible sites i is carried out. In the following, we write the two cases. For sake of simplicity, we substitute \bar{n}_i by f_1 and \bar{n}_j by f_2 . The two cases then are

$$H_{\text{linear}} = \begin{cases} -2t \sum_j \sqrt{\frac{f_2}{f_1}} \Delta n_i + U f_1 \Delta n_i + V \sum_j f_2 \Delta n_i - \mu \Delta n_i \\ -2t \sum_j \sqrt{\frac{f_1}{f_2}} \Delta n_i + U f_2 \Delta n_i + V \sum_j f_1 \Delta n_i - \mu \Delta n_i. \end{cases} \tag{5.15}$$

Here, we assume that the quantities f_1 and f_2 are independent of i and j . This is a simplification for the further evaluation. Thus, the two cases can be rewritten as

$$H_{\text{linear}} = \begin{cases} \left(-2tz \sqrt{\frac{f_2}{f_1}} + U f_1 + zV f_2 - \mu \right) \Delta n_i =: g_1 \Delta n_i \\ \left(-2tz \sqrt{\frac{f_1}{f_2}} + U f_2 + zV f_1 - \mu \right) \Delta n_i =: g_2 \Delta n_i. \end{cases} \tag{5.16}$$

Hence, the Rotor-Hamiltonian part H_{linear} , which is of linear order in Δn_i can now be written in a compact form

$$H_{\text{linear}} = g_i \Delta n_i, \tag{5.17}$$

it depends on the considered lattice site i , where the function g_i is

$$g_i = \begin{cases} g_1 \\ g_2. \end{cases} \tag{5.18}$$

The function g_i can be expressed in a way, that its fluctuating nature, becomes obvious

$$g_i = \frac{g_1 + g_2}{2} + \left(\frac{g_1 - g_2}{2} \right) \cos(kR_i), \tag{5.19}$$

with R_i being the lattice site coordinate. This means, that the function g_i is a fluctuating function, which depends on the considered lattice site.

Since H_{linear} eq. (5.17) has to vanish, we have to determine the functions g_i in such a way, that it is always zero. In eq. (5.19) we see, that g_i consists of two parts. The second part is multiplied by a cosine, which lets the second part become zero, only at certain values of kR_i . We are interested in a case, where g_i is always zero, thus both parts of g_i eq. (5.19) have to be zero separately. Therefore

$$\frac{g_1 + g_2}{2} \stackrel{!}{=} 0 \quad \wedge \quad \frac{g_1 - g_2}{2} \stackrel{!}{=} 0. \quad (5.20)$$

The right hand side of eq. (5.20) becomes zero, when $\cos(kR_i)$ does, despite that, it still has to be zero for any R_i , as argued before.

As a next step, we calculate both parts consisting in g_i eq. (5.19). At first, we compute the left hand side of eq. (5.20)

$$\begin{aligned} \frac{g_1 + g_2}{2} &= \frac{1}{2} \left\{ \left(-2tz \sqrt{\frac{f_2}{f_1}} + Uf_1 + zVf_2 - \mu \right) + \left(-2tz \sqrt{\frac{f_1}{f_2}} + Uf_2 + zVf_1 - \mu \right) \right\} \\ &= \frac{1}{2} \left\{ -2tz \left[\sqrt{\frac{f_2}{f_1}} + \sqrt{\frac{f_1}{f_2}} \right] + U \left[\underbrace{f_1 + f_2}_{=2n} \right] + zV \left[\underbrace{f_2 + f_1}_{=2n} \right] - 2\mu \right\} \\ &= \left\{ -tz \left[\frac{\overbrace{f_2 + f_1}^{=2n}}{\sqrt{f_1 f_2}} \right] + n[U + zV] - \mu \right\} \\ &= \left\{ -\frac{2tzn}{\sqrt{f_1 f_2}} + n[U + zV] - \mu \right\} \stackrel{!}{=} 0, \end{aligned} \quad (5.21)$$

the brackets marked with "2n" results in the fact, that if functions f_1 and f_2 are summed, they equal twice the mean particle number per lattice site. This can easily be proofed by inserting the definitions for the functions $f_{1,2}$, see appendix B.1.

With eq. (5.21), we are now able to calculate the chemical potential μ for our system

$$\mu = n \left[-\frac{2tz}{\sqrt{f_1 f_2}} + (U + zV) \right]. \quad (5.22)$$

The chemical potential still depends on the function $\sqrt{f_1 f_2}$, thus we have to determine the right hand side of eq. (5.20)

$$\begin{aligned} \frac{g_1 - g_2}{2} &= \frac{1}{2} \left\{ \left[-2tz \sqrt{\frac{f_2}{f_1}} + Uf_1 + zVf_2 - \mu \right] - \left[-2tz \sqrt{\frac{f_1}{f_2}} + Uf_2 + zVf_1 - \mu \right] \right\} \\ &= \frac{1}{2} \left\{ -2tz \left[\frac{f_2 - f_1}{\sqrt{f_1 f_2}} \right] + U[f_1 - f_2] + zV[f_2 - f_1] \right\}. \end{aligned} \quad (5.23)$$

To further compute eq. (5.23), we introduce the following substitution

$$\Delta = f_1 - f_2, \quad (5.24)$$

this can be inserted into eq. (5.23). It has to be kept in mind, that $\Delta \neq \Delta n_i$. The right side of eq. (5.20) thus becomes

$$\frac{g_1 - g_2}{2} = \frac{1}{2} \left\{ -2tz \left[\frac{-\Delta}{\sqrt{f_1 f_2}} \right] + U \Delta + zV(-\Delta) \right\} \quad (5.25)$$

$$= \frac{\Delta}{2} \left\{ \frac{2tz}{\sqrt{f_1 f_2}} + (U - zV) \right\} \stackrel{!}{=} 0. \quad (5.26)$$

Since neither Δn_i nor Δ can be zero, the bracket has to be and this leads us to the determination of the desired function $\sqrt{f_1 f_2}$

$$\begin{aligned} 0 &= \frac{2tz}{\sqrt{f_1 f_2}} + (U - zV) \\ \Rightarrow \sqrt{f_1 f_2} &= \frac{2tz}{(zV - U)}. \end{aligned} \quad (5.27)$$

With the function $\sqrt{f_1 f_2}$ being obtained, the chemical potential μ eq. (5.22) can be expressed in terms without functions f_1 and f_2

$$\mu = 2Un. \quad (5.28)$$

If the chemical potential μ eq. (5.28) and the functions $\sqrt{f_1 f_2}$ eq. (5.27) are inserted into the function g_i eq. (5.19), we find, that it is always zero, independent of the considered lattice site.

The Rotor-Hamiltonian eq. (5.13) without the linear parts in Δn_i thus is

$$\begin{aligned} H = & -2t \sum_{\langle i, j \rangle} \sqrt{\bar{n}_i \bar{n}_j} \left(1 - \frac{1}{2} (\varphi_i - \varphi_j)^2 \right) + \frac{U}{2} \sum_i \bar{n}_i^2 + \frac{V}{2} \sum_{\langle i, j \rangle} \bar{n}_i \bar{n}_j - \mu \sum_i \bar{n}_i \\ & + \frac{1}{2} \sum_{\langle i, j \rangle} \Delta n_i \Delta n_j \left[V - \frac{t}{\sqrt{\bar{n}_i \bar{n}_j}} \right] + \frac{t}{2} \sum_{\langle i, j \rangle} \frac{\sqrt{\bar{n}_i \bar{n}_j}}{\bar{n}_i^2} \Delta n_i^2 + \frac{U}{2} \sum_i \Delta n_i^2, \end{aligned} \quad (5.29)$$

where eq. (5.28) for the chemical potential μ and eq. (5.27) for the function $\sqrt{f_1 f_2}$ still need to be inserted.

5.1.2 Comparing the Hamiltonians

Until now, we computed the Rotor-Hamiltonian for our system and cancelled out all the linear terms in the quantum fluctuations Δn_i . This was done by evaluating the function g_i eq. (5.19) to be zero independent of the lattice site i . The next step is to further reduce the Rotor-Hamiltonian eq. (5.29), by analyzing its behavior at different lattice site occupations n_i or n_j . Therefore we write the Rotor-Hamiltonian eq. (5.29) for the two types of lattice site occupation

$$\begin{aligned}
H' &= -2t \sum_j \sqrt{f_1 f_2} \left(1 - \frac{1}{2} (\varphi_i - \varphi_j)^2\right) + \frac{U}{2} f_1^2 + \frac{V}{2} \sum_j f_1 f_2 - \mu f_1 \\
&\quad + \frac{1}{2} \sum_j \Delta n_i \Delta n_j \left[V - \frac{t}{\sqrt{f_1 f_2}} \right] + \frac{t}{2} \sum_j \frac{\sqrt{f_1 f_2}}{\bar{n}_i^2} \Delta n_i^2 + \frac{U}{2} \Delta n_i^2 \\
&= -2t \sum_j \underbrace{\sqrt{f_1 f_2} \left(1 - \frac{1}{2} (\varphi_i - \varphi_j)^2\right)}_1 + \underbrace{\frac{U}{2} f_1^2}_2 + \underbrace{\frac{zV}{2} f_1 f_2}_3 - \underbrace{\mu f_1}_4 \\
&\quad + \frac{1}{2} \sum_j \underbrace{\Delta n_i \Delta n_j \left[V - \frac{t}{\sqrt{f_1 f_2}} \right]}_5 + \frac{\Delta n_i^2}{2} \left[\underbrace{zt \frac{\sqrt{f_1 f_2}}{\bar{n}_i^2}}_6 + \underbrace{U}_7 \right], \tag{5.30}
\end{aligned}$$

$$\begin{aligned}
H'' &= -2t \sum_j \sqrt{f_2 f_1} \left(1 - \frac{1}{2} (\varphi_i - \varphi_j)^2\right) + \frac{U}{2} f_2^2 + \frac{V}{2} \sum_j f_2 f_1 - \mu f_2 \\
&\quad + \frac{1}{2} \sum_j \Delta n_i \Delta n_j \left[V - \frac{t}{\sqrt{f_2 f_1}} \right] + \frac{t}{2} \sum_j \frac{\sqrt{f_2 f_1}}{\bar{n}_i^2} \Delta n_i^2 + \frac{U}{2} \Delta n_i^2 \\
&= -2t \sum_j \underbrace{\sqrt{f_2 f_1} \left(1 - \frac{1}{2} (\varphi_i - \varphi_j)^2\right)}_{1'} + \underbrace{\frac{U}{2} f_2^2}_{2'} + \underbrace{\frac{zV}{2} f_2 f_1}_{3'} - \underbrace{\mu f_2}_{4'} \\
&\quad + \frac{1}{2} \sum_j \underbrace{\Delta n_i \Delta n_j \left[V - \frac{t}{\sqrt{f_2 f_1}} \right]}_{5'} + \frac{\Delta n_i^2}{2} \left[\underbrace{zt \frac{\sqrt{f_2 f_1}}{\bar{n}_i^2}}_{6'} + \underbrace{U}_{7'} \right], \tag{5.31}
\end{aligned}$$

where the Hamiltonian H' considers a site with many particles n_i and H'' one with few n_j . The functions \bar{n}_i and \bar{n}_j were substituted by f_1 and f_2 as introduced earlier. Those terms containing an underbrace, are the interesting ones, we want to analyze further.

Before the Hamiltonians H' and H'' for the different lattice site occupations can be summed, we have to consider the different behaviors of those terms. Some terms can be added together, where others can not and thus the summation of the possible lattice sites can only be carried out to $N/2$. Now we want to consider the different parts of the Rotor-Hamiltonians eq. (5.30 + 5.31)

- part 1, 1': are the same in both cases, thus the parts can be added together and the summation can be done to N
- part 2, 2': are different, since the on-site interaction depends on the number of particles in each site, hence each summation can only be done to $N/2$
- part 3, 3': equal terms, because in one case the interaction between particles at site i with f_1 and at site j with f_2 particles are considered, and at the other case vice versa,

thus the terms can be added together and the summation can be done to N

- part 4, 4': terms differ from each other, there are different number of particles in the according sites, hence the summation can only be done to N/2
- part 5, 5': are the same terms, the reasoning goes as in the case for the nearest-neighbor interaction, the terms can be added together and the summation can be carried out to N
- part 6, 6': are not the same terms, their are fluctuating functions, a summation can only go to N/2 and the summation index has to be changed in one case to i'
- part 7, 7': same terms, can be added together and summation is carried out to N

After this analysis of the different Rotor-Hamiltonians eq. (5.30) and eq. (5.31), we can sum them as argued before

$$\begin{aligned}
H = & -2t \sum_{\langle i,j \rangle}^N \sqrt{f_1 f_2} \left(1 - \frac{1}{2} (\varphi_i - \varphi_j)^2 \right) + \frac{U}{2} \left(\sum_i^{N/2} f_1^2 + \sum_i^{N/2} f_2^2 \right) \\
& + \sum_i^N \frac{zV}{2} f_1 f_2 - \mu \left(\sum_i^{N/2} f_1 + \sum_i^{N/2} f_2 \right) + \frac{1}{2} \sum_{\langle i,j \rangle}^N \Delta n_i \Delta n_j \left[V - \frac{t}{\sqrt{f_1 f_2}} \right] \\
& + \sum_i^N \frac{U}{2} \Delta n_i + \frac{zt}{2} \sqrt{f_1 f_2} \left[\sum_i^{N/2} \frac{\Delta n_i^2}{\bar{n}_i^2} + \sum_{i'}^{N/2} \frac{\Delta n_{i'}^2}{\bar{n}_{i'}^2} \right].
\end{aligned}$$

We further reduce the above Rotor-Hamiltonian by carrying out possible summations

$$\begin{aligned}
H = & -2t \sqrt{f_1 f_2} \sum_{\langle i,j \rangle}^N \left(1 - \frac{1}{2} (\varphi_i - \varphi_j)^2 \right) + \frac{UN}{4} (f_1^2 + f_2^2) + \frac{NzV}{2} f_2 f_1 \\
& - \frac{N\mu}{2} (f_1 + f_2) + \frac{1}{2} \sum_{\langle i,j \rangle}^N \Delta n_i \Delta n_j \left[V - \frac{t}{\sqrt{f_1 f_2}} \right] + \sum_i^N \frac{U}{2} \Delta n_i \\
& + \frac{zt}{2} \sqrt{f_1 f_2} \left[\sum_i^{N/2} \frac{\Delta n_i^2}{\bar{n}_i^2} + \sum_{i'}^{N/2} \frac{\Delta n_{i'}^2}{\bar{n}_{i'}^2} \right]. \tag{5.32}
\end{aligned}$$

Now we sort the Rotor-Hamiltonian eq. (5.32) in parts

$$\begin{aligned}
H = & -2t\sqrt{f_1 f_2} \sum_{\langle i, j \rangle}^N (1) + \frac{UN}{4} (f_1^2 + f_2^2) + \frac{NzV}{2} f_1 f_2 - \frac{N\mu}{2} (f_1 + f_2) \\
& + 2t\sqrt{f_1 f_2} \sum_{\langle i, j \rangle}^N \left(\frac{1}{2} (\varphi_i - \varphi_j)^2 \right) + \frac{1}{2} \sum_{\langle i, j \rangle}^N \Delta n_i \Delta_j \left[V - \frac{t}{\sqrt{f_1 f_2}} \right] + \frac{U}{2} \sum_i^N \Delta n_i^2 \\
& + \frac{zt}{2} \sqrt{f_1 f_2} \left[\sum_i^{N/2} \frac{\Delta n_i^2}{\bar{n}_i^2} + \sum_i^{N/2} \frac{\Delta n_{i'}^2}{\bar{n}_{i'}^2} \right]. \tag{5.33}
\end{aligned}$$

5.1.3 Calculating the mean-field part

In the next step, we want to evaluate the mean-field energy for the considered system. This is done by taking the parts of the Rotor-Hamiltonian eq. (5.33), which are independent of the phase φ_i and the quantum fluctuations Δn_i

$$\begin{aligned}
E_{\text{MF}} = & -2t\sqrt{f_1 f_2} \sum_{\langle i, j \rangle}^N (1) + \frac{UN}{4} (f_1^2 + f_2^2) + \frac{NzV}{2} f_1 f_2 - \frac{N\mu}{2} (f_1 + f_2) \\
= & -2t\sqrt{f_1 f_2} Nz + \frac{UN}{4} (f_1^2 + f_2^2) + \frac{NzV}{2} f_1 f_2 - \frac{N\mu}{2} (f_1 + f_2). \tag{5.34}
\end{aligned}$$

Now we insert the determined value for the function $\sqrt{f_1 f_2}$, as calculated in eq. (5.27). We also include the substitution done earlier, where we set $f_1 = \bar{n}_i$ and $f_2 = \bar{n}_j$. The quantities \bar{n}_i are as defined in eq. (5.2). The values \bar{c} and \bar{d} , which construct the mean-field number of particles \bar{n}_i are

$$\bar{c} = \sqrt{\frac{n}{2} - \frac{zt}{(U - zV)}}, \tag{5.35}$$

$$\bar{d} = \sqrt{\frac{n}{2} + \frac{zt}{(U - zV)}}, \tag{5.36}$$

as computed in section 4.6.1.

All this can be plugged into eq. (5.34) to calculate the mean-field energy E_{MF}

$$\begin{aligned}
E_{\text{MF}} = & -2t \left(-\frac{2tz}{(U - zV)} \right) Nz + \frac{NU}{4} \left((\bar{c} + \bar{d})^4 + (\bar{c} - \bar{d})^4 \right) \\
& + \frac{NzV}{2} \left(-\frac{2tz}{(U - zV)} \right)^2 - \frac{N\mu}{2} (2n) \\
= & \frac{4t^2 z^2 N}{(U - zV)} + \frac{UN}{4} \left(2(\bar{c}^4 + 6\bar{c}^2 \bar{d}^2 + \bar{d}^4) \right) + \frac{NzV}{2} \frac{4t^2 z^2}{(U - zV)^2} - N\mu n. \tag{5.37}
\end{aligned}$$

At this point, we insert the computed values for \bar{c} of eq. (4.89) and \bar{d} of eq. (4.88). The mean-field energy thus becomes

$$\begin{aligned}
E_{\text{MF}} &= \frac{4t^2z^2N}{(U-zV)} + \frac{UN}{2} \left[\left(\frac{n}{2} - \frac{zt}{U-zV} \right)^2 + 6 \left(\frac{n}{2} - \frac{zt}{U-zV} \right) \right. \\
&\quad \left. \times \left(\frac{n}{2} + \frac{zt}{U-zV} \right) + \left(\frac{n}{2} + \frac{zt}{U-zV} \right)^2 \right] \\
&\quad + NzV \frac{2t^2z^2}{(U-zV)^2} - N\mu n \\
&= \frac{4t^2z^2N}{(U-zV)} + UN \left[n^2 - 2 \frac{z^2t^2}{(U-zV)} \right] + NzV \frac{2z^2t^2}{(U-zV)} - N\mu n \\
&= \frac{4t^2z^2N}{(U-zV)} + UNn^2 - \mu Nn - \frac{2z^2t^2N}{(U-zV)^2} (U-zV) \\
&= \frac{2t^2z^2N}{(U-zV)} + Un^2N - \mu Nn. \tag{5.38}
\end{aligned}$$

If eq. (5.38) the mean-field energy for the considered grand canonical ensemble is compared to the energy density of the ground state, in the previously done mean-field calculations eq. (4.91), we find, that it only differs by a part $-\mu Nn$. This part originates in the fact, that we have included the chemical potential μ into the evaluation done so far. Thus, our calculations so far, are consistent with the mean-field considerations done in chapter 4.

To obtain the mean-field energy for the grand canonical ensemble, we have to insert the calculated chemical potential eq. (5.28) into the mean-field energy eq. (5.38). Therefore we get the value for the mean-field energy E_{MF}

$$E_{\text{MF}} = N \left[\frac{2t^2z^2}{U-zV} - Un^2 \right], \tag{5.39}$$

where N is the number of lattice sites, t the hopping constant, z the number of nearest neighbors, U the on-site interaction, V the nearest-neighbor interaction and n is the mean number of particles in a lattice site.

5.1.4 The final Rotor-Hamiltonian in real space

After completing the above calculation, we are closer to finally write the Rotor-Hamiltonian in real space. To do so, we rewrite the Rotor-Hamiltonian in eq. (5.33) as

$$\begin{aligned}
H &= E_{\text{MF}} + t\sqrt{f_1f_2} \sum_{\langle i,j \rangle} (\varphi_i - \varphi_j)^2 + \frac{1}{2} \sum_{\langle i,j \rangle} \Delta n_i \Delta n_j \left[V - \frac{t}{\sqrt{f_1f_2}} \right] \\
&\quad + \frac{U}{2} \sum_i \Delta n_i^2 + \frac{zt}{2} \sqrt{f_1f_2} \left[\sum_i^{N/2} \frac{\Delta n_i^2}{\bar{n}_i^2} + \sum_{i'}^{N/2} \frac{\Delta n_{i'}^2}{\bar{n}_{i'}^2} \right]. \tag{5.40}
\end{aligned}$$

In the next step, we insert the value of the function $\sqrt{f_1 f_2}$, as obtained in eq. (5.27) and then get

$$\begin{aligned} H = & E_{\text{MF}} + t \left(\frac{2tz}{(zV-U)} \right) \sum_{\langle i,j \rangle}^N (\varphi_i - \varphi_j)^2 + \frac{1}{2} \sum_{\langle i,j \rangle}^N \Delta n_i \Delta n_j \left[V - \frac{t}{\left(\frac{2zt}{(zV-U)} \right)} \right] \\ & + \frac{U}{2} \sum_i \Delta n_i^2 + \frac{zt}{2} \left(\frac{2tz}{(zV-U)} \right) \left[\sum_i^{N/2} \frac{\Delta n_i^2}{\bar{n}_i^2} + \sum_{i'}^{N/2} \frac{\Delta n_{i'}^2}{\bar{n}_{i'}^2} \right]. \end{aligned} \quad (5.41)$$

Within the proceeding reduction we have to introduce new coefficients allowing us to construct the above equation in a terse form. These coefficients are

$$E_1 = \frac{2t^2 z}{(zV-U)}, \quad (5.42)$$

$$E_2 = \frac{1}{4} \left[V + \frac{U}{z} \right], \quad (5.43)$$

$$E_3 = \frac{U}{2}, \quad (5.44)$$

$$E_4 = \frac{t^2 z^2}{(zV-U)}. \quad (5.45)$$

Thus we can write the Rotor-Hamiltonian eq. (5.41) as

$$\begin{aligned} H = & E_{\text{MF}} + E_1 \sum_{\langle i,j \rangle}^N (\varphi_i - \varphi_j)^2 + E_2 \sum_{\langle i,j \rangle}^N \Delta n_i \Delta n_j \\ & + E_3 \sum_i \Delta n_i^2 + E_4 \left[\sum_i^{N/2} \frac{\Delta n_i^2}{\bar{n}_i^2} + \sum_{i'}^{N/2} \frac{\Delta n_{i'}^2}{\bar{n}_{i'}^2} \right]. \end{aligned} \quad (5.46)$$

5.2 Fourier Transformation of the Rotor-Hamiltonian

Our goal for the whole calculation done so far, is to reach the dispersion relation for our system. With the Rotor-Hamiltonian eq. (5.46) brought into a compact form, we now have to Fourier transform it.

5.2.1 Fourier Transformation Part 1

We start the transformation by considering the Rotor-Hamiltonian eq. (5.46) without the fluctuating part. This part is the last term in eq. (5.46). It has to be analyzed, before a Fourier transformation can be done. The next section is going to do this.

Thus, the Rotor-Hamiltonian eq. (5.46) without fluctuations is

$$\begin{aligned}
H &= E_{\text{MF}} + E_1 \sum_{\langle i, j \rangle}^N (\varphi_i - \varphi_j)^2 \\
&\quad + E_2 \sum_{\langle i, j \rangle}^N \Delta n_i \Delta n_j + E_3 \sum_i \Delta n_i^2.
\end{aligned} \tag{5.47}$$

The Fourier transformation of the Hamiltonian eq. (5.47) can be done similarly as in the previous chapter in section 4.2. Therefore only the result of the transformation is given

$$\begin{aligned}
H &= E_{\text{MF}} + E_1 \sum_k 2\varphi_k \varphi_{-k} \left[z - 2 \sum_{\alpha} \cos(k_{\alpha} a) \right] \\
&\quad + E_2 \sum_{k, \alpha} 2\Delta n_k \Delta n_{-k} \cos(k_{\alpha} a) + E_3 \sum_k \Delta n_k \Delta n_{-k},
\end{aligned} \tag{5.48}$$

where the mean-field energy E_{MF} is as in eq. (5.39) and the coefficients $E_1 - E_3$ are as defined in equations (5.42 - 5.44).

By introducing again new coefficients

$$E'_1 = \frac{4t^2 z}{(zV - U)}, \tag{5.49}$$

$$E'_2 = \frac{1}{2} \left[\left(V + \frac{U}{z} \right) \sum_{\alpha} \cos(k_{\alpha} a) + U \right], \tag{5.50}$$

we can rewrite the Fourier transformed Rotor-Hamiltonian eq. (5.48) as

$$H(k) = E_{\text{MF}} + E'_1 \sum_k \varphi_k \varphi_{-k} \left[z - 2 \sum_{\alpha} \cos(k_{\alpha} a) \right] + \sum_k \Delta n_k \Delta n_{-k} E'_2. \tag{5.51}$$

This Hamiltonian can now be diagonalized with the same technique as introduced in section 4.3 of the previous chapter. It can be diagonalized, because it is of the same form as in section 4.3. Thus, we can give the diagonal Rotor-Hamiltonian for the case without the fluctuating part

$$H = E_{\text{MF}} + \sum_k \sqrt{\frac{8t^2 z}{(zV - U)} \left[z - 2 \sum_{\alpha} \cos(k_{\alpha} a) \right] \left[\left(V + \frac{U}{z} \right) \sum_{\alpha} \cos(k_{\alpha} a) + U \right]} \left(\alpha_k^{\dagger} \alpha_k + \frac{1}{2} \right). \tag{5.52}$$

The evaluation the the diagonal Rotor-Hamiltonian is only given for sake of completeness. The fluctuating part of the Rotor-Hamiltonian eq. (5.46) has to be taken into account too, at diagonalizing the Hamiltonian.

5.2.2 Fourier Transformation Part2

As argued above, the Fourier transformation of the fourth part of the Rotor-Hamiltonian eq. (5.46) is still due. In this section, we want to get more insight of the fluctuating part

$$H_4 = E_4 \left[\sum_i^{N/2} \frac{\Delta n_i^2}{\bar{n}_i^2} + \sum_{i'}^{N/2} \frac{\Delta n_{i'}^2}{\bar{n}_{i'}^2} \right], \quad (5.53)$$

where the coefficient E_4 is, as defined in eq. (5.45) .

The equation above can be written with a lattice site depending coefficient U_i

$$H_4 = E_4 \sum_i^N U_i \Delta n_i^2, \quad (5.54)$$

where the introduced coefficient U_i is

$$U_i = \begin{cases} \frac{1}{f_1^2} = \frac{1}{\bar{n}_i^2}, & \text{at site } n_i \\ \frac{1}{f_2^2} = \frac{1}{\bar{n}_{i'}^2} & \text{at site } n_{i'}. \end{cases} \quad (5.55)$$

The Fourier transformation can now be carried out. In this case, the coefficient U_i has to be transformed too. This is done with

$$U_i = \sum_q e^{iqx_i} U_q. \quad (5.56)$$

The Fourier transformation for the quadratic quantum fluctuations is done similarly as in section 4.2.2 of the previous chapter. The routine is now carried out in the same way, except for the inclusion of the coefficient U_i

$$\begin{aligned} \sum_i^N U_i \Delta n_i^2 &= \sum_i \left(\sum_q e^{iqx_i} U_q \right) \left(\frac{1}{\sqrt{N}} \sum_k e^{ikx_i} \Delta n_k \right) \left(\frac{1}{N} \sum_{k'} e^{ik'x_i} \Delta n_{k'} \right) \\ &= \frac{1}{N} \sum_{i, k, k', q} U_q \Delta n_k \Delta n_{k'} e^{i(q+k+k')x_i} \\ &= \frac{1}{N} \sum_{k, k', q} U_q \Delta n_k \Delta n_{k'} N \delta_{k-(k+q)} \\ &= \sum_{k, q} U_q \Delta n_k \Delta n_{-(k+q)}. \end{aligned} \quad (5.57)$$

There are two possible cases for the Fourier transformed coefficient U_q . Either we are interested in the value of the coefficient at the center of the first Brillouin zone at $q = 0$ or at the boundary $q = K$. The quantity K is a reciprocal lattice vector. Thus, the fluctuating functions eq. (5.57) splits up into two parts

$$H_4 = E_4 \left(\underbrace{\sum_k U_0 \Delta n_k \Delta n_{-k}}_1 + \underbrace{\sum_k U_1 \Delta n_k \Delta n_{-(k+K)}}_2 \right) \quad (5.58)$$

where the two coefficients U_0 and U_1 are

$$U_0 = \frac{1}{2} \left(\frac{1}{f_1^2} + \frac{1}{f_2^2} \right) \quad (5.59)$$

$$U_1 = \frac{1}{2} \left(\frac{1}{f_1^2} - \frac{1}{f_2^2} \right). \quad (5.60)$$

This tells us, that the fluctuating parts contribute two different parts to the Fourier transformed Rotor-Hamiltonian. Thus, the first part with the coefficient U_0 is responsible for further diagonal contributions to the Rotor-Hamiltonian. The second part in eq. (5.58) with the coefficient U_1 delivers off-diagonal contributions.

Next, the first part of eq. (5.58) with the diagonal contributions is added to the Rotor-Hamiltonian in eq. (5.51)

$$\begin{aligned} H(k) = & E_{\text{MF}} + E'_1 \sum_k \varphi_k \varphi_{k'} \left[z - 2 \sum_{\alpha} \cos(k_{\alpha} a) \right] \\ & + \sum_k \Delta n_k \Delta n_{-k} \left[E'_2 + \frac{E_4}{2} \left(\frac{1}{f_1^2} + \frac{1}{f_2^2} \right) \right]. \end{aligned} \quad (5.61)$$

We then have to calculate the coefficient U_0 eq. (5.59). This is done by inserting the values for \bar{c} eq. (4.89) and \bar{d} eq. (4.88), since the coefficient f_1 and f_2 consist of these two values. The calculation is straight forward and presented in the appendix B.2.

With the coefficient U_0 determined, the quantities E'_2 of eq. (5.50) and E_4 of eq. (5.45) are plugged into above equation, together with U_0

$$\begin{aligned} H(k) = & E_{\text{MF}} + E'_1 \sum_k \varphi_k \varphi_{-k} \left[z - 2 \sum_{\alpha} \cos(k_{\alpha} a) \right] \\ & + \sum_k \Delta n_k \Delta n_{-k} \left[\frac{1}{2} \left[\left(V + \frac{U}{z} \right) \sum_{\alpha} \cos(k_{\alpha} a) + U \right] \right. \\ & \left. + \frac{(zV - U)}{4} \left(\frac{n^2 (U - zV)^2}{2z^2 t^2} - 1 \right) \right]. \end{aligned} \quad (5.62)$$

The above Rotor-Hamiltonian can now be diagonalized in the same manner as done earlier in section 4.3 by introducing relations between the phases φ_i , the quantum fluctuations Δn_i and the new creation a_k^{\dagger} and annihilation operators a_k . The diagonalized Rotor-Hamiltonian then, again, becomes of the harmonic oscillator form

$$H = E_{\text{MF}} + \sum_k E''(k) \left(\alpha_k^{\dagger} \alpha_k + \frac{1}{2} \right), \quad (5.63)$$

with the dispersion relation $E''(k)$ being

$$\begin{aligned}
E''(k) = & \left\{ \frac{8t^2z}{zV-U} \left[z - 2 \sum_{\alpha} \cos(k_{\alpha}a) \right] \right. \\
& \times \left. \left[\left(V + \frac{U}{z} \right) \sum_{\alpha} \cos(k_{\alpha}a) + U + \frac{zV-U}{2} \left(\frac{n^2(U-zV)^2}{2z^2t^2} - 1 \right) \right] \right\}^{1/2}. \quad (5.64)
\end{aligned}$$

5.2.3 Fourier Transformation Part3

So far we have diagonalized the Rotor-Hamiltonian eq. (5.46) without considering the contributions of the fluctuating part eq. (5.53). Then, we took the fluctuating part along, but only with the diagonal contributions to the Rotor-Hamiltonian and thus found the diagonalized Hamiltonian eq. (5.63). The next logical step would be, to also consider the off-diagonal terms of the fluctuating Hamiltonian part eq. (5.53).

The coefficient U_1 , which contributes the off-diagonal parts, is calculated in the appendix B.3. In the following, only the result of this computation is used.

The whole Rotor-Hamiltonian eq. (5.46) Fourier transformed, with off-diagonal terms, reads

$$\begin{aligned}
\mathbb{H} = & E_{\text{MF}} + E'_1 \sum_k \varphi_k \varphi_{-k} \left[z - 2 \sum_{\alpha} \cos(k_{\alpha}a) \right] \\
& + \sum_k \Delta n_k \Delta n_{-k} \left\{ \frac{1}{2} \left[\left(V + \frac{U}{z} \right) \sum_{\alpha} \cos(k_{\alpha}a) + U \right] \right. \\
& \quad \left. + \frac{(zV-U)}{4} \left(\frac{n^2(U-zV)^2}{2z^2t^2} - 1 \right) \right\} \\
& + \sum_k \Delta n_k \Delta n_{-(k+K)} \left\{ \frac{(zV-U)^2 n}{4zt} \left(\frac{n^2(U-zV)^2}{4z^2t^2} \right)^{1/2} \right\}. \quad (5.65)
\end{aligned}$$

The diagonalization of the Rotor-Hamiltonian above, is a bit tricky. Despite that, we present the procedure of doing so.

The Rotor-Hamiltonian eq. (5.65) can be rewritten in a more compact form, by introducing new coefficients

$$\mathbb{H} = E_{\text{MF}} + \sum_k \varphi_k \varphi_{-k} \chi_k + \sum_k \Delta n_k \Delta n_{-k} \zeta_k + \sum_k \Delta n_k \Delta n_{-(k+K)} \xi, \quad (5.66)$$

where K is still a reciprocal lattice vector and

$$\chi_k = E'_1 \left[z - 2 \sum_{\alpha} \cos(k_{\alpha} a) \right] = \frac{4t^2 z}{(zV - U)} \left[z - 2 \sum_{\alpha} \cos(k_{\alpha} a) \right], \quad (5.67)$$

$$\zeta_k = \frac{1}{2} \left[\left(V + \frac{U}{z} \right) \sum_{\alpha} \cos(k_{\alpha} a) + U \right] + \frac{(zV - U)}{4} \left(\frac{n^2 (U - zV)^2}{2z^2 t^2} - 1 \right), \quad (5.68)$$

$$\xi = E_4 \cdot U_1 = \frac{(zV - U)^2 n}{4zt} \left(\frac{n^2 (U - zV)^2}{4z^2 t^2} - 1 \right)^{1/2}. \quad (5.69)$$

We know, that there are two different lattice site fillings, therefore we have to write the Rotor-Hamiltonian eq. (5.66) for the two types. In this procedure we neglect the mean-field energy E_{MF} , because it does not effect the diagonalization. The Rotor-Hamiltonian thus is

$$\begin{aligned} H = & \sum_k [\varphi_{k_1} \varphi_{-k_1} \chi_{k_1} + \varphi_{k_2} \varphi_{-k_2} \chi_{k_2}] \\ & + \sum_k [\Delta n_{k_1} \Delta n_{-k_1} \zeta_{k_1} + \Delta n_{k_2} \Delta n_{-k_2} \zeta_{k_2}] \\ & + \xi \sum_k [\Delta n_{k_1} \Delta n_{-k_2} + \Delta n_{k_2} \Delta n_{-k_1}]. \end{aligned} \quad (5.70)$$

To reduce the Hamiltonian above eq. (5.70), it can also be expressed in a matrix representation

$$H = \sum_k \left\{ \begin{pmatrix} \varphi_{k_1} \\ \varphi_{k_2} \end{pmatrix} \begin{pmatrix} \chi_{k_1} & 0 \\ 0 & \chi_{k_2} \end{pmatrix} + \begin{pmatrix} \Delta n_{k_1} \\ \Delta n_{k_2} \end{pmatrix} \begin{pmatrix} \zeta_{k_1} & \xi \\ \xi & \zeta_{k_2} \end{pmatrix} \begin{pmatrix} \Delta n_{-k_1} \\ \Delta n_{-k_2} \end{pmatrix} \right\}. \quad (5.71)$$

The further computation and diagonalization of above the Hamiltonian is done by lending a useful tool of classical mechanics, the Hamiltonian equations. For a introduction into the Hamiltonian equations of motion in classical mechanics, see [29]. The Hamiltonian equations of motion are

$$\dot{q}_k = \frac{\partial H}{\partial p_k} \quad (5.72)$$

and

$$\dot{p}_k = -\frac{\partial H}{\partial q_k}. \quad (5.73)$$

In our case we interpret the phase of the quasi-condensate φ_k as the classical momentum p_k , because the motion of particles in the system is due to the change of the different phases. The quantum fluctuations Δn_k in the system is referred to as the classical position q_k , since the quantum fluctuations are responsible for the change of the particle number at the lattice sites.

With these assumptions, we write the Hamiltonian equations of motion, first for the time derivative of the positions q_k eq. (5.72)

$$\begin{pmatrix} \partial_t q_{k_1} \\ \partial_t q_{k_2} \end{pmatrix} = \begin{pmatrix} 2\chi_{k_1} & 0 \\ 0 & 2\chi_{k_2} \end{pmatrix} \begin{pmatrix} p_{k_1} \\ p_{k_2} \end{pmatrix} \quad (5.74)$$

$$\begin{pmatrix} \frac{1}{2\chi_{k_1}} \partial_t q_{k_1} \\ \frac{1}{2\chi_{k_2}} \partial_t q_{k_2} \end{pmatrix} = \begin{pmatrix} p_{k_1} \\ p_{k_2} \end{pmatrix}, \quad (5.75)$$

then for the momentums eq.(5.73)

$$\begin{pmatrix} \partial_t p_{k_1} \\ \partial_t p_{k_2} \end{pmatrix} = -2 \begin{pmatrix} \zeta_{k_1} & \xi \\ \xi & \zeta_{k_2} \end{pmatrix} \begin{pmatrix} q_{k_1} \\ q_{k_2} \end{pmatrix}. \quad (5.76)$$

In the next step, we want eliminate one of the variables q_{k_i} or p_{k_i} from equations (5.75 or 5.76). Therefore we insert eq. (5.75) into eq. (5.76) and obtain a relation between p_{k_i} and q_{k_i}

$$\partial_t \begin{pmatrix} p_{k_1} \\ p_{k_2} \end{pmatrix} = \frac{1}{2} \begin{pmatrix} \frac{1}{\chi_{k_1}} \partial_t^2 q_{k_1} \\ \frac{1}{\chi_{k_2}} \partial_t^2 q_{k_2} \end{pmatrix}. \quad (5.77)$$

This relation eq. (5.77) is plugged into eq. (5.76) to get equations of motion, which only depend on the position of particles q_{k_i}

$$\frac{1}{2} \begin{pmatrix} \frac{1}{\chi_{k_1}} \partial_t^2 q_{k_1} \\ \frac{1}{\chi_{k_2}} \partial_t^2 q_{k_2} \end{pmatrix} = -2 \begin{pmatrix} \zeta_{k_1} & \xi \\ \xi & \zeta_{k_2} \end{pmatrix} \begin{pmatrix} q_{k_1} \\ q_{k_2} \end{pmatrix}. \quad (5.78)$$

The above matrix equations can be brought to a more convenient form

$$\begin{pmatrix} \chi_{k_2} \partial_t^2 q_{k_1} \\ \chi_{k_1} \partial_t^2 q_{k_2} \end{pmatrix} = -4\chi_{k_1}\chi_{k_2} \begin{pmatrix} \zeta_{k_1} & \xi \\ \xi & \zeta_{k_2} \end{pmatrix} \begin{pmatrix} q_{k_1} \\ q_{k_2} \end{pmatrix}. \quad (5.79)$$

The two equations of motion, which can be obtained from the above matrices, are

$$\chi_{k_2} \partial_t^2 q_{k_1}(n) = -4\chi_{k_1}\chi_{k_2} (\zeta_{k_1} q_{k_1}(n) + \xi q_{k_2}(n-1)) \quad (5.80)$$

$$\chi_{k_1} \partial_t^2 q_{k_2}(n) = -4\chi_{k_1}\chi_{k_2} (\xi q_{k_1}(n+1) + \zeta_{k_2} q_{k_2}(n)). \quad (5.81)$$

They are of the form of coupled oscillators. In the further calculations, they need to be decoupled. The form reminds us of the equations of motion for a two atomic basis in a solid.

To solve these equations we need to propose an ansatz, which reads

$$q_{k_1} = A e^{i(kr_i n - \omega t)} \quad q_{k_2} = B e^{i(kr_i n - \omega t)}, \quad (5.82)$$

where the coefficients A, B are amplitudes. The ansatz above is the same as in solid state physics, if equations of motions for a solid with a basis of two atoms needs to be solved. For an introduction into the field of solid state physics, see [3].

The second derivative of the ansatz for q_{k_i} eq. (5.82) is done

$$\ddot{q}_{1(2)} = -A(B) \omega^2 e^{i(knr_i - \omega t)}. \quad (5.83)$$

This is now inserted into the first equation of motion eq. (5.80)

$$\chi_{k_2} \left(-\omega^2 A e^{i(kr_i n - \omega t)} \right) = -4\chi_{k_1} \chi_{k_2} \left(\zeta_{k_1} A e^{i(kr_i n - \omega t)} + \xi B e^{i(kr_i (n-1) - \omega t)} \right) \quad (5.84)$$

$$\Rightarrow 0 = (4\chi_{k_1} \zeta_{k_1} - \omega^2) A + 4\chi_{k_1} \xi e^{-ikr_i} B. \quad (5.85)$$

Now the second derivative, eq. (5.83), is put into eq. (5.81) to further reduce that equation

$$\chi_{k_1} \left(-B \omega^2 e^{i(knr_i - \omega t)} \right) = -4\chi_{k_1} \chi_{k_2} \left(\xi A e^{i(kr_i (n+1) - \omega t)} + \zeta_{k_2} B e^{i(knr_i - \omega t)} \right) \quad (5.86)$$

$$\Rightarrow 0 = (4\chi_{k_2} \zeta_{k_2} - \omega^2) B + 4\chi_{k_2} \xi e^{ikr_i}. \quad (5.87)$$

The two computed equations (5.85 + 5.87) can be rewritten in a matrix representation

$$0 = \begin{pmatrix} (4\chi_{k_1} \zeta_{k_1} - \omega^2) & 4\chi_{k_1} \xi e^{-ikr_i} \\ 4\chi_{k_2} \xi e^{ikr_i} & (4\chi_{k_2} \zeta_{k_2} - \omega^2) \end{pmatrix} \begin{pmatrix} A \\ B \end{pmatrix}. \quad (5.88)$$

To solve these equations in matrix representation, either the matrix or the vector has to be zero. Since the vector consisting of the amplitudes A and B can not be zero, the matrix has to be. This tells us, that the determinant of the matrix has to vanish

$$0 \stackrel{!}{=} (4\chi_{k_1} \zeta_{k_1} - \omega^2) (4\chi_{k_2} \zeta_{k_2} - \omega^2) - 16\chi_{k_1} \chi_{k_2} \xi^2. \quad (5.89)$$

Let us recall, which quantity we are interested in. We started with a Rotor-Hamiltonian in the grand canonical ensemble and proposed an ansatz for the number of particles at the lattice sites n_i . Next we cancelled all linear orders of quantum fluctuations out and obtained the desired Rotor-Hamiltonian in real space. The obvious next step was the Fourier transformation of the determined Rotor-Hamiltonian. By doing this, we found that the quantum fluctuations deliver off-diagonal contributions to the diagonalization of the Rotor-Hamiltonian. Therefore, we could not apply our scheme of introducing creation and annihilation operators to do the diagonalization. Despite that, our goal was to diagonalize the Rotor-Hamiltonian to obtain the dispersion relation. We needed to know, if the new supersolid phase is stable or not. To find out, if an instability in the dispersion relation of the supersolid phase occurs or not. Hence, the whole steps done so far were to calculate the dispersion relation $\varepsilon(k)$ of our supersolid phase. Since our previously done techniques of diagonalization can not solve the problem, we helped ourselves with the trick by relating to problems that have already been solved, like the behavior of a solid with a two atomic basis. Therefore our desired quantity is the dispersion relation ω .

After this excursion, it is clear, for what quantity we need to solve eq. (5.89), thus for ω^2

$$\omega_{1/2}^2 = 2(\chi_{k_1} \zeta_{k_1} + \chi_{k_2} \zeta_{k_2}) \pm 2\sqrt{(\chi_{k_1} \zeta_{k_1} - \chi_{k_2} \zeta_{k_2})^2 + 4\chi_{k_1} \chi_{k_2} \xi^2}. \quad (5.90)$$

By inserting the definitions of equations (5.67 - 5.69) renaming $k_1 = k$ and $k_2 = k + K$ we obtain the dispersion relation for our supersolid phase

$$\begin{aligned}
\omega_{1/2}^2 = & \frac{2t^2}{g} \left(\left[z - 2 \sum_{\alpha} \cos(k_{\alpha}a) \right] \left[2 \left(g + \frac{\kappa}{z} \right) \sum_{\alpha} \cos(k_{\alpha}a) + \kappa + zg(2g^2 - 1) \right] \right. \\
& + \left. \left[z - 2 \sum_{\alpha} \cos((k_{\alpha} + K)a) \right] \left[2 \left(g + \frac{\kappa}{z} \right) \sum_{\alpha} \cos((k_{\alpha} + K)a) + \kappa + zg(2g^2 - 1) \right] \right) \\
& \pm 2t^2 \left(\frac{1}{g^2} \left\{ \left[z - 2 \sum_{\alpha} \cos(k_{\alpha}a) \right] \left[2 \left(g + \frac{\kappa}{z} \right) \sum_{\alpha} \cos(k_{\alpha}a) + \kappa + zg(2g^2 - 1) \right] \right. \right. \\
& - \left. \left. \left[z - 2 \sum_{\alpha} \cos((k_{\alpha} + K)a) \right] \left[2 \left(g + \frac{\kappa}{z} \right) \sum_{\alpha} \cos((k_{\alpha} + K)a) + \kappa + zg(2g^2 - 1) \right] \right\}^2 \right. \\
& \left. + 8z^2g^2 \left[z - 2 \sum_{\alpha} \cos(k_{\alpha}a) \right] \left[z - 2 \sum_{\alpha} \cos((k_{\alpha} + K)a) \right] (g^2 - 1) \right)^{1/2}, \tag{5.91}
\end{aligned}$$

where K is again a reciprocal lattice vector, the introduced coefficient g thereby is

$$g = \frac{n(zV - U)}{2zt}, \tag{5.92}$$

and the coefficient κ is as

$$\kappa = \frac{nU}{t}. \tag{5.93}$$

The coefficients g and κ were introduced into eq. (5.91) to allow to write a more compact form for the dispersion relation.

Since we want to consider the off-diagonal terms too, we set the reciprocal lattice vector as $K = \frac{\pi}{a}$. The dispersion relation eq. (5.91) then can be written in a dimensionless form

$$\begin{aligned}
\frac{\omega_{1/2}^2}{2t^2} = & \frac{1}{g} \left(\left[z - 2 \sum_{\alpha} \cos(k_{\alpha}a) \right] \left[2 \left(g + \frac{\kappa}{z} \right) \sum_{\alpha} \cos(k_{\alpha}a) + \kappa + zg(2g^2 - 1) \right] \right. \\
& + \left. \left[z - 2 \sum_{\alpha} \cos\left(\left(k_{\alpha} + \frac{\pi}{a}\right)a\right) \right] \left[2 \left(g + \frac{\kappa}{z} \right) \sum_{\alpha} \cos\left(\left(k_{\alpha} + \frac{\pi}{a}\right)a\right) + \kappa + zg(2g^2 - 1) \right] \right) \\
& \pm \left(\frac{1}{g^2} \left\{ \left[z - 2 \sum_{\alpha} \cos(k_{\alpha}a) \right] \left[2 \left(g + \frac{\kappa}{z} \right) \sum_{\alpha} \cos(k_{\alpha}a) + \kappa + zg(2g^2 - 1) \right] \right. \right. \\
& - \left. \left. \left[z - 2 \sum_{\alpha} \cos\left(\left(k_{\alpha} + \frac{\pi}{a}\right)a\right) \right] \left[2 \left(g + \frac{\kappa}{z} \right) \sum_{\alpha} \cos\left(\left(k_{\alpha} + \frac{\pi}{a}\right)a\right) + \kappa + zg(2g^2 - 1) \right] \right\}^2 \right. \\
& \left. + 8z^2g^2 \left[z - 2 \sum_{\alpha} \cos(k_{\alpha}a) \right] \left[z - 2 \sum_{\alpha} \cos\left(\left(k_{\alpha} + \frac{\pi}{a}\right)a\right) \right] (g^2 - 1) \right)^{1/2}. \tag{5.94}
\end{aligned}$$

Figure 5.1 shows the dimensionless dispersion relation of eq. (5.94). We find that no instability occurs, despite any ratios of nearest-neighbor to on-site interaction. Thus we propose that the presented supersolid phase is stable against quantum fluctuations.

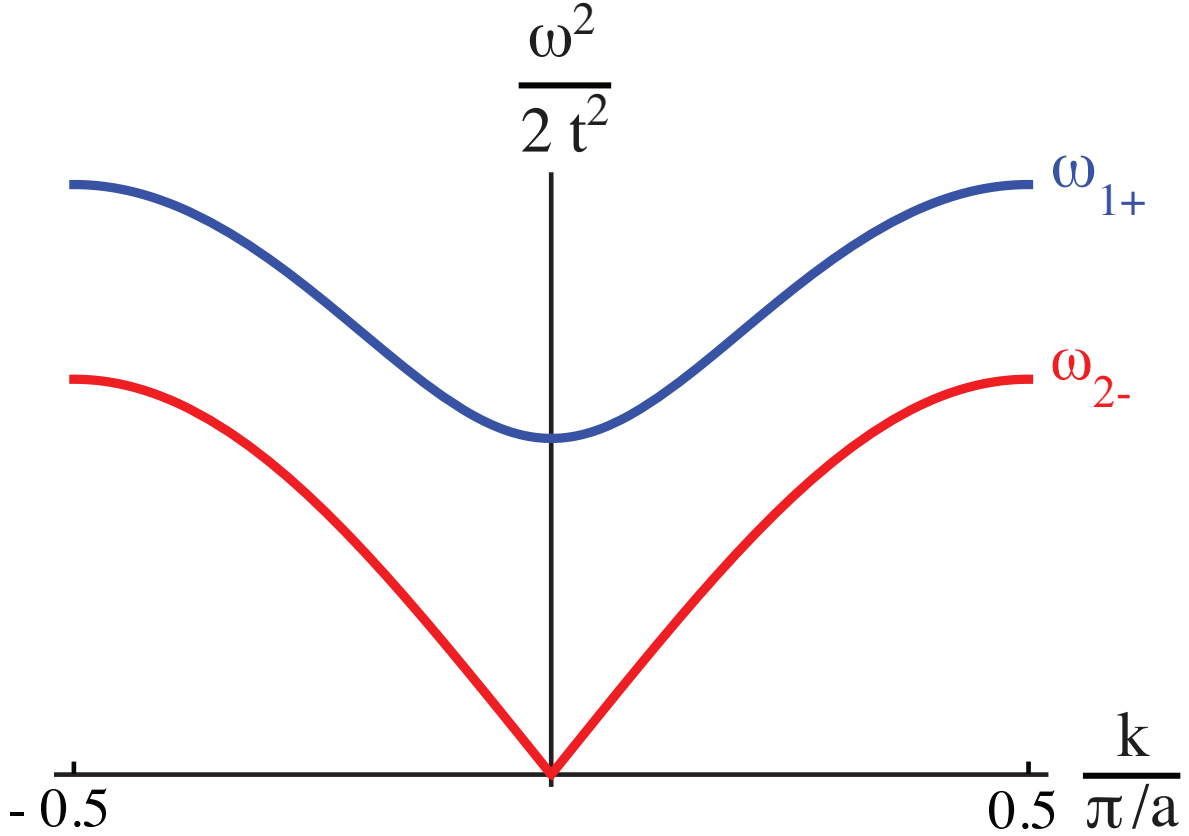


Figure 5.1: Dispersion relation of the supersolid phase in one dimension in orders of $k = \pi/a$. Despite the ratio γ of nearest-neighbor to on-site interaction the system is stable. No instability occurs. For more insight see text.

The dispersion relation in figure 5.1 can be explained as follows: The lower branch, marked as ω_{1+} , corresponds to the first solution of eq. (5.94), if the + sign is considered. The upper branch is marked as ω_{2-} and is the solution of eq. (5.94) for the case of the – sign. The lower branch can be considered as the acoustic modes of the supersolid. There, the condensates in the lattice sites oscillate in phase. The upper branch can be assigned as the optical mode, where the condensates oscillate out of phase by π .

Chapter 6

Experimental Realization

In the previous chapters we first calculated the instability of the dispersion relation within the Bogoliubov theory. Then we went into the Rotor-Model to determine the instability within a mean-field theory, since the description of the Bogoliubov theory becomes invalid at higher filling factors n . There we discovered, that the instability occurs at the same critical ratio γ as in the Bogoliubov theory. After that, we proposed an ansatz to describe the new phase. Previously within chapter 5 we investigated the stability of the supersolid phase and found that no instability occurs. Thus, the theory done so far is conclusive and seems to be valid. Our next step is to consider the experimental realization of the done theory.

A possibility for an experimental set up would be the application of chromium atoms to an optical lattice. The group of Tilman Pfau at the University of Stuttgart intensively investigated the properties of ^{52}Cr atoms and possible applications.

In the following sections we want to determine a possible experimental setup and if the dipolar chromium BEC is stable, while being in a trap. The stability of the Cr-BEC is necessary to carry out the loading into an optical lattice and applying the needed ratio γ .

6.1 Energy of the BEC in a trap

At first we start with the calculation of the energy of a Cr-BEC within a cylindrical shaped trap. Therefore we use the Gross-Pitaevskii energy functional with an external trapping potential of cylindrical shape

$$E[\Phi] = \int \left[\underbrace{\frac{\hbar^2}{2m} |\nabla\Phi|^2}_1 + \underbrace{V_{\text{trap}} |\Phi|^2}_2 - \underbrace{\mu |\Phi|^2}_3 + \underbrace{\frac{1}{2} |\Phi|^2 \int U_{\text{dd}}(\mathbf{r} - \mathbf{r}') |\Phi(\mathbf{r}')|^2 d\mathbf{r}'}_4 + \underbrace{\frac{g}{2} |\Phi|^4}_5 \right] d\mathbf{r}, \quad (6.1)$$

where V_{trap} is the potential of the cylindrical trap and U_{dd} is the dipole-dipole interaction potential

$$V_{\text{trap}} = \frac{m}{2} (\omega_\rho^2 \rho^2 + \omega_z^2 z^2), \quad (6.2)$$

$$U_{\text{dd}}(\mathbf{r} - \mathbf{r}') = \frac{\mu_0 \mu^2}{4\pi} \frac{1 - 3 \cos^2 \theta}{|\mathbf{r} - \mathbf{r}'|^3}, \quad (6.3)$$

and the coefficient g being

$$g = \frac{4\pi \hbar^2 a}{m}. \quad (6.4)$$

The first part in eq. (6.1) accounts the kinetic part, the second considers the potential of the trap V_{trap} , the third the chemical potential μ , the fourth part stands for the dipole-dipole interaction and the fifth part is for the contact interaction. In the equation above, a is the scattering length, m the atomic mass of the particles, \hbar the planck's constant, μ_0 the permeability of vacuum, μ the permanent magnetic dipole moment and θ is the angle between the direction of polarization and the relative position of the particles. For a further introduction into the detailed calculation of the dipolar BEC confined in a cylindrical shape see [30].

Following ansatz is used for the wave function, it is of a Gaussian form

$$\Phi(\rho, z) = \sqrt{\frac{N}{\pi^{3/2} \sigma_\rho^2 \sigma_z a_{\text{ho}}^3}} e^{-\frac{1}{2a_{\text{ho}}^2} \left(\frac{\rho^2}{\sigma_\rho^2} + \frac{z^2}{\sigma_z^2} \right)}, \quad (6.5)$$

where the coefficient σ_ρ is the radial size of the BEC cloud, σ_z the expansion in the z -direction, ω_z is the trap size in z -direction and ω_ρ the trap size in radial direction. The coefficient N is the number of particles in the trap and a_{ho} is the harmonic oscillator length with

$$a_{\text{ho}} = \sqrt{\frac{\hbar}{m\bar{\omega}}}. \quad (6.6)$$

The coefficient $\bar{\omega}$ is mean trap frequency with

$$\bar{\omega} = (\omega_\rho^2 \omega_z)^{1/3}. \quad (6.7)$$

The ansatz eq. (6.5) is being inserted into the Gross-Pitaevskii energy functional eq. (6.1) and reveals the energy for the BEC in the confining trap

$$E = \frac{N}{4} \hbar \bar{\omega} \left\{ \left[\frac{2}{\sigma_\rho^2} + \frac{1}{\sigma_z^2} \right] + \frac{1}{\lambda^{2/3}} [2\sigma_\rho^2 + \lambda^2 \sigma_z^2] - \frac{4\mu}{\hbar \bar{\omega}} + \frac{4Na_{\text{dd}}}{\sqrt{2\pi} a_{\text{ho}} \sigma_\rho^2 \sigma_z} \left(\frac{a}{a_{\text{dd}}} - f(\kappa) \right) \right\}, \quad (6.8)$$

where following coefficients are introduced

$$\lambda = \frac{\omega_z}{\omega_\rho} \quad (6.9)$$

$$a_{\text{dd}} = \frac{\mu_0 \mu^2 m}{12\pi \hbar^2} \quad (6.10)$$

$$f(\kappa) = \frac{1 + 2\kappa^2}{1 - \kappa^2} - \frac{3\kappa^2 \text{Artanh} \sqrt{1 - \kappa^2}}{(1 - \kappa^2)^{3/2}}. \quad (6.11)$$

The coefficient λ is the ratio of the confining trap in z - to ρ -direction, a_{dd} is the dipolar length as introduced in [30] and the function $f(\kappa)$ comes out at the integration of the dipole-dipole interaction term. It depends on the aspect ratio $\kappa = \sigma_\rho/\sigma_z$ of the BEC cloud.

6.2 Calculation of U, V, t

In the upcoming sections we want to determine relations for the on-site interaction U , the nearest-neighbor interaction V and the hopping term t , expressed in experimental available quantities, e.g. like the aspect ratio of the cloud κ . To reach this, we begin our calculations with the above result for the energy of a BEC in a trap and modify it to our needs.

6.2.1 Calculation of the on-site interaction U

We start with the evaluation of the on-site interaction U . Here, we consider the BEC to be of Gaussian form and being confined in a cylindrical shaped trap, see figure 6.1.

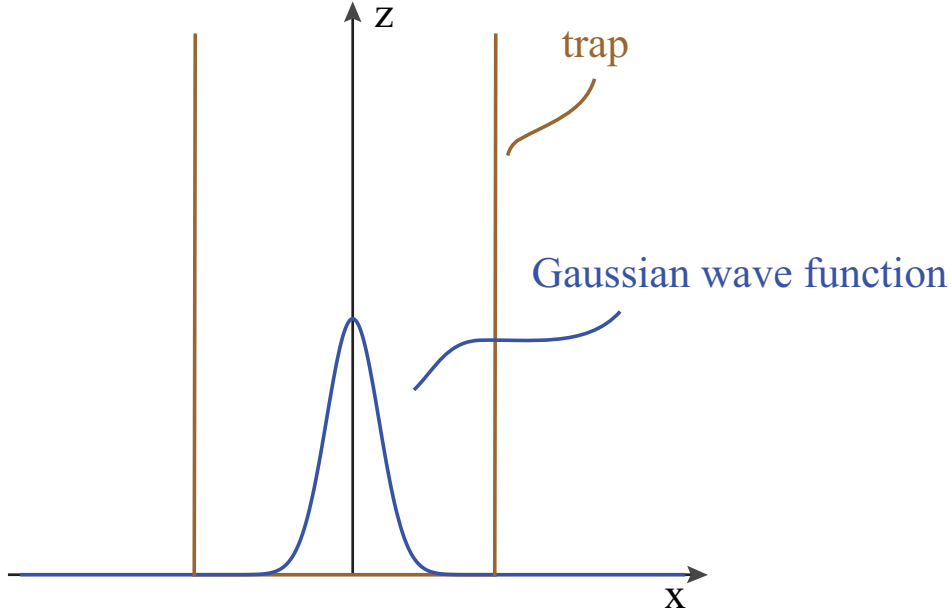


Figure 6.1: Dipolar BEC, described by a Gaussian wave function, confined in a cylindrical shaped trap.

Instead of a calculation for fixed particle number N , as done before, we now consider a variable particle number. For this reason we replace the particle number N by the mean number of particles per trap \bar{n} and introduce mean-field particle fluctuations δn

$$N \rightarrow \bar{n} + \delta n. \quad (6.12)$$

Since we work with a fluctuating particle number, we also have to introduce a chemical potential μ , for controlling purposes, into the energy eq. (6.8). Next, we replace every particle number N by the proposed eq. (6.12) and obtain

$$E = \frac{(\bar{n} + \delta n)}{4} \hbar\bar{\omega} \left(\frac{2}{\sigma_\rho^2} + \frac{1}{\sigma_z^2} \right) + \frac{(\bar{n} + \delta n)}{4\lambda^{2/3}} \hbar\bar{\omega} (2\sigma_\rho^2 + \lambda^2\sigma_z^2) + \frac{(\bar{n} + \delta n)^2 \hbar\bar{\omega} a_{\text{dd}}}{\sqrt{2\pi} a_{\text{ho}} \sigma_\rho^2 \sigma_z} \left(\frac{a}{a_{\text{dd}}} - f(\kappa) \right) - \mu (\bar{n} + \delta n). \quad (6.13)$$

Now, we sort the above energy in orders of δn

$$\begin{aligned} E &= \bar{n} \left[\frac{\hbar\bar{\omega}}{4} \left(\frac{2}{\sigma_\rho^2} + \frac{1}{\sigma_z^2} \right) + \frac{\hbar\bar{\omega}}{4\lambda^{2/3}} (2\sigma_\rho^2 + \lambda^2\sigma_z^2) + \frac{\bar{n} \hbar\bar{\omega} a_{\text{dd}}}{\sqrt{2\pi} a_{\text{ho}} \sigma_\rho^2 \sigma_z} \left(\frac{a}{a_{\text{dd}}} - f(\kappa) \right) - \mu \right] \\ &+ \bar{n} \left[\frac{2 \hbar\bar{\omega} a_{\text{dd}}}{\sqrt{2\pi} a_{\text{ho}} \sigma_\rho^2 \sigma_z} \left(\frac{a}{a_{\text{dd}}} - f(\kappa) \right) \right] \delta n \\ &+ \left[\frac{\hbar\bar{\omega}}{4} \left(\frac{2}{\sigma_\rho^2} + \frac{1}{\sigma_z^2} \right) + \frac{\hbar\bar{\omega}}{4\lambda^{2/3}} (2\sigma_\rho^2 + \lambda^2\sigma_z^2) - \mu \right] \delta n \\ &+ \left[\frac{\hbar\bar{\omega} a_{\text{dd}}}{\sqrt{2\pi} a_{\text{ho}} \sigma_\rho^2 \sigma_z} \left(\frac{a}{a_{\text{dd}}} - f(\kappa) \right) \right] \delta n^2. \end{aligned} \quad (6.14)$$

We seek, that there are only quadratic orders of mean-fluctuations in our system. Therefore, we determine the chemical potential μ in such a way, that all linear terms in δn vanish. Thus

$$\mu = \frac{\hbar\bar{\omega}}{4} \left(\frac{2}{\sigma_\rho^2} + \frac{1}{\sigma_z^2} \right) + \frac{\hbar\bar{\omega}}{4\lambda^{2/3}} (2\sigma_\rho^2 + \lambda^2\sigma_z^2) + \frac{2\bar{n} \hbar\bar{\omega} a_{\text{dd}}}{\sqrt{2\pi} a_{\text{ho}} \sigma_\rho^2 \sigma_z} \left(\frac{a}{a_{\text{dd}}} - f(\kappa) \right). \quad (6.15)$$

With the chemical potential μ eq. (6.15) inserted into the energy eq. (6.14), we get the following structure for the energy of our considered system

$$E(\bar{n} + \delta n) = E(\bar{n}) + \frac{U}{2} \delta n^2, \quad (6.16)$$

where the energy of the mean number of particles $E(\bar{n})$ is

$$E(\bar{n}) = \frac{\bar{n}^2 \hbar\bar{\omega} a_{\text{dd}}}{\sqrt{2\pi} a_{\text{ho}} \sigma_\rho^2 \sigma_z} \left(f(\kappa) - \frac{a}{a_{\text{dd}}} \right). \quad (6.17)$$

The pre-factor of the quadratic part in eq. (6.16) is the desired on-site interaction, expressed in experimentally accessible values

$$U = \frac{2\hbar\bar{\omega} a_{\text{dd}}}{\sqrt{2\pi} a_{\text{ho}} \sigma_\rho^2 \sigma_z} \left(\frac{a}{a_{\text{dd}}} - f(\kappa) \right). \quad (6.18)$$

The above value for U is only an upper boundary for the exact value of the on-site interaction. To find the exact value for U , the derivative of eq. (6.17) with respect to σ_ρ and σ_z has to be done. Then this determined equation has to be solved, to obtain the critical scattering length a_{crit} , this has to be inserted into eq. (6.18) to achieve the exact value. Derivatives with respect

to N , λ or \bar{w} can not be carried out, because $E(\bar{n} + \delta n)$ does not depend on these values. For further insight into the exact calculation of U , a first step is to consider [30].

In this work we only present the upper boundary for U , because the exact value can only be obtained with numerical efforts. For an estimate of U the upper boundary is sufficient.

6.2.2 Calculation of the nearest-neighbor interaction V

With the upper boundary for the on-site interaction U , an upper boundary for the nearest-neighbor interaction V is due. This is done in the following.

We assume two cylindrical shaped traps, each occupied by a BEC. The two traps are apart by a distance b and one trap contains N_1 particles, the other N_2 , see figure 6.2.

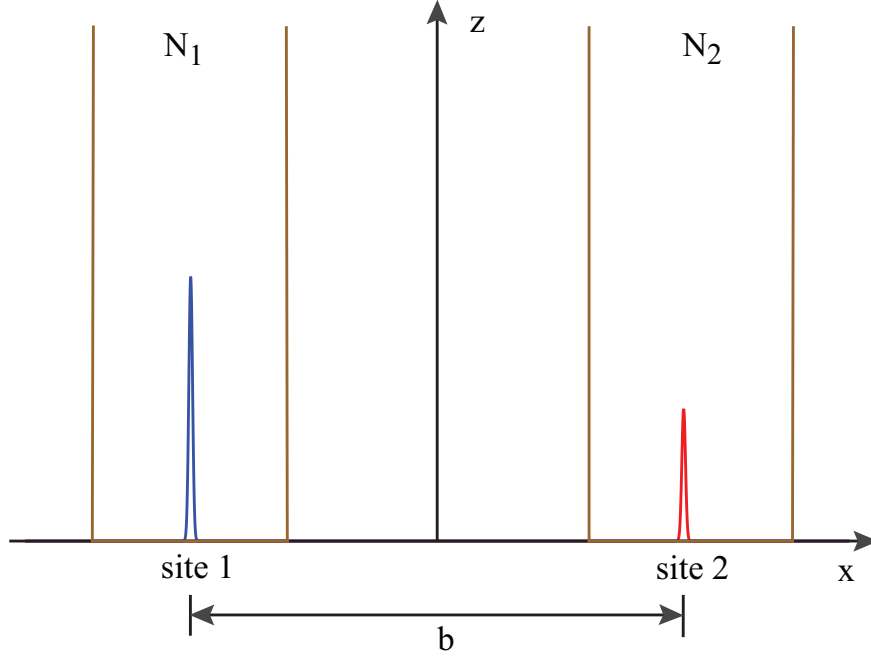


Figure 6.2: Two dipolar BECs, each assumed to be a sharp peak function to prevent an overlap, confined in cylindrical shaped traps. The left BEC contains N_1 particles, the right N_2 .

For this case the energy functional for two cylindrical shaped traps, where each holds one BEC, has to be written as

$$E[\Phi_1, \Phi_2] = E[\Phi_1] + E[\Phi_2] + WW[\Phi_1, \Phi_2], \quad (6.19)$$

where $E[\Phi_1]$ is the energy functional of eq. (6.1) for trap1 and $E[\Phi_2]$ for trap2. The term $WW[\Phi_1, \Phi_2]$ is the energy functional for the interaction between the BECs in trap1 and trap2.

To solve the above Gross-Pitaevskii equations, we need to propose an ansatz for the two wave functions, where again the fixed particle number N is replaced by a fluctuating particle number $\bar{n} + \delta n_i$. Thus

$$\Phi_1(\rho, z) = \sqrt{\frac{\bar{n} + \delta n_1}{\pi^{3/2} \sigma_\rho^2 \sigma_z a_{\text{ho}}^3}} e^{-\frac{1}{2a_{\text{ho}}^2} \left(\frac{\rho^2}{\sigma_\rho^2} + \frac{z^2}{\sigma_z^2} \right)}, \quad (6.20)$$

$$\Phi_2(\rho, z) = \sqrt{\frac{\bar{n} + \delta n_2}{\pi^{3/2} \sigma_\rho^2 \sigma_z a_{\text{ho}}^3}} e^{-\frac{1}{2a_{\text{ho}}^2} \left(\frac{\rho^2}{\sigma_\rho^2} + \frac{z^2}{\sigma_z^2} \right)}. \quad (6.21)$$

The given ansatz above need to be inserted into the Gross-Pitaevskii energy functional of eq. (6.19) to determine the energy of the considered system. The calculation for the energy functionals $E[\Phi_1]$ and $E[\Phi_2]$ can be done identically as in section 6.1, by inserting the appropriate wave function eq. (6.20) or eq. (6.21). To evaluate the chemical potential μ in this case, the interaction energy functional has to be calculated at first. It reads

$$WW[\Phi_1, \Phi_2] = \frac{1}{2} \int |\Phi_1(\mathbf{r})|^2 U_{\text{dd}}(\mathbf{r} - \mathbf{r}') |\Phi_2(\mathbf{r}')|^2 d\mathbf{r}' d\mathbf{r}. \quad (6.22)$$

where U_{dd} is as in eq. (6.3) given. An analytic calculation can not be carried out, because one integration can not be done analytically. Therefore we compute an upper boundary, again, for the nearest-neighbor interaction. We use the following simplification: Here, the two wave functions are considered to be of a delta shape, instead of a Gaussian. Thus eq. (6.20) and eq. (6.21) have to be multiplied by $\delta(x \pm \frac{b}{2})$, where b is the fixed distance between the traps. Since the wave functions are now delta shaped, all particles in the two traps can be considered being parallel, which leads to following simplifications of eq. (6.3)

$$|\mathbf{r} - \mathbf{r}'| \rightarrow b \quad (6.23)$$

$$\theta \rightarrow \frac{\pi}{2} \Rightarrow \cos\left(\frac{\pi}{2}\right) \rightarrow 0. \quad (6.24)$$

The angle θ is the angle between the direction of polarization and the relative position of the particles. For these simplifications, the dipole-dipole potential is

$$U_{\text{dd}}(\mathbf{r} - \mathbf{r}') \rightarrow U_{\text{dd}}(b) = \frac{\mu_0 \mu^2}{4\pi b^3}. \quad (6.25)$$

The ansatz for the wave functions of the different BECs now are

$$\Phi_1(x, y, z) = \sqrt{\frac{N_1}{\pi^{3/2} \sigma_\rho^2 \sigma_z a_{\text{ho}}^3}} e^{-\frac{1}{2a_{\text{ho}}^2} \left(\frac{(x+\frac{b}{2})^2}{\sigma_\rho^2} + \frac{y^2}{\sigma_\rho^2} + \frac{z^2}{\sigma_z^2} \right)} \delta\left(x + \frac{b}{2}\right), \quad (6.26)$$

$$\Phi_2(x', y', z') = \sqrt{\frac{N_2}{\pi^{3/2} \sigma_\rho^2 \sigma_z a_{\text{ho}}^3}} e^{-\frac{1}{2a_{\text{ho}}^2} \left(\frac{(x'-\frac{b}{2})^2}{\sigma_\rho^2} + \frac{y'^2}{\sigma_\rho^2} + \frac{z'^2}{\sigma_z^2} \right)} \delta\left(x' - \frac{b}{2}\right), \quad (6.27)$$

where we further assume, that trap sizes and the size of the BECs are the same for the two sites.

Next we insert the above wave functions into the simplified interaction energy functional

$$WW[\Phi_1, \Phi_2] = \frac{1}{2} \int |\Phi_1(\mathbf{r})|^2 U_{\text{dd}}(b) |\Phi_2(\mathbf{r}')|^2 d\mathbf{r}' d\mathbf{r}, \quad (6.28)$$

and integrate over the coordinates y', z', y, z . This leads to the following expression

$$WW[\Phi_1, \Phi_2] = \gamma (\pi^2 a_{\text{ho}}^4 \sigma_\rho^2 \sigma_z^2) \int e^{-\frac{1}{a_{\text{ho}}^2 \sigma_\rho^2} (x^2 + x'^2 + b(x-x') + \frac{b^2}{2})} dx dx'. \quad (6.29)$$

Here we introduce the coefficient γ as

$$\gamma = \frac{1}{2} \left(\frac{N_1}{\pi^{3/2} \sigma_\rho^2 \sigma_z a_{\text{ho}}^3} \right) \left(\frac{\mu_0 \mu^2}{4\pi b^3} \right) \left(\frac{N_2}{\pi^{3/2} \sigma_\rho^2 \sigma_z a_{\text{ho}}^3} \right). \quad (6.30)$$

The introduced coefficient γ should not be misunderstood, it is not the ratio of nearest-neighbor to on-site interaction $\gamma \neq \gamma_c$.

Next, we integrate over the coordinate x' and get

$$WW[\Phi_1, \Phi_2] = \gamma (\pi^2 a_{\text{ho}}^4 \sigma_\rho^2 \sigma_z^2) \int e^{-\frac{1}{4a_{\text{ho}}^2 \sigma_\rho^2} (b+2x)^2} dx (\sqrt{\pi} a_{\text{ho}} \sigma_\rho), \quad (6.31)$$

where an integration over the last coordinate x gives

$$WW[\Phi_1, \Phi_2] = \gamma (\pi^2 a_{\text{ho}}^4 \sigma_\rho^2 \sigma_z^2) (\sqrt{\pi} a_{\text{ho}} \sigma_\rho) (\sqrt{\pi} a_{\text{ho}} \sigma_\rho). \quad (6.32)$$

The introduced coefficient γ eq. (6.30) is now being put into the above computed equation and thus reveals the final value for interaction energy functional $WW[\Phi_1, \Phi_2]$

$$WW[\Phi_1, \Phi_2] = \frac{\mu_0 \mu^2 N_1 N_2}{8\pi b^3}. \quad (6.33)$$

Until now, we have evaluated the energy of the interaction term $WW[\Phi_1, \Phi_2]$. To obtain the energy of the whole considered system, we need to insert eq. (6.33) into the energy functional eq. (6.19), together with the results for the energies $E[\Phi_1]$ and $E[\Phi_2]$. Hence we get

$$\begin{aligned} E_{\text{ges}}[\Phi_1, \Phi_2] &= E[\Phi_1] + E[\Phi_2] + WW[\Phi_1, \Phi_2] \\ &= N_1 (\alpha - \mu + N_1 \beta) + N_2 (\alpha - \mu + N_2 \beta) + \eta N_1 N_2. \end{aligned} \quad (6.34)$$

The coefficients α, β and η are

$$\alpha = \frac{\hbar \bar{\omega}}{4} \left\{ \left[\frac{2}{\sigma_\rho^2} + \frac{1}{\sigma_z^2} \right] + \frac{1}{\lambda^{2/3}} [2\sigma_\rho^2 + \lambda^2 \sigma_z^2] \right\}, \quad (6.35)$$

$$\beta = \frac{a_{\text{dd}} \hbar \bar{\omega}}{\sqrt{2\pi} a_{\text{ho}} \sigma_\rho^2 \sigma_z} \left(\frac{a}{a_{\text{dd}}} - f(\kappa) \right), \quad (6.36)$$

$$\eta = \frac{\mu_0 \mu^2}{8\pi b^3}, \quad (6.37)$$

and were introduced for simplification and to allow a more compact form for the energy of the system E_{ges} .

In the next step, we plug in the values for the particle numbers N_1 and N_2 , namely $\bar{n} + \delta n_i$ and sort the revealing equation by orders of the mean-field fluctuations δn_i

$$E_{\text{ges}} = \bar{n}^2 (2\beta + \eta) + \beta (\delta n_1^2 + \delta n_2^2) + 2\bar{n} [\alpha - \mu] + \eta \delta n_1 \delta n_2 + (\delta n_1 + \delta n_2) [2\bar{n}\beta + \alpha - \mu + \eta\bar{n}]. \quad (6.38)$$

Again, we have to determine the chemical potential μ in such a way, that the linear parts of the mean-field fluctuations δn_i vanish. Thus we get the chemical potential as

$$0 \stackrel{!}{=} (\delta n_1 + \delta n_2) [2\bar{n}\beta + \alpha - \mu + \eta\bar{n}] \Rightarrow \mu = 2\bar{n}\beta + \alpha + \eta\bar{n}. \quad (6.39)$$

We can now achieve the energy for the system expressed with the introduced coefficients α , β , η , by inserting the chemical potential eq. (6.39) into eq. (6.38)

$$E_{\text{ges}} = \bar{n}^2 (-2\beta - \eta) + \beta (\delta n_1^2 + \delta n_2^2) + \eta \delta n_1 \delta n_2. \quad (6.40)$$

Now the definitions (6.35 - 6.37) are put into the equation above, to get the energy expressed in the experimental parameters. After that we bring eq. (6.40) into a form, where the values for the nearest-neighbor and on-site interaction are shown. Hence we get

$$E_{\text{ges}} = E(\bar{n}^2) + \frac{U}{2} (\delta n_1^2 + \delta n_2^2) + \frac{V}{2} \delta n_1 \delta n_2, \quad (6.41)$$

whereby the energy of the mean number of particles $E(\bar{n}^2)$, the on-site interaction U and the nearest-neighbor interactions V are

$$E(\bar{n}^2) = \bar{n}^2 \left(\frac{2a_{\text{dd}}\hbar\bar{\omega}}{\sqrt{2\pi}a_{\text{ho}}\sigma_\rho^2\sigma_z} \left(f(\kappa) - \frac{a}{a_{\text{dd}}} \right) - \frac{\mu_0\mu^2}{8\pi b^3} \right), \quad (6.42)$$

$$U = \frac{2a_{\text{dd}}\hbar\bar{\omega}}{\sqrt{2\pi}a_{\text{ho}}\sigma_\rho^2\sigma_z} \left(\frac{a}{a_{\text{dd}}} - f(\kappa) \right), \quad (6.43)$$

$$V = \frac{\mu_0\mu^2}{4\pi b^3}. \quad (6.44)$$

Thus we found an upper boundary for the nearest-neighbor interaction V with eq. (6.44). The value for the on-site interaction eq. (6.43) is identical to the value in calculated in eq. (6.18) and proofs the consistency for our calculations.

6.2.3 Expressing the Instability

Since we now have upper boundaries for the on-site U and nearest-neighbor interaction V , we can express the critical ratio of V/U in coefficients, which are accessible in an experiment. This is done by using the value for the on-site interaction eq. (6.18) and the nearest-neighbor interaction V eq. (6.44)

$$\gamma = \frac{V}{U} = \frac{12a_{\text{ho}}^3 \sigma_\rho^2 \sigma_z}{\sqrt{2\pi} b^3 \left(\frac{a}{a_{\text{dd}}} - f(\kappa) \right)}. \quad (6.45)$$

The upper equation, can be given in a more convenient form, where only proportions between values are important

$$\gamma \approx \left(\frac{\sigma_\rho a_{\text{ho}}}{b} \right)^2 \frac{\sigma_z a_{\text{ho}}}{b} \frac{1}{\left(\frac{a}{a_{\text{dd}}} - f(\kappa) \right)}. \quad (6.46)$$

With the ratio γ expressed in quantities accessible in an experiment, we now have to consider, how γ can be tuned to the critical value γ_c . First, we start with the investigation for the radial size of the cloud, the first part in eq. (6.46). In the radial direction, the expansion of the cloud is limited at

$$\sigma_{\rho \text{max}} = \frac{b}{4},$$

because we assumed that the two BEC clouds do not overlap. The assumption was, that the two BEC wave functions have a Gaussian delta shape and therefore no expansion of the wave functions were considered. To be sure, that no overlapping between the two wave functions appear, the cloud is limited in radial-direction. The harmonic oscillator length a_{ho} is of the order of one. Thus, we obtain for the first part in eq. (6.46)

$$\left(\frac{\sigma_\rho a_{\text{ho}}}{b} \right)^2 \rightarrow \mathcal{O}\left(\frac{1}{16}\right).$$

This means, we are not able to tune γ in the radial direction.

Next, we investigate the constraints in the z-direction. Since there are now constraints concerning the z-direction, therefore the system can be fully tuned. Now, we want to take a closer look at the last part of eq. (6.46). The function

$$\frac{1}{\left(\frac{a}{a_{\text{dd}}} - f(\kappa) \right)}, \quad (6.47)$$

results from the calculation of the energy of a dipolar BEC. It is responsible for the stability of a dipolar BEC within a cylindrical shaped trap and gives the dependency of the scattering length for the collapse. For trap aspect ratios $\lambda < 1$, the cloud is cigar shaped and only stable for scattering lengths $a > a_{\text{dd}}$. If the trap aspect ratio is chosen to be oblate, $\lambda > 1$, even negative scattering lengths until $a \approx -2a_{\text{dd}}$ can be realized, before collapsing. For a stability discussion see [30]. Still due is, how we should choose the trap ratio. First of all, we need the ratio of nearest-neighbor to on-site interaction to be positive and larger than one. Therefore the function eq. (6.47) has to be larger than one. To accomplish that, we need

$$\left(\frac{a}{a_{\text{dd}}} - f(\kappa) \right) < 1, \quad (6.48)$$

to be smaller than one. This can only be achieved, if we choose a cigar shaped trap and a scattering length a of $a \geq a_{\text{dd}}$. With this, the function eq. (6.47) becomes smaller than one. Hence, the ratio γ can be tuned to reach the critical ratio γ_c , where the instability in the

superfluid phase occurs and the supersolid phase begins, by setting the trap to be prolate and the scattering length to be $a \geq a_{\text{dd}}$.

6.2.4 The hopping term t

For sake of completeness the hopping term is given

$$t = \frac{4}{\sqrt{\pi}} E_r \left(\frac{V_0}{E_r} \right)^{3/4} \exp \left[-2 \left(\frac{V_0}{E_r} \right)^{1/2} \right], \quad (6.49)$$

where $E_r = \frac{\hbar^2 k^2}{2m}$ is the recoil energy and V_0 the tuneable amplitude of the optical lattice.

The equation for the hopping term is valid for the lowest Bloch band $n = 0$ and in the limit $V_0 \gg E_r$, see also [7]. It can be used for the analysis, since the assumption is made, that the system stays in the lowest Bloch band and excitations to higher bands can be neglected.

The hopping matrix elements $t_n(\mathbf{R})$ are uniquely determined by the energies of the Bloch bands $\varepsilon_n(\mathbf{q})$ via

$$\sum_{\mathbf{R}} t_n(\mathbf{R}) e^{i\mathbf{q}\cdot\mathbf{R}} = \varepsilon_n(\mathbf{q}), \quad (6.50)$$

and \mathbf{R} is a lattice vector.

Alternatively the hopping term can be calculated, as proposed by Jaksch *et al.* [22], as

$$t = \int d^3x w_0^*(\mathbf{x} - \mathbf{x}_i) \left[-\frac{\hbar^2}{2m} \nabla^2 + V_0(\mathbf{x}) \right] w(\mathbf{x} - \mathbf{x}_j), \quad (6.51)$$

where $w(\mathbf{x} - \mathbf{x}_i)$ is the Wannier function of lattice site i or j and $V_0(\mathbf{x})$ is the optical lattice potential.

6.3 Experimental Proposal

In this section, we want to propose an experimental setup to achieve the described supersolid phase. In the previous section 6.2.3 we argued, that cigar shaped traps are needed. Therefore we consider a 2D optical lattice, which consist of cigar shaped traps, arranged in a plane to form a two dimensional lattice, see section 2.1.

Now we want to give estimates for the needed frequencies of the on-site U and nearest-neighbor interaction V . The critical ratio γ_c is

$$\gamma_c = \frac{2t}{nU} + \frac{1}{z}. \quad (6.52)$$

Since we desire to be in the supersolid phase, the hopping t should be small compared to the superfluid phase, were t dominates. Therefore the first part of eq. (6.52) is small. Hereby, t is small and U too, but in the order of t , thus the term should be of the order of $1/z$. The quantity z is the number of nearest neighbors. Hence, in our experiment, we consider the critical ratio γ_c to be of the order of

$$\gamma_c = \frac{V}{U} \approx \frac{2}{z}. \quad (6.53)$$

This is one relation to consider. The other one, as argued is

$$nU \approx 2zt, \quad (6.54)$$

since the first part in eq. (6.52) should be

$$\frac{1}{z} \approx \frac{2t}{Un}. \quad (6.55)$$

With the equations above, we have relations for calculating the desired frequencies. Typically frequencies for the hopping t is $\sim 10\text{Hz}$, [32]. Usually the number of particles confined in a cigar shaped trap ranges between 10^1 and $3 \cdot 10^2$, depending on the used laser power [18], [53], [38], [26]. Therefore, we can carry out the determination of U and V , in a 1D system with 20 particles per lattice site. Inserting these values into equations (6.53 + 6.54) we find that the on-site interaction U is of the order

$$U \approx 2 \text{ Hz}, \quad (6.56)$$

and the nearest-neighbor interaction V thus

$$V \approx 2 \text{ Hz}, \quad (6.57)$$

depending on the considered dimension.

Another proof for the possible experimental application of our theory is to insert the needed values for chromium atoms into eq. (6.44). The typically distance between two cigar shaped traps is in the order of 10^{-6}m . The other needed values for the calculation are

$$\begin{aligned} \mu_0 &= 4\pi \cdot 10^{-7} \frac{\text{Vs}}{\text{Am}}, \\ \mu &= 6 \cdot 9.2740154 \cdot 10^{-24} \text{ Am}^2, \\ b &\approx 10^{-6} \text{ m}. \end{aligned}$$

With this inserted into the upper boundary for the nearest-neighbor interaction eq. (6.44), we obtain a value of

$$V \approx 0.5 \text{ Hz}. \quad (6.58)$$

Thus the value for the calculated nearest-neighbor interaction of chromium is of the order of the estimated value for the nearest-neighbor interaction eq. (6.57) needed for the instability to occur.

Chapter 7

Summary & Outlook

In the presented work, we have in detail showed the possibility of a supersolid phase on an optical lattice by rigorous calculations. We have proofed in several ways, that an instability occurs in the energy spectrum of the superfluid phase. Therefore we propose the existence of a supersolid phase on an optical lattice.

Our calculations started with the Bogoliubov theory for a dilute Bose gas. Within this theory, where the system is assumed to be in the ground state and interactions are only allowed between particles in the ground state and in low excited states, we found that the superfluid phase is unstable. To find this, we took a Hamiltonian, which considers on-site and nearest-neighbor interactions and then diagonalized it. In this way, we achieved the dispersion relation of the system. Next, we tuned the ratio between the nearest-neighbor and on-site interaction and discovered, that at a critical ratio γ_c , the superfluid phase suffers an instability in its dispersion relation. This was the first sign of the appearance of a new quantum phase. This new phase could not be interpreted as the known Mott Insulator phase, since hopping was not fully suppressed. To proof, that the superfluid phase really undergoes a phase transition, we changed the description from the Bogoliubov to a mean-field picture. In the mean-field theory, we started our considerations with a Rotor-Hamiltonian. We used it, because we assumed, that every optical lattice site contains a quasi-condensate, which can be described by a macroscopic wave function. This kind of system then could be considered as a Josephson Junction array. After the determination of the dispersion relation, we discovered, that the instability occurs even at this description. We then took a closer look at the system, determined the number of particles and the mean-field fluctuations at each lattice site. This told us, that there are fluctuations of particle numbers, depending on the lattice site and the phase difference between sites. Next, we proposed an ansatz, where the different occupations of lattice sites were considered. This proposal was strengthened by the fluctuating particle numbers of the different lattice sites and the adjustability of them. Then we evaluated the new ground state energy for the new phase, which enters at the instability of the superfluid phase. Afterwards we investigated the phase transition between the superfluid and the new phase. The conclusion was, that it is of second order, thus the system undergoes a smooth transition. The new phase was proposed to be a supersolid, because it has properties of the superfluid, i.e. the hopping, and it forms a crystalline ordering, like solids. In the last section of the mean-field considerations the validity of the calculations was discussed and argued to be appropriate. The following chapter investigated the stability of the supersolid phase and if it holds against

quantum fluctuations introduced to the system. The conclusion, that the supersolid phase is stable, even against quantum fluctuations, strengthened our proposal of the occurrence of this phase on an optical lattice. In the last chapter, we discussed a possible experimental realization for the supersolid phase. There we proposed, that a BEC with chromium atoms confined to an optical lattice would be a promising candidate. We also calculated the on-site and nearest-neighbor interaction expressed in values, which are experimental accessible. To close the chapter of experimental realization, we assumed the frequencies of the on-site and nearest-neighbor interaction needed to tune the system to the critical ratio.

The next step of this work would be an experimental setup to realize the calculations carried out in this work. For this, a Bose-Einstein condensate of much more particles in the condensate is needed, than achieved today. With this accomplished, the future would look really promising to finally realize a supersolid.

Appendix A

Sortation of Rotor-Hamiltonian

As argued in section 5.1, we are going to sort the Rotor-Hamiltonian

$$\begin{aligned}
H = & -2t \sum_{\langle i,j \rangle} \sqrt{\bar{n}_i \bar{n}_j} \left[1 + \frac{1}{2} \left(\frac{\Delta n_j}{\bar{n}_j} + \frac{\Delta n_i}{\bar{n}_i} \right) + \frac{1}{4} \frac{\Delta n_j \Delta n_i}{\bar{n}_j \bar{n}_i} \right. \\
& \left. - \frac{1}{8} \left(\left(\frac{\Delta n_j}{\bar{n}_j} \right)^2 + \left(\frac{\Delta n_i}{\bar{n}_i} \right)^2 \right) - \frac{1}{2} (\varphi_i - \varphi_j)^2 \right] \\
& + \frac{U}{2} \sum_i (\bar{n}_i^2 + \Delta n_i^2 + 2\bar{n}_i \Delta n_i) \\
& + \frac{V}{2} \sum_{\langle i,j \rangle} (\bar{n}_i \bar{n}_j + \bar{n}_i \Delta n_j + \bar{n}_j \Delta n_i + \Delta n_i \Delta n_j) \\
& - \mu \sum_i (\bar{n}_i + \Delta n_i) .
\end{aligned} \tag{A.1}$$

by orders of Δn_i

$$\begin{aligned}
H = & -2t \sum_{\langle i,j \rangle} \sqrt{\bar{n}_i \bar{n}_j} \left(1 - \frac{1}{2} (\varphi_i - \varphi_j)^2 \right) + \frac{U}{2} \sum_i \bar{n}_i^2 + \frac{V}{2} \sum_{\langle i,j \rangle} \bar{n}_i \bar{n}_j - \mu \sum_i \bar{n}_i \\
& - 2t \sum_{\langle i,j \rangle} \sqrt{\bar{n}_i \bar{n}_j} \frac{1}{2} \left(\frac{\Delta n_i}{\bar{n}_i} + \frac{\Delta n_j}{\bar{n}_j} \right) + \frac{U}{2} \sum_i 2\bar{n}_i \Delta n_i \\
& + \frac{V}{2} \sum_{\langle i,j \rangle} (\bar{n}_i \Delta n_j + \bar{n}_j \Delta n_i) - \mu \sum_i \Delta n_i \\
& - 2t \sum_{\langle i,j \rangle} \sqrt{\bar{n}_i \bar{n}_j} \frac{1}{4} \frac{\Delta n_i \Delta n_j}{\bar{n}_i \bar{n}_j} + \frac{V}{2} \sum_{\langle i,j \rangle} \Delta n_i \Delta n_j \\
& - 2t \sum_{\langle i,j \rangle} \sqrt{\bar{n}_i \bar{n}_j} \left(-\frac{1}{8} \left(\left(\frac{\Delta n_i}{\bar{n}_i} \right)^2 + \left(\frac{\Delta n_j}{\bar{n}_j} \right)^2 \right) \right) + \frac{U}{2} \sum_i \Delta n_i^2
\end{aligned}$$

$$\begin{aligned}
&= -2t \sum_{\langle i, j \rangle} \sqrt{\bar{n}_i \bar{n}_j} \left(1 - \frac{1}{2} (\varphi_i - \varphi_j)^2 \right) + \frac{U}{2} \sum_i \bar{n}_i^2 + \frac{V}{2} \sum_{\langle i, j \rangle} \bar{n}_i \bar{n}_j - \mu \sum_i \bar{n}_i \\
&\quad - t \sum_{\langle i, j \rangle} \left(\sqrt{\frac{\bar{n}_j}{\bar{n}_i}} \Delta n_i + \sqrt{\frac{\bar{n}_i}{\bar{n}_j}} \Delta n_j \right) + U \sum_i \bar{n}_i \Delta n_i \\
&\quad + \frac{V}{2} \sum_{\langle i, j \rangle} (\bar{n}_i \Delta n_j + \bar{n}_j \Delta n_i) - \mu \sum_i \Delta n_i \\
&\quad + \sum_{\langle i, j \rangle} \Delta n_i \Delta n_j \left[\frac{V}{2} - \frac{t}{2} \frac{1}{\sqrt{\bar{n}_i \bar{n}_j}} \right] + \sum_{\langle i, j \rangle} \frac{t}{4} \sqrt{\bar{n}_i \bar{n}_j} \left(2 \left(\frac{\Delta n_i}{\bar{n}_i} \right)^2 \right) + \frac{U}{2} \sum_i \Delta n_i^2 \\
&= E' - t \sum_{\langle i, j \rangle} \underbrace{\left(\sqrt{\frac{\bar{n}_j}{\bar{n}_i}} \Delta n_i + \sqrt{\frac{\bar{n}_i}{\bar{n}_j}} \Delta n_j \right)}_{\text{same structure}} + U \sum_i \Delta n_i \bar{n}_i + \frac{V}{2} \sum_{\langle i, j \rangle} \underbrace{\left(\bar{n}_i \Delta n_j + \bar{n}_j \Delta n_i \right)}_{\text{same structure}} - \mu \sum_i \Delta n_i \\
&\quad + \sum_{\langle i, j \rangle} \frac{\Delta n_i \Delta n_j}{2} \left[V - \frac{t}{\sqrt{\bar{n}_i \bar{n}_j}} \right] + \frac{t}{2} \sum_{\langle i, j \rangle} \frac{\sqrt{\bar{n}_i \bar{n}_j}}{\bar{n}_i^2} \Delta n_i^2 + \frac{U}{2} \sum_i \Delta n_i^2, \tag{A.2}
\end{aligned}$$

where the coefficient E' is

$$E' = -2t \sum_{\langle i, j \rangle} \sqrt{\bar{n}_i \bar{n}_j} \left(1 - \frac{1}{2} (\varphi_i - \varphi_j)^2 \right) + \frac{U}{2} \sum_i \bar{n}_i^2 + \frac{V}{2} \sum_{\langle i, j \rangle} \bar{n}_i \bar{n}_j - \mu \sum_i \bar{n}_i. \tag{A.3}$$

The terms in eq. (A.2) labeled as "same structure" reveal the same values, when the summation over $\langle i, j \rangle$ is carried out. Therefore the terms can be put together in each case. Thus, the Rotor-Hamiltonian reduces further to

$$\begin{aligned}
H &= E' - 2t \sum_{\langle i, j \rangle} \sqrt{\frac{\bar{n}_j}{\bar{n}_i}} \Delta n_i + U \sum_i \Delta n_i \bar{n}_i + 2 \frac{V}{2} \sum_{\langle i, j \rangle} (\bar{n}_j \Delta n_i) - \mu \sum_i \Delta n_i \\
&\quad + \frac{1}{2} \sum_{\langle i, j \rangle} \Delta n_i \Delta n_j \left[V - \frac{t}{\sqrt{\bar{n}_i \bar{n}_j}} \right] + \frac{t}{2} \sum_{\langle i, j \rangle} \frac{\sqrt{\bar{n}_i \bar{n}_j}}{\bar{n}_i^2} \Delta n_i^2 + \frac{U}{2} \sum_i \Delta n_i^2. \tag{A.4}
\end{aligned}$$

Finally we obtain the sorted Rotor-Hamiltonian by orders of the quantum fluctuations Δn_i

$$\begin{aligned}
H &= -2t \sum_{\langle i, j \rangle} \sqrt{\bar{n}_i \bar{n}_j} \left(1 - \frac{1}{2} (\varphi_i - \varphi_j)^2 \right) + \frac{U}{2} \sum_i \bar{n}_i^2 + \frac{V}{2} \sum_{\langle i, j \rangle} \bar{n}_i \bar{n}_j - \mu \sum_i \bar{n}_i \\
&\quad - 2t \sum_{\langle i, j \rangle} \sqrt{\frac{\bar{n}_j}{\bar{n}_i}} \Delta n_i + U \sum_i \bar{n}_i \Delta n_i + V \sum_{\langle i, j \rangle} \bar{n}_j \Delta n_i - \mu \sum_i \Delta n_i \\
&\quad + \frac{1}{2} \sum_{\langle i, j \rangle} \Delta n_i \Delta n_j \left[V - \frac{t}{\sqrt{\bar{n}_i \bar{n}_j}} \right] + \frac{t}{2} \sum_{\langle i, j \rangle} \frac{\sqrt{\bar{n}_i \bar{n}_j}}{\bar{n}_i^2} \Delta n_i^2 + \frac{U}{2} \sum_i \Delta n_i^2. \tag{A.5}
\end{aligned}$$

Appendix B

Calculations of Chapter 5

B.1 Computing $2n$

As argued in section 5.1.1, $f_1 + f_2 = 2n$. In the following this is computed.

We need following values

$$f_1 = \bar{n}_i = (\bar{c} + \bar{d})^2 \quad , \quad f_2 = \bar{n}_j = (\bar{c} - \bar{d})^2 \quad , \quad (\text{B.1})$$

the values for \bar{c} eq. (4.89) and \bar{d} eq. (4.88)

$$\bar{c}^2 = \frac{n}{2} - \frac{zt}{U - zV} \quad , \quad (\text{B.2})$$

$$\bar{d}^2 = \frac{n}{2} + \frac{zt}{U - zV} \quad . \quad (\text{B.3})$$

Now we can begin the calculation

$$\begin{aligned} f_1 + f_2 &= \bar{n}_i + \bar{n}_j = (\bar{c} + \bar{d})^2 + (\bar{c} - \bar{d})^2 \\ &= (\bar{c}^2 + 2\bar{c}\bar{d} + \bar{d}^2) + (\bar{c}^2 - 2\bar{c}\bar{d} + \bar{d}^2) \\ &= 2(\bar{c}^2 + \bar{d}^2) = 2\left(\frac{n}{2} - \frac{zt}{U - zV} + \frac{n}{2} + \frac{zt}{U - zV}\right) \\ &= 2\left(\frac{n}{2} + \frac{n}{2}\right) = 2n \end{aligned} \quad (\text{B.4})$$

B.2 Calculation of U_0

Here we want to refer to the postponed calculation of U_0 in section 5.2.2

$$U_0 = \frac{1}{2} \left(\frac{1}{f_1^2} + \frac{1}{f_2^2} \right), \quad (\text{B.5})$$

where

$$f_1^2 = \bar{n}_i^2 = \left((\bar{c} + \bar{d})^2 \right)^2, \quad (\text{B.6})$$

$$f_2^2 = \bar{n}_j^2 = \left((\bar{c} - \bar{d})^2 \right)^2, \quad (\text{B.7})$$

and with eq. (B.2 + B.3).

Inserting the values for f_1^2 and f_2^2 into eq. (B.5)

$$\begin{aligned} U_0 &= \frac{1}{2} \left(\frac{1}{\left((\bar{c} + \bar{d})^2 \right)^2} + \frac{1}{\left((\bar{c} - \bar{d})^2 \right)^2} \right) \\ &= \frac{1}{2} \left(\frac{1}{\left(\bar{c}^2 + 2\bar{c}\bar{d} + \bar{d}^2 \right)^2} + \frac{1}{\left(\bar{c}^2 - 2\bar{c}\bar{d} + \bar{d}^2 \right)^2} \right) \\ &= \frac{1}{2} \left(\frac{1}{\left(\frac{n}{2} - \frac{zt}{U-zV} + 2 \left(\frac{n^2}{4} - \frac{z^2t^2}{(U-zV)^2} \right)^{1/2} + \frac{n}{2} + \frac{zt}{U-zV} \right)^2} \right. \\ &\quad \left. + \frac{1}{\left(\frac{n}{2} - \frac{zt}{U-zV} - 2 \left(\frac{n^2}{4} - \frac{z^2t^2}{(U-zV)^2} \right)^{1/2} + \frac{n}{2} + \frac{zt}{U-zV} \right)^2} \right) \\ &= \frac{1}{2} \left(\frac{1}{\left(n + \left(n^2 - \frac{4z^2t^2}{(U-zV)^2} \right)^{1/2} \right)^2} + \frac{1}{\left(n - \left(n^2 - \frac{4z^2t^2}{(U-zV)^2} \right)^{1/2} \right)^2} \right) \end{aligned}$$

$$\begin{aligned}
&= \frac{1}{2} \left(\frac{1}{\left(2n^2 - \frac{4z^2t^2}{(U-zV)^2} + 2n \left(n^2 - \frac{4z^2t^2}{(U-zV)^2}\right)^{1/2}\right)^2} + \frac{1}{\left(2n^2 - \frac{4z^2t^2}{(U-zV)^2} - 2n \left(n^2 - \frac{4z^2t^2}{(U-zV)^2}\right)^{1/2}\right)^2} \right) \\
&= \frac{1}{2} \left(\frac{2n^2 - 2n \left(n^2 - \frac{4z^2t^2}{(U-zV)^2}\right)^{1/2} - \frac{4z^2t^2}{(U-zV)^2} + 2n^2 + 2n \left(n^2 - \frac{4z^2t^2}{(U-zV)^2}\right)^{1/2} - \frac{4z^2t^2}{(U-zV)^2}}{\left(2n^2 + 2n \left(n^2 - \frac{4z^2t^2}{(U-zV)^2}\right)^{1/2} - \frac{4z^2t^2}{(U-zV)^2}\right) \left(2n^2 - 2n \left(n^2 - \frac{4z^2t^2}{(U-zV)^2}\right)^{1/2} - \frac{4z^2t^2}{(U-zV)^2}\right)} \right) \\
&= \frac{2n^2 - \frac{4z^2t^2}{(U-zV)^2}}{\left(4n^2 - \frac{16z^2t^2n^2}{(U-zV)^2} - 4n^2 + \frac{16z^2t^2n^2}{(U-zV)^2} + \frac{16z^4t^4}{(U-zV)^4}\right)} \\
&= \frac{n^2 - \frac{2z^2t^2}{(U-zV)^2}}{\frac{8z^4t^4}{(U-zV)^4}} \\
&= \frac{n^2 (U-zV)^4}{8z^4t^4} - \frac{(U-zV)^2}{4z^2t^2} \\
&= \frac{(U-zV)^2}{4z^2t^2} \left(\frac{n^2 (U-zV)^2}{2z^2t^2} - 1 \right) = \frac{1}{2} \left(\frac{1}{f_1^2} + \frac{1}{f_2^2} \right). \tag{B.8}
\end{aligned}$$

B.3 Calculation of U_1

With U_0 being calculated above, U_1 is due. The coefficient U_1 is

$$U_1 = \frac{1}{2} \left(\frac{1}{f_1^2} - \frac{1}{f_2^2} \right), \tag{B.9}$$

and

$$f_1^2 = \bar{n}_i^2 = \left((\bar{c} + \bar{d})^2 \right)^2, \tag{B.10}$$

$$f_2^2 = \bar{n}_j^2 = \left((\bar{c} - \bar{d})^2 \right)^2, \tag{B.11}$$

where the coefficients \bar{c} and \bar{d} are as in eq. (B.2 + B.3).

Now the computation can be carried out

$$\begin{aligned}
U_1 &= \frac{1}{2} \left(\frac{1}{(\bar{c} + \bar{d})^4} - \frac{1}{(\bar{c} - \bar{d})^4} \right) \\
&= \frac{1}{2} \left(\frac{1}{(\bar{c}^2 + \bar{d}^2 + 2\bar{c}\bar{d})^2} - \frac{1}{(\bar{c}^2 + \bar{d}^2 - 2\bar{c}\bar{d})^2} \right) \\
&= \frac{1}{2} \left(\frac{1}{\left(n + \left(n^2 - \frac{4z^2t^2}{(U-zV)^2} \right)^{1/2} \right)^2} - \frac{1}{\left(n - \left(n^2 - \frac{4z^2t^2}{(U-zV)^2} \right)^{1/2} \right)^2} \right) \\
&= \frac{1}{2} \left(\frac{1}{2n^2 - \frac{4z^2t^2}{(U-zV)^2} + 2n \left(n^2 - \frac{4z^2t^2}{(U-zV)^2} \right)^{1/2}} - \frac{1}{2n^2 - \frac{4z^2t^2}{(U-zV)^2} - 2n \left(n^2 - \frac{4z^2t^2}{(U-zV)^2} \right)^{1/2}} \right) \\
&= \frac{1}{2} \left(\frac{-4n \left(n^2 - \frac{4z^2t^2}{(U-zV)^2} \right)^{1/2}}{4n^4 - \frac{16z^2t^2n^2}{(U-zV)^2} + \frac{16z^4t^4}{(U-zV)^4} - 4n^4 + \frac{16z^2t^2n^2}{(U-zV)^2}} \right) \\
&= \frac{-2n \left(n^2 - \frac{4z^2t^2}{(U-zV)^2} \right)^{1/2}}{\frac{16z^4t^4}{(U-zV)^4}} \\
&= \frac{-n \left(n^2 - \frac{4z^2t^2}{(U-zV)^2} \right)^{1/2}}{\frac{8z^4t^4}{(U-zV)^4}} \\
&= \frac{-(U-zV)^4 n \left(n^2 - \frac{4z^2t^2}{(U-zV)^2} \right)^{1/2}}{8z^4t^4} \\
&= \frac{-(U-zV)^3 n \left(\frac{n^2 (U-zV)^2}{4z^2t^2} - 1 \right)^{1/2}}{4z^3t^3} \\
&= \frac{(zV-U)^3 n \left(\frac{n^2 (U-zV)^2}{4z^2t^2} - 1 \right)^{1/2}}{4z^3t^3} = \frac{1}{2} \left(\frac{1}{f_1^2} - \frac{1}{f_2^2} \right). \tag{B.12}
\end{aligned}$$

Bibliography

- [1] A.A. Abrikosov, L.P. Gorkov, and I.E. Dzyaloshinski. *Methods Of Quantum Field Theory In Statistical Physics*. Dover Publications, revised english edition, 1963.
- [2] P. W. ANDERSON. Considerations on the flow of superfluid helium. *Rev. Mod. Phys.*, 38(2):298–310, Apr 1966.
- [3] N. W. Ashcroft and N. D. Mermin. *Solid State Physics*. Harcourt Brace College Publishers, international edition edition, 1975.
- [4] G. G. Batrouni, F. Hébert, and R. T. Scalettar. Supersolid phases in the one-dimensional extended soft-core bosonic hubbard model. *Phys. Rev. Lett.*, 97(8):087209, Aug 2006.
- [5] G. G. Batrouni and R. T. Scalettar. Phase separation in supersolids. *Phys. Rev. Lett.*, 84(7):1599–1602, Feb 2000.
- [6] G. G. Batrouni, R. T. Scalettar, G. T. Zimanyi, and A. P. Kampf. Supersolids in the bose-hubbard hamiltonian. *Phys. Rev. Lett.*, 74(13):2527–2530, Mar 1995.
- [7] Immanuel Bloch, Jean Dalibard, and Wilhelm Zwerger. Many-body physics with ultracold gases. *Rev. Mod. Phys.*, 80(3):885–964, Jul 2008.
- [8] R. M. Bradley and S. Doniach. Quantum fluctuations in chains of josephson junctions. *Phys. Rev. B*, 30(3):1138–1147, Aug 1984.
- [9] H. P. Büchler. Lecture notes: Physik der kalten Gase, 2008.
- [10] H. P. Büchler and G. Blatter. Supersolid versus phase separation in atomic bose-fermi mixtures. *Phys. Rev. Lett.*, 91(13):130404, Sep 2003.
- [11] F. S. Cataliotti, S. Burger, C. Fort, P. Maddaloni, F. Minardi, A. Trombettoni, A. Smerzi, and M. Inguscio. Josephson junction arrays with bose-einstein condensates. *Science*, 293(5531):843–846, Aug 2001.
- [12] P. M. Chaikin and T. C. Lubensky. *Principles of condensed matter physics*. Cambridge University Press, first edition, 1995.
- [13] G. V. Chester. Speculations on bose-einstein condensation and quantum crystals. *Phys. Rev. A*, 2(1):256–258, Jul 1970.
- [14] Bryan K. Clark and D. M. Ceperley. Off-diagonal long-range order in solid *he4*. *Phys. Rev. Lett.*, 96(10):105302, Mar 2006.

- [15] Franco Dalfovo, Stefano Giorgini, Lev P. Pitaevskii, and Sandro Stringari. Theory of bose-einstein condensation in trapped gases. *Rev. Mod. Phys.*, 71(3):463–512, Apr 1999.
- [16] N. Elstner and H. Monien. Dynamics and thermodynamics of the bose-hubbard model. *Phys. Rev. B*, 59(19):12184–12187, May 1999.
- [17] K. Góral, L. Santos, and M. Lewenstein. Quantum phases of dipolar bosons in optical lattices. *Phys. Rev. Lett.*, 88(17):170406, Apr 2002.
- [18] Markus Greiner, Immanuel Bloch, Olaf Mandel, Theodor W. Hänsch, and Tilman Esslinger. Exploring phase coherence in a 2d lattice of bose-einstein condensates. *Phys. Rev. Lett.*, 87(16):160405, Oct 2001.
- [19] Markus Greiner, Olaf Mandel, Tilman Esslinger, Theodor W. Hänsch, and Immanuel Bloch. Quantum phase transition from a superfluid to a mott insulator in a gas of ultracold atoms. *Nature*, 415(6867):39, Jan 2002.
- [20] Axel Griesmaier, Jörg Werner, Sven Hensler, Jürgen Stuhler, and Tilman Pfau. Bose-einstein condensation of chromium. *Phys. Rev. Lett.*, 94(16):160401, Apr 2005.
- [21] R. A. Guyer. Superfluidity in quantum crystals. *Phys. Rev. Lett.*, 26(4):174–177, Jan 1971.
- [22] D. Jaksch, C. Bruder, J. I. Cirac, C. W. Gardiner, and P. Zoller. Cold bosonic atoms in optical lattices. *Phys. Rev. Lett.*, 81(15):3108–3111, Oct 1998.
- [23] D. Jaksch and P. Zoller. The cold atom hubbard toolbox. *Science*, 315(1):52–79, Jan 2005.
- [24] Juha Javanainen. Oscillatory exchange of atoms between traps containing bose condensates. *Phys. Rev. Lett.*, 57(25):3164–3166, Dec 1986.
- [25] E. Kim and M. H. W. Chan. Probable observation of a supersolid helium phase. *Nature*, 427(6971):225, Jan 2004.
- [26] T. Kinoshita, T. Wenger, and D. S. Weiss. Observation of a one-dimensional tonks-girardeau gas. *Science Express*, 305(5687):1125–1128, Jul 2004.
- [27] Tobias Koch, Thierry Lahaye, Jonas Metz, Bernd Fröhlich, Marco Fattori, Axel Griesmaier, and Tilman Pfau. Stabilization of a purely dipolar quantum gas against collapse. *Nat Phys*, 4(3):218, Mar 2008.
- [28] Konrad Kopitzki and Peter Herzog. *Einführung in die Festkörperphysik*. Teubner Studienbücher, sixth edition, 2007.
- [29] F. Kuypers. *Klassische Mechanik*. Wiley-VCH Verlag, seventh edition, 2005.
- [30] T. Lahaye, C. Menotti, L. Santos, M. Lewenstein, and T. Pfau. The physics of dipolar bosonic quantum gases. *Reports on Progress in Physics*, 72(12):126401, Nov 2009.
- [31] Thierry Lahaye, Tobias Koch, Bernd Fröhlich, Marco Fattori, Jonas Metz, Axel Griesmaier, Stefano Giovanazzi, , and Tilman Pfau. Strong dipolar effects in a quantum ferrofluid. *Nature*, 448(7154):672, Aug 2007.

- [32] Thierry Lahaye, Tilman Pfau, and Luis Santos. Mesoscopic ensembles of polar bosons in triple-well potentials, 2009.
- [33] A. J. Leggett. Can a solid be "superfluid"? *Phys. Rev. Lett.*, 25(22):1543–1546, Nov 1970.
- [34] Gerald D. Mahan. *Many-Particle Physics*. Plenum Press, second edition, 1990.
- [35] Christophe Mora and Yvan Castin. Extension of bogoliubov theory to quasicondensates. *Phys. Rev. A*, 67(5):053615, May 2003.
- [36] Oliver Morsch and Markus Oberthaler. Dynamics of bose-einstein condensates in optical lattices. *Rev. Mod. Phys.*, 78(1):179–215, Feb 2006.
- [37] William J. Mullin. Cell model of a bose-condensed solid. *Phys. Rev. Lett.*, 26(11):611–614, Mar 1971.
- [38] B. Paredes, A. Widera, V. Murg, O. Mandel, S. Folling, I. Cirac, G. V. Shlyapnikov, T. W. Hänsch, and I. Bloch. Tonks-girardeau gas of ultracold atoms in an optical lattice. *Nature*, 429(6989):277–281, May 2004.
- [39] Oliver Penrose and Lars Onsager. Bose-einstein condensation and liquid helium. *Phys. Rev.*, 104(3):576–584, Nov 1956.
- [40] Yves Pomeau and Sergio Rica. Dynamics of a model of supersolid. *Phys. Rev. Lett.*, 72(15):2426–2429, Apr 1994.
- [41] Nikolay Prokof'ev and Boris Svistunov. Supersolid state of matter. *Phys. Rev. Lett.*, 94(15):155302, Apr 2005.
- [42] Eric Roddick and D. Stroud. Mean-field theory for underdamped josephson-junction arrays with an offset voltage. *Phys. Rev. B*, 48(22):16600–16606, Dec 1993.
- [43] S. Sachdev. *Quantum Phase Transitions*. Cambridge University Press, first edition, 1999.
- [44] J. J. Sakurai. *Modern Quantum Mechanics*. Addison Wesley Longman Publishing Company, revised edition edition, 1994.
- [45] R. T. Scalettar, G. G. Batrouni, A. P. Kampf, and G. T. Zimanyi. Simultaneous diagonal and off-diagonal order in the bose-hubbard hamiltonian. *Phys. Rev. B*, 51(13):8467–8480, Apr 1995.
- [46] V. W. Scarola and S. Das Sarma. Quantum phases of the extended bose-hubbard hamiltonian: Possibility of a supersolid state of cold atoms in optical lattices. *Phys. Rev. Lett.*, 95(3):033003, Jul 2005.
- [47] V. W. Scarola, E. Demler, and S. Das Sarma. Searching for a supersolid in cold-atom optical lattices. *Phys. Rev. A*, 73(5):051601, May 2006.
- [48] Gerd Schön and A. D. Zaikin. Quantum coherent, phase transitions, and the dissipative dynamics of ultra small tunnel junctions. *Physics Reports*, 198(5-6):237–412, Dec 1990.

- [49] Pinaki Sengupta, Leonid P. Pryadko, Fabien Alet, Matthias Troyer, and Guido Schmid. Supersolids versus phase separation in two-dimensional lattice bosons. *Phys. Rev. Lett.*, 94(20):207202, May 2005.
- [50] A. Smerzi, S. Fantoni, S. Giovanazzi, and S. R. Shenoy. Quantum coherent atomic tunneling between two trapped bose-einstein condensates. *Phys. Rev. Lett.*, 79(25):4950–4953, Dec 1997.
- [51] J. Stuhler, A. Griesmaier, T. Koch, M. Fattori, T. Pfau, S. Giovanazzi, P. Pedri, and L. Santos. Observation of dipole-dipole interaction in a degenerate quantum gas. *Phys. Rev. Lett.*, 95(15):150406, Oct 2005.
- [52] Guang-Shan Tian. A rigorous theorem on off-diagonal long-range order of boson systems. *Journal of Physics. A: Mathematical and General.*, 25(10):2989–2995, Jan 1992.
- [53] B. Laburthe Tolra, K. M. O’Hara, J. H. Huckans, W. D. Phillips, S. L. Rolston, and J. V. Porto. Observation of reduced three-body recombination in a correlated 1d degenerate bose gas. *Phys. Rev. Lett.*, 92(19):190401, May 2004.
- [54] D. van Oosten, P. van der Straten, and H. T. C. Stoof. Quantum phases in an optical lattice. *Phys. Rev. A*, 63(5):053601, Apr 2001.
- [55] Anne van Otterlo and Karl-Heinz Wagenblast. Coexistence of diagonal and off-diagonal long-range order: A monte carlo study. *Phys. Rev. Lett.*, 72(22):3598–3601, May 1994.
- [56] Stefan Wessel and Matthias Troyer. Supersolid hard-core bosons on the triangular lattice. *Phys. Rev. Lett.*, 95(12):127205, Sep 2005.
- [57] C. N. Yang. Concept of off-diagonal long-range order and the quantum phases of liquid he and of superconductors. *Rev. Mod. Phys.*, 34(4):694–704, Oct 1962.
- [58] Chen Ning Yang. η pairing and off-diagonal long-range order in a hubbard model. *Phys. Rev. Lett.*, 63(19):2144–2147, Nov 1989.

Ehrenwörtliche Erklärung

Ich erkläre, dass ich diese Arbeit selbstständig verfasst und keine anderen als die angegebenen Quellen und Hilfsmittel benutzt habe.

January 15, 2011

Adam Bühler

Acknowledgements

First of all, I want to thank my parents for giving me the possibility to study physics and supporting me through my career. Second of all, I want to thank my supervisor H. P. Büchler for the opportunity to write this thesis, for his support through it and for all the discussions about one of the most exciting hobby there is. Then I want to thank my family and friends for the beautiful time we share, especially: Kaethe , Edda , Klaus , Patrick, Christopher, Mirjam, Thomas, Nina, Christian R. , Bernd, Rike, Vanessa, Nico, Dominik, and the rest of the RP-guys: Ben, Benji, Chris, Thomas F; the people through my studies: Matthias S., Stefan, Matthias Z., Gerald, Ling, Emanuel, Eli; and all the other members of the DLRG Ortsgruppe Kornwestheim. Then I want to thank all the members of the ITP3 for all the nice talks and discussions we had, no matter what topic. Especially considered here should be my former room mate Jan, the guy next door Jürgen, Steffen, Andreas, Thorsten and the new room mate Elke.

Also I want to thank H. P. Büchler, my mother Sigrid, Jerome and Elke for reading this thesis and giving comments about corrections.

Last but not least, I want to thank Prof. Wunner for taking care of the second report for my thesis.